**FY98 Interim Technical Report**

**Strategic Environmental Research and Development Program**
**Project 1094**

# Environmental Impacts to the Chemical Signature Emanating from Buried Unexploded Ordnance

James M. Phelan
Environmental Restoration Technologies Department

Stephen W. Webb
Mission Analysis and Simulation Department

Sandia National Laboratories
Albuquerque, NM

Daniel C. Leggett
U.S. Army Corps of Engineers,
Cold Regions Research and Engineering Laboratory
Hanover, NH

William A. Jury
University of California Riverside

# REPORT DOCUMENTATION PAGE

*Form Approved*
*OMB No. 074-0188*



| 1. AGENCY USE ONLY (Leave blank) | 2. REPORT DATE | 3. REPORT TYPE AND DATES COVERED |
|---|---|---|
| | December 1998 | Technical Report |

**4. TITLE AND SUBTITLE**
Environmental Impacts to the Chemical Signature Emanating from Buried Unexploded Ordnance

**5. FUNDING NUMBERS**
N/A

**6. AUTHOR(S)**
James M. Phelan, Stephen W. Webb, Daniel C. Leggett and Wiliam A. Jury

**7. PERFORMING ORGANIZATION NAME(S) AND ADDRESS(ES)**
Sandia National Laboratories, Albuquerque, NM

U.S. Army Corps of Engineers, Cold Regions Research and Engineering Laboratory, Hanover, NH

University of California, Riverside

**8. PERFORMING ORGANIZATION REPORT NUMBER**
N/A

**9. SPONSORING / MONITORING AGENCY NAME(S) AND ADDRESS(ES)**
SERDP
901 North Stuart St. Suite 303
Arlington, VA 22203

**10. SPONSORING / MONITORING AGENCY REPORT NUMBER**
N/A

**11. SUPPLEMENTARY NOTES**


**12a. DISTRIBUTION / AVAILABILITY STATEMENT**
Approved for public release: distribution is unlimited.

**12b. DISTRIBUTION CODE**
A

**13. ABSTRACT *(Maximum 200 Words)***
The goal of locating buried UXO and landmines is a significant challenge to science and technology. Technology development efforts are under way to use chemical sensors that can discriminate inert ordnance and clutter from live munitions that continue to be a threat. However, the chemical signature is affected by multiple environmental phenomena that can enhance or reduce its presence and transport behavior, and can affect the distribution of the chemical signature in the environment. For example, the chemical among these phases, including the spatial distribution, is the key in designing appropriate detectors, e.g., gas, aqueous or solid phase sampling instruments. A fundamental understanding of the environmental conditions that affect the chemical signature is needed to describe the favorable and unfavorable conditions of a chemical detector based survey to minimize the consequences of a false negative.

**14. SUBJECT TERMS**
SERDP, SERDP Collection, chemical signature, UXO, landmines

**15. NUMBER OF PAGES**
72

**16. PRICE CODE**

| 17. SECURITY CLASSIFICATION OF REPORT | 18. SECURITY CLASSIFICATION OF THIS PAGE | 19. SECURITY CLASSIFICATION OF ABSTRACT | 20. LIMITATION OF ABSTRACT |
|---|---|---|---|
| unclass | unclass | unclass | UL |

CV
JM

**Sandia National Laboratories**

Operated for the U.S. Department of Energy by
**Sandia Corporation**

**James M Phelan**
Environmental Restoration Technologies Department

P.O. Box 5800
Albuquerque, NM 87185-0719

Phone: (505)845-9892
Fax: (505)844-0543
Internet: jmphela@sandia.gov

December 23, 1998

Mr. Brad Smith
Executive Director
Strategic Environmental Research and Development Program
901 North Stuart Street
Suite 303
Arlington, VA 22203

Dear Mr. Smith,

Attached please find the FY98 Annual Interim Technical Report for the SERDP Project 1094, "Environmental Impacts to the Chemical Signature Emanating from Buried UXO." The authors hope that this documentation will provide sufficient technical documentation of progress for the first year of this exciting project. We feel that the findings will provide the needed information to scientific and operational groups to further the development of chemical sensing for detection of UXO. If there are any questions, please contact myself at your convenience.

Sincerely,

James M. Phelan

## 1.0 Project Background

The goal of locating buried UXO and landmines is a significant challenge to science and technology. Technology development efforts are under way to use chemical sensors that can discriminate inert ordnance and clutter from live munitions that continue to be a threat. However, the chemical signature is affected by multiple environmental phenomena that can enhance or reduce its presence and transport behavior, and can affect the distribution of the chemical signature in the environment. For example, the chemical can be present in the vapor, aqueous, and solid phases. The distribution of the chemical among these phases, including the spatial distribution, is key in designing appropriate detectors, e.g., gas, aqueous or solid phase sampling instruments. A fundamental understanding of the environmental conditions that affect the chemical signature is needed to describe the favorable and unfavorable conditions of a chemical detector based survey to minimize the consequences of a false negative. Figures 1 and 2 show the principal subsurface phenomena and the principal surface boundary conditions that are being explored in this project.

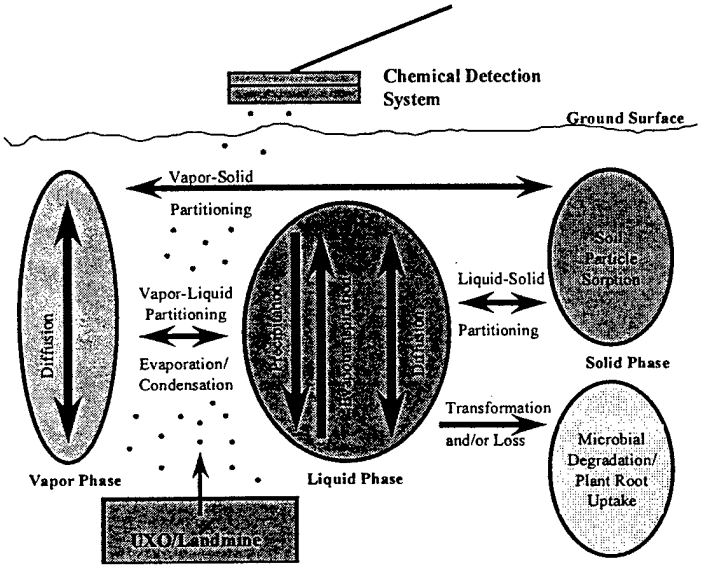


Figure 1. Subsurface Environmental Fate and Transport Phenomena

## 2.0 Objective

The objective of this project is to develop a validated subsurface transport model that can be used to predict the spatial, temporal, and phase specific concentration of chemical signature molecules derived from shallow UXO and buried landmines under the influence of specific environmental conditions. Other government programs are developing chemical detector platforms that can provide a separate unique signal to classify subsurface objects identified with existing geophysical systems. It is estimated that eleven million acres of land needs assessment to identify subsurface UXO - with costs estimated to be about $1.4M/acre. The ranges where UXO can be found are distributed throughout the country where environmental conditions vary significantly. It is the hypothesis of this project that these environmental conditions will have a

significant impact on the transport of chemical signature molecules from subsurface UXO and buried landmines to the surface before presentation to a chemical detector system.

If through this systems analysis, one can show the ranges and/or combinations of environmental parameters that improve the transport of chemical signature molecules to the chemical detector system, and conversely, those that constrain this movement, end-users seeking to locate buried UXO will be better positioned to understand the merits and limitations when looking to deploy the chemical detector technology.

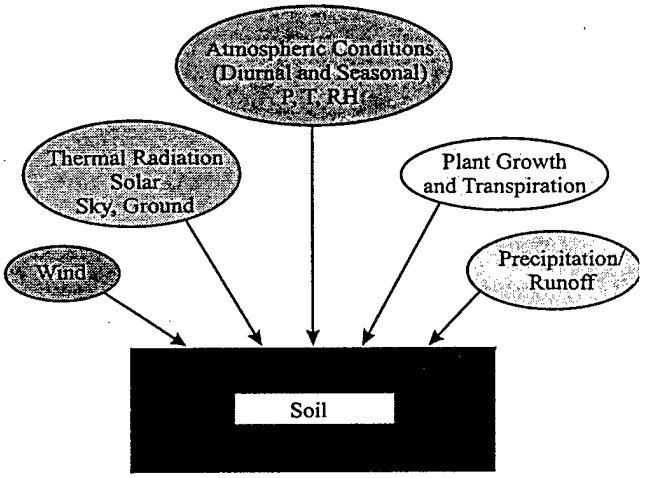


Figure 2. Soil Surface Boundary Conditions

## 3.0 Technical Approach

This project is a cooperative effort involving Sandia National Laboratories, US Army Corps of Engineers - Cold Regions Research and Engineering Laboratory, the University of California Riverside and Lawrence Berkeley Laboratory. This project has been co-funded by the DARPA program for the chemical/biological detection of explosives in landmines. The project is divided into five major tasks.

Task 1: Model Development/Utilization - The task involves completion of a sensitivity analysis of known input parameters in a one-dimensional analytical contaminant transport model, expanding this model to assess two-dimensions to explore the surface area footprint from buried UXO, and modifying an existing numerical simulation code (TOUGH2) (surface boundary conditions, multiple chemical components, liquid diffusion) for use as the complete systems analysis tool. Inverse modeling will be used to assess input parameter sensitivity and as a tool for the design of laboratory validation experiments in task three.

Task 2: Fundamental Properties - This task involves the measurement of specific transport parameters currently not available in the literature for explosive signature

molecules. These include temperature dependent water solubility, vapor-solid sorption as a function of soil moisture content and source-term emission rates.

Task 3: Laboratory-Scale Experiments – This task involves a laboratory validation study that will confirm the most critical parameters included in the simulation model through soil column transport experiments.

Task 4: Operational Strategy – This task will utilize the simulation tools to assess the impacts of environmental conditions on the transport of chemical signature molecules from shallow UXO and support end-user queries on the utility of chemical sensor platforms for the classification stage in the identification of true unexploded ordnance.

Task 5: Ordnance Source Term – This task was added in August 1998 to evaluate the source term from actual ordnance items.

## 4.0 Project Accomplishments

### Task One – Model Development/Utilization

The environmental fate and transport of organic chemicals including volatilization and leaching losses has been used to explore the distribution of agricultural pesticides in soils (Mayer et al. 1974, Farmer et al. 1980, and Jury et al. 1980). These models were primarily intended to simulate specific circumstances. However, Jury et al. (1983, 1984a, 1984b, 1984c) developed and validated a general screening model (Behavior Assessment Model, BAM) that included volatilization, leaching, and degradation to explore the major loss pathways of agricultural pesticides as a function of specific environmental conditions. The Behavior Assessment Model was adapted for evaluation of chemicals in buried soils and has been termed the Buried Chemical Model (BCM)(Jury et al., 1990). The model simulations can be used to assess the behavior of different chemicals under particular environmental conditions, but are not intended to predict a definitive concentration distribution in the field. As such, the predictions from the screening model are only an indication of expected conditions.

***A. Phase Partitioning Phenomena***

The formulations of the BAM and BCM models begin by defining phase partitioning phenomena. These are valuable in that they can express the total concentration of a chemical in the gas, aqueous and sorbed phases. The total concentration is expressed as

$$C_T = \rho_b C_S + \theta C_L + a C_G \qquad [1]$$

where $C_S$ is the concentration sorbed to the soil, $C_L$ is the solute concentration in the aqueous phase, and $C_G$ is the gas phase concentration. In addition, Jury (1983) shows how equation [1] can be rewritten in terms of one of the variables alone

$$C_T = R_S C_S = R_L C_L = R_G C_G \qquad [2]$$

where

$$R_S = \rho_b + \frac{\theta}{K_d} + a\frac{K_H}{K_d} \qquad [3]$$

$$R_L = \rho_b K_d + \theta + aK_H, \text{ and} \quad [4]$$

$$R_G = \rho_b \frac{K_d}{K_H} + \frac{\theta}{K_H} + a \quad [5]$$

are the solid, liquid and gas phase partition coefficients, respectively.

In their evaluation of vapor phase transport in soils, Ong et al., 1992, added vapor-solid sorption such that equations [1] and [2] become

$$C_T = \theta C_L + aC_G + C_L K_d \rho_b + C_G K_{SG} \rho_b \quad [6]$$

and

$$C_T = R_S C_S = R_L C_L = R_G C_G = R_{SG} C_{SG} \quad [7]$$

where

$$R_L = \rho_b K_d + \theta + aK_H + \rho_b K_H K_{SG} \quad [8]$$

$$R_G = \rho_b \frac{K_d}{K_H} + \frac{\theta}{K_H} + a + \rho_b K_{SG} \quad [9]$$

$$R_{SL} = \rho_b + \frac{\theta}{K_d} + a\frac{K_H}{K_d} + \frac{\rho_b K_H K_{SG}}{K_d}, \text{ and} \quad [10]$$

$$R_{SG} = \frac{\rho_b K_d}{K_H K_{SG}} + \frac{\theta}{K_H K_{SG}} + \frac{a}{K_{SG}} + \rho_b \quad [11]$$

are the liquid, gas and solid-liquid and solid-gas phase partition coefficients, respectively. This formulation introduces a new term, $K_{SG}$ that is a function of the overall vapor partition coefficient ($K'_d$), which is highly dependent on the soil moisture content. $K_{SG}$ is defined as (Ong et al., 1992)

$$K_{SG} = K'_d(w) - \frac{K_d}{K_H} + \frac{w}{100 K_H \gamma \rho_w} \quad [12]$$

Below four monomolecular layers of water coverage on soils, $K'_d$ is an exponential function described by

$$A = \log(K'_d) \quad [13]$$

$$A = (A_0 - \beta(w))e^{-\alpha\omega} + \beta(w) \quad [14]$$

$$\alpha = \frac{-\ln\left[\frac{A_4 - \beta}{A_0 - \beta}\right]}{w_4} \quad [15]$$

$$\beta(w) = \log\left(\frac{K_d}{K_H} + \frac{w}{K_H \gamma \rho_w}\right) \quad [16]$$

Above four monomolecular layers of water coverage on soil, $K'_d$ is a function of $K_H$ and is described by

$$A = \log\left(\frac{K_d}{K_H} + \frac{w}{K_H \gamma \rho_w}\right) \quad [17]$$

Ong et al, 1990, characterize the vapor-solid partitioning in this region as being controlled by Henry's Law Constant (HLC). This is because the vapor must first partition into the soil water prior to partitioning onto the soil particle. The moisture content at four monomolecular layers of soil water is a function of the soil specific surface area and is described by

$$w_4 = 4\left(\frac{S_A MW_w}{MA_w A_n}\right) \quad [18]$$

The specific surface area ($S_A$) of soils range from 10 $m^2/g$ for sand to 100's $m^2/g$ for some types of clay. Figure 3 shows the correlation of soil specific surface area to the moisture content at four monomolecular layers of water. The proportion of clay in soils strongly influences the soil specific surface area. This is due to the small size of the clay soil particles.

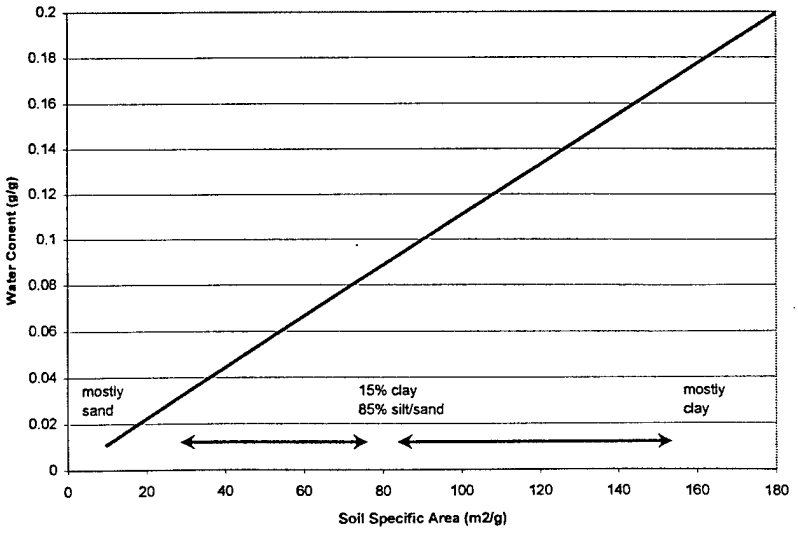


Figure 3. Soil Water Content at 4 Monomolecular Layers as a Function of Soil Specific Area

In their evaluation of toluene and trichloroethene, $K_d$ increased about $10^4$ from the point of four monomolecular layers to oven dry soil moisture contents. The impact of the vapor solid partitioning is significant at moderately low soil moisture contents. Figure 4 shows how the relative soil gas concentration can decline rapidly as the soil moisture content declines. Note that the soil moisture contents at four monomolecular layers are at levels that are not unusually low, and are typically observed in soils after precipitation and drainage events have occurred. With an extended absence of precipitation, the surface soil moisture approaches the extremely dry region. It is a potential that this dry layer could act as a barrier to vapor emission from soils and be a preconcentrator of analyte signal. Whether this process is fully reversible with the addition of water is unknown, and may represent an opportunity for enhancement of the chemical signature.

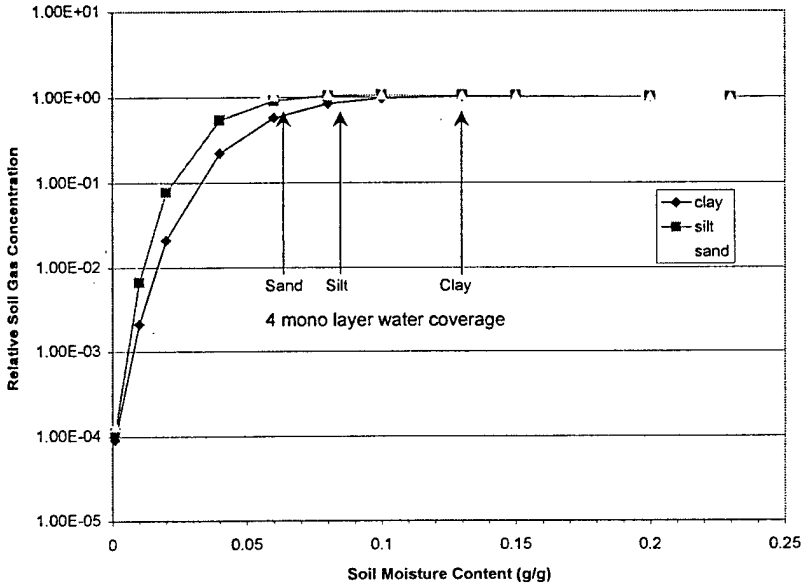


Figure 4. Relative Soil Gas Concentrations Impacted by Low Soil Moisture Content

In order to understand this phenomenon more, a Monte Carlo simulation approach was employed. This method specifies a statistical distribution function for various input parameters, then randomly selects particular values for each input variable within the specified statitical distribution, and tracks the output of one or more variables. The following input assumptions and distributions were defined for the soil bulk density, soil particle density, soil moisture content, soil water partition coefficient, soil specific surface area and soil vapor partition coefficient at oven dry conditions ($A_0$). Other parameters that were fixed included soil temperature (22 °C), which defines the Henry's Law Constant, the soil specific surface area (80 $m^2/g$) which defines the soil moisture content at four monomolecular layers (0.089 g/g) and the total soil concentration ($C_T$= 1000 ug/kg). The chemical chosen for this simulation was 2,4-DNT, as it may likely be one of the best signature compounds for chemical detection.

Two forecast evaluations were performed. The first was for soil moisture contents that were above the four monomolecular layers of soil water (0.13 to 0.30 $cm^3/cm^3$) such that the vapor solid partition coefficient was in the region controlled by the HLC. The volumetric moisture content of 0.13 $cm^3/cm^3$ is equivalent to a gravimetric soil mositure content of 0.089 g/g at a soil bulk density of 1.5 $g/cm^3$, which is the soil moisture content

at four monomolecular layers for a soil with a specific area of 80 $m^2/g$. The output variable is the soil gas concentration. The second forecast evaluation was performed in the dry region, below four monomolecular layers of soil water (0.01 to 0.13 $cm^3/cm^3$), where the soil vapor partioning is highly non-linear.

**Assumption: Soil Bulk Density**

Triangular distribution with parameters:

| | |
|---|---|
| Minimum | 1.04 |
| Likeliest | 1.51 |
| Maximum | 1.68 |

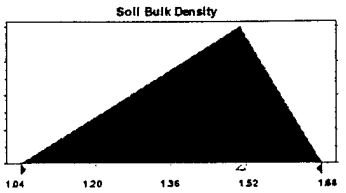


Selected range is from 1.04 to 1.68
Mean value in simulation was 1.41

**Assumption: Soil Particle Density**

Normal distribution with parameters:

| | |
|---|---|
| Mean | 2.60 |
| Standard Dev. | 0.01 |

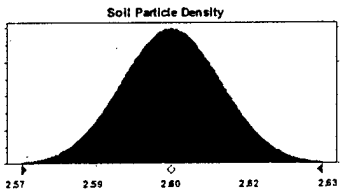


Selected range is from -Infinity to +Infinity
Mean value in simulation was 2.60

**Assumption: Soil Moisture Content**

Uniform distribution with parameters:

| | |
|---|---|
| Minimum | 0.13 |
| Maximum | 0.30 |

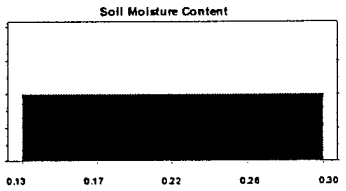


Mean value in simulation was 0.22

**Assumption: Soil Water Partition Coeff (Kd)**

Lognormal distribution with parameters:

| | |
|---|---|
| Mean | 3.0 |
| Standard Dev. | 1.0 |

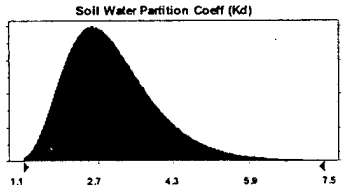


Selected range is from 0.0 to +Infinity
Mean value in simulation was 3.0

**Assumption: A zero**

Uniform distribution with parameters:

| | |
|---|---|
| Minimum | 10.00 |
| Maximum | 11.00 |

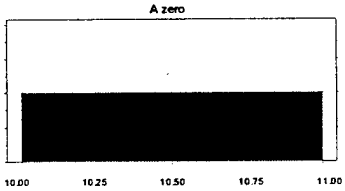


Mean value in simulation was 10.50

The following forecast of soil gas concentrations shows that there is an apparent normal or log normal distribution of values.

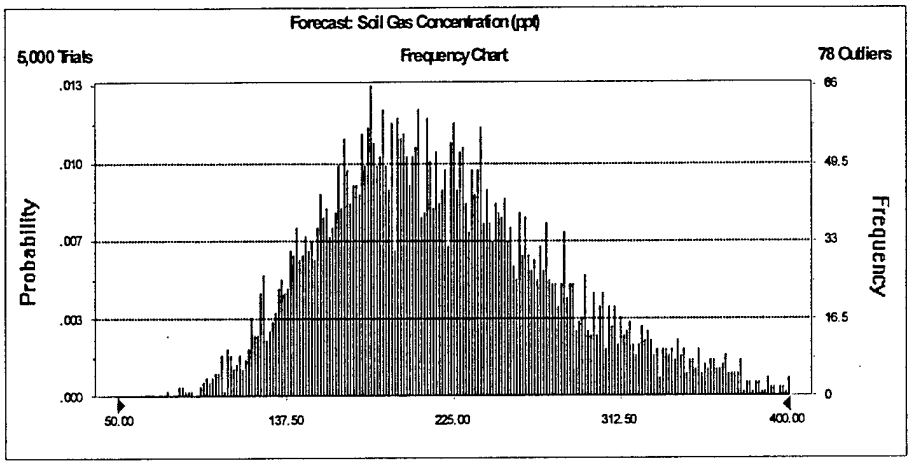


Figure 5. Soil Gas Concentration – Wet

Figure 6 shows a sensitivity analysis of the input parameters. The strongest parameter is the soil water partition coefficient, which is clear from a closer examination of equation [9]. The shape of the histogram in Figure 5 is consistent with that for the soil water partition coefficient, which is also supported by the strength of the association as shown in the sensitivity analysis (Figure 6).

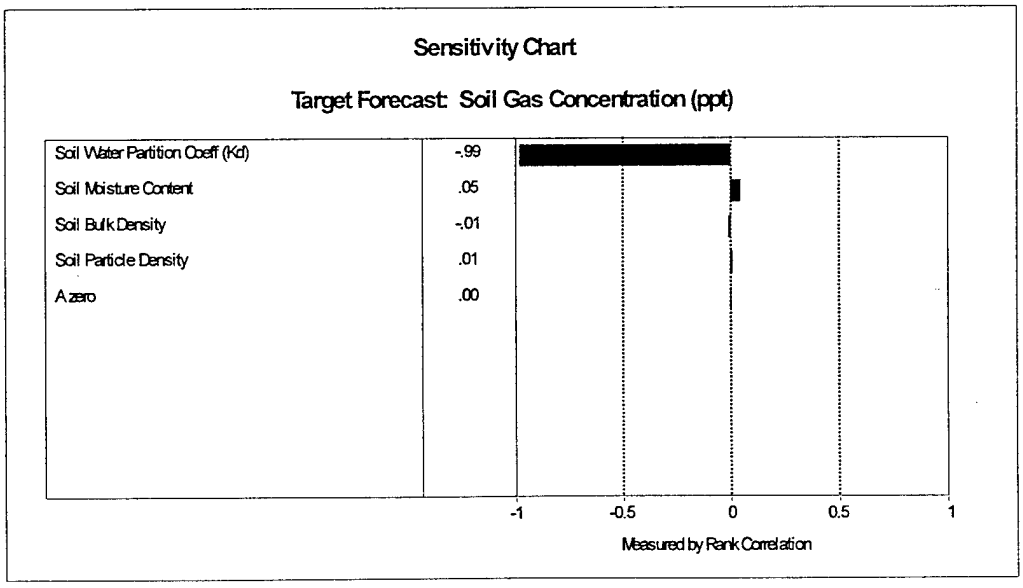


Figure 6. Sensitivity Analysis – Wet

The next simulation was performed by altering only the input values for the soil moisture content. In this case, the soil moisture range is set to be below four monomolecular layers of water.

**Assumption: Soil Moisture Content**

Uniform distribution with parameters:

| | |
|---|---|
| Minimum | 0.01 |
| Maximum | 0.13 |

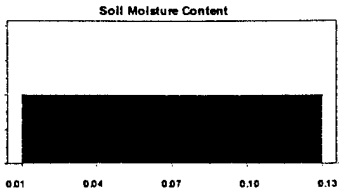


Mean value in simulation was 0.07

Figure 7 shows that most of the forecast values for the soil gas concentration are well below those for the higher moisture content simulation. In addition, the sensitivity analysis (Figure 8) shows that the principal parameter is now the moisture content, as $K'_d(w)$ becomes dominant (equations [9] and [12]).

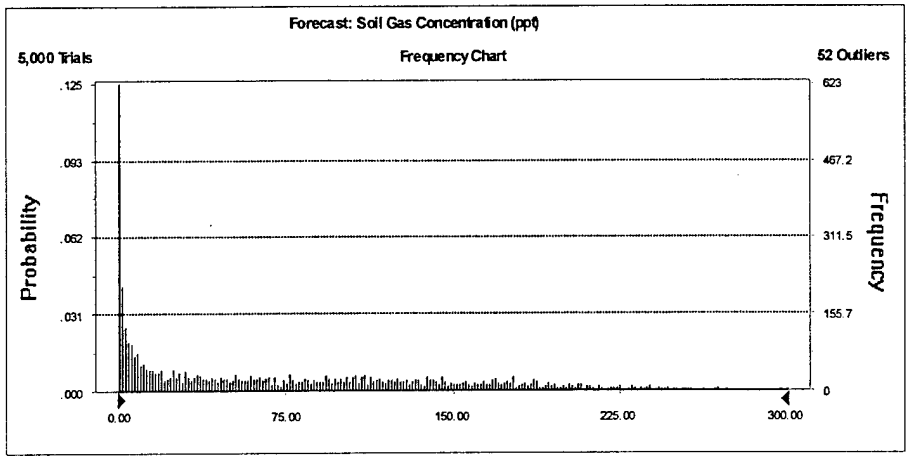


Figure 7. Soil Gas Concentration - Dry

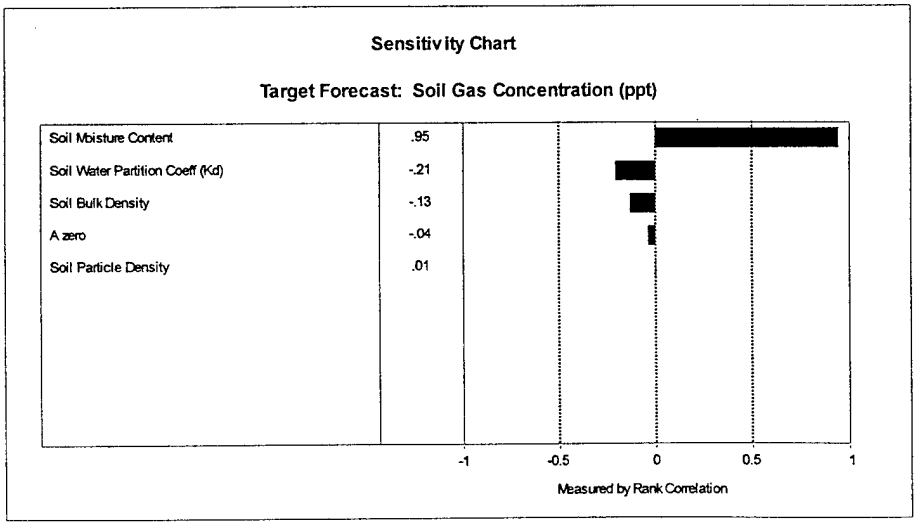


Figure 8. Sensitivity Analysis – Dry

This analysis shows that when employing vapor sniffing chemical sensing technology, optimum conditions would be found when the soils contained more moisture than four monomolecular layers.

***B. 1-Dimensional Transport Sensitivity Analysis***

A one-dimensional model sensitivity analysis was used to examine the impact of changes to a single parameter for a given environmental scenario. The output that was evaluated was the surface vapor flux. The model that was used was the Buried Chemical Model from Jury et al., 1990. This sensitivity analysis was presented in three conference proceedings (Appendix A, B and C) and in a report from Dr. Jury (Appendix D). Table one shows the parameters evaluated and a summary of the impact.

| Parameter | Impact on steady state surface flux |
|---|---|
| Soil Bulk Density | Direct inversely proportional |
| Henry's Law Constant | Directly proportional |
| Soil-Water Partition Coefficient | Direct inversely proportional |
| Source Flux | Insignificant compared to initial surface concentration |
| Initial Surface Concentration | Directly proportional |
| Burial Depth | Increases lag time (very sensitive) |
| Water Flux (Precipitation or Evaporation) | Evaporation enhances, precipitation depresses |
| Biochemical Half-life | Insensitive if > 1 year, very sensitive if < 60 days |

Dr. Bill Jury performed a 2-dimensional analysis, which is included in Appendix E. This showed that the surface vapor flux was greatest directly above a source with a small halo up to twice the length of the buried source. However, the flux drops off exponentially with lateral distance.

***C. Numerical Model Development***

A more detailed mechanistic numerical model is being developed. This model is being based on TOUGH2 (Pruess, 1991) with modifications pertinent to the UXO/landmine application and is called T2TNT. The first round of modifications to TOUGH2 has been completed including:

1. Addition of TNT, DNT, and DNB vapor components – UXO/landmines typically emit TNT, DNT, and DNB vapors. The behavior of each of these chemicals is different (vapor pressure, vapor/liquid, liquid/solid, and vapor/solid partitioning), so each component is modeled separately. Additional components could be added if necessary.
2. Dusty Gas Model for gas diffusion – Gas diffusion can be a dominant transport mode for explosive vapors in the subsurface, especially for low moisture content conditions. In order to mechanistically model gas diffusion in a porous medium, the Dusty Gas Model (Webb, 1998) has been implemented.
3. Liquid diffusion of dissolved explosive gases – Liquid diffusion can be a dominant transport mode for explosive vapors in the subsurface, especially for moderate and high moisture content conditions. Liquid diffusion was not present in the original version of TOUGH2. Liquid diffusion using Fick's Law has been included because of the significant chemical concentration in the liquid phase.

4. Partition coefficient as a function of saturation – The solid partition coefficient may be a strong function of saturation, especially at low moisture content where the partition coefficient may increase dramatically (Petersen, et al. 1995). The capability of including a saturation-dependent partition coefficient has been included.
5. Biodegradation – A simple half-life approach has been implemented to model biodegradation of the explosive vapors.
6. Surface Boundary Conditions – Due to the shallow burial depth of many UXO/landmines, the fluid conditions surrounding the UXO/landmine are strongly influenced by the surface conditions. The parameters necessary to adequately model the surface boundary conditions are numerous, including solar and long-wave radiation, the surface boundary layer which is a function of wind speed and other parameters, precipitation and evaporation at the surface, plants and their root systems, and the diurnal and seasonal variation of these parameters. The models used for these boundary conditions are discussed in more detail below.

The surface boundary conditions discussed above are complex in their own right. Numerous models have been developed to analyze the soil-air-plant system. In order to expedite the inclusion of the important surface conditions into T2TNT, a number of existing models have been evaluated. As a result, the SiSPAT model developed by Braud et al. (1995, 1996) has been selected for inclusion into T2TNT with the kind permission of M. Vauchlin of LTHE in Grenoble, France. Subroutines from SiSPAT have been included directly into T2TNT as necessary.

SiSPAT has been applied to a number of field studies as documented by Braud et al. (1995, 1995), and Boulet et al. (1997), and more are in progress. Therefore, SiSPAT should provide a well-documented and tested approach for modeling the soil-plant-atmosphere interface in the T2TNT code.

At the present time, the surface boundary conditions for a bare soil have been implemented, including the surface boundary layer, solar and long-wave radiation, precipitation, and other conditions including the diurnal and seasonal variation of the parameters. Incorporation of the plant portion of the SiSPAT model into T2TNT is expected in 1999.

As part of the verification process for T2TNT, comparison to results of the one-dimensional screening model presented by Phelan and Webb (1997) have been performed. The conditions are for a low desert environment with moderate moisture content; the parameters are summarized in Table 1 as presented by Phelan and Webb (1997). The precipitation/evaporation cycles have not been included in this simulation in order to provide comparison with the buried chemical analytical solution of Jury et al. (1990).

Note that some of the assumptions made in the analytical model can only be approximated in the numerical code, such as uniform moisture content. In addition, there are differences in the gas diffusion model, which could lead to slightly different answers. However, in general, the analytical and numerical problems are essentially equivalent.

Table 1. Simulation Parameters

| Parameter | units | base case |
|---|---|---|
| $\theta$ | $cm^3/cm^3$ | 0.25 |
| $\phi$ | $cm^3/cm^3$ | 0.434 |
| $\rho_b$ | $g/cm^3$ | 1.5 |
| $K_d$ | $cm^3/g$ | 2.5 |
| $K_H$ | -- | 5.9E-7 |
| air boundary layer | cm | 0.5 |
| $t_{1/2}$ | days | 180 |
| $C_o$ | $\mu g/cm^3$ | 4.6E-3 |
| $J_c$ | $\mu g/cm^2$-day | 8.6E-6 |
| $D_l^w$ | $cm^2$/day | 0.432 |
| $D_g^a$ | $cm^2$/day | 4320 |
| burial depth, top | cm | 5 |
| burial depth, bottom | cm | 15 |

Figure 9 compares the TNT flux at the surface from the analytical solution and from T2TNT. The predicted surface flux values are higher than the analytical solution, especially at smaller times. The difference is due to numerical diffusion of the numerical method and is expected. At longer times, the agreement between the analytical and T2TNT solutions is good.

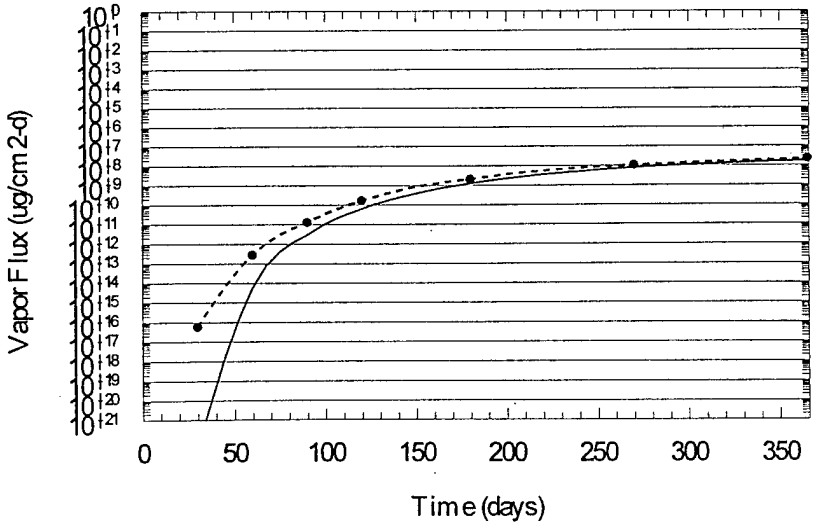


Figure 9. Comparison of TNT surface flux from Analytical and Numerical Models

Figure 10 shows the subsurface distribution of TNT after 1 year for the Jury et al. (1990) model and from T2TNT. The agreement in the concentration distribution is excellent at all locations. Overall, the solution from T2TNT agrees well with the analytical solution of Jury et al. (1990) except for some surface flux differences at early times due to numerical diffusion.

Figure 10. Comparison of Depth Profile from Analytical and Numerical Models

Additional verification and sensitivity studies will be performed with the newly-developed model, including the effect of the boundary layer on the results, drying

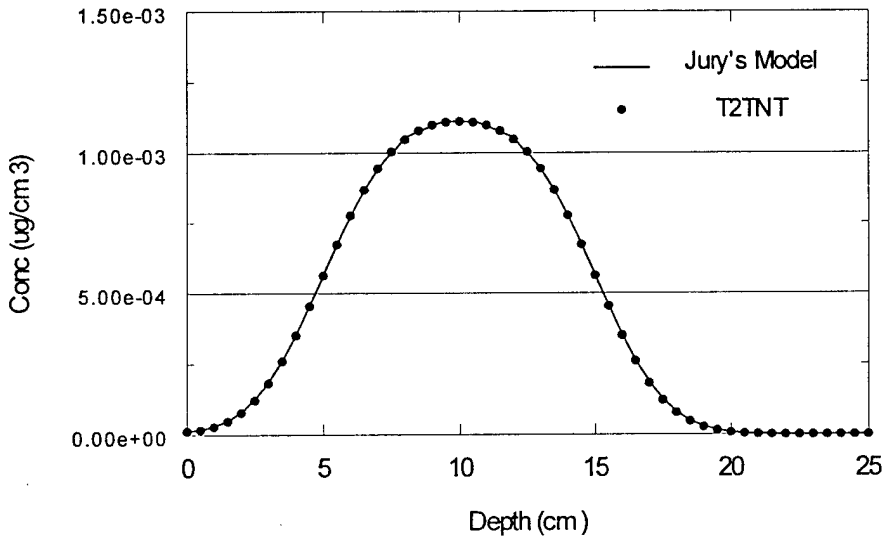


simulations including non-uniform moisture content, diurnal and seasonal variations, and multidimensional effects to determine the degree of lateral spreading including the "footprint" of a landmine.

Task Two – Fundamental Property Measurement

Early on in this project, 2,4-DNT was identified as a potential key chemical constituent that had more favorable properties for chemical detection, than that of 2,4,6-TNT. However, the only water solubility vs. temperature data available was only room temperature. We began to evaluate water solubility with a method called Dynamic Coupled Column Liquid Chromatographic method that was developed at the National Bureau of Standards (now NIST) for polycyclic aromatic hydrocarbons in water (May and Wasik, 1978). The method is based on generating saturated solutions by pumping water through a column packed with glass beads that have been coated with the compound of interest. This method is recommended for low solubility compounds (such as explosives) and can avert problems such as incomplete equilibration of the solid phase in water, avoidance of microcrystals in solution and adsorptive loss on containers, filters and transfers devices. The results from this effort were not satisfactory. The effluent concentration was dependent on the flow rate passing through the column. The results

were not uniform, with some runs showing the concentration to be a positive relationship with flow rate, and others with a negative slope. Our method used a modified dynamic system, which used direct collection of effluent rather than an extractor column as described in the published method. Subsequent to this effort, additional data for 2,4-DNT were located (Army, 1971) and has been used in the modeling efforts. However, this data set is lean and additional effort will be spent to fill in the data gaps.

The literature has shown the importance of vapor-solid sorption for environmental pollutants such as toluene and trichloroethene (Ong et al., 1990). The principal parameter for evaluating this phenomenon is the vapor-solid sorption coefficient (K'd). A method has been developed (Petersen et al., 1988) that is based on the equilibrium partitioning in closed spaces method. Upon closer evaluation of this method for compounds such as 2,4,6-TNT and 2,4-DNT, it was found that it would be physically impossible due to the low vapor densities. In July 1998, the DARPA co-sponsor of this project requested support for field data collection of soil gas concentrations surrounding buried landmines. The vapor-solid sorption coefficient data collection effort was tabled and a change was placed in the September quarterly progress report pushing the milestone to December 30, 1998. After consultation with the USA CRREL, an alternate method has been identified that might be suitable for this measurement. Work is currently in progress to complete this data collection.

As part of this SERDP/DARPA co-funded effort, the U.S. Army Corps of Engineers, Cold Regions Research and Engineering Laboratory has been performing research on the source term from landmine materials and actual landmines. This effort has found that the initial surface concentration of explosives varies widely, but is about the same magnitude as data reported by Hogan, 1992 of about 10 ng/cm$^2$. The source flux values were evaluated by two methods. One is immersion of pieces of the plastic mine case in water and measurement of the concentration in water over time. The other method uses whole landmines in tedlar bags with measurement of the gas and tedlar bag sorbed concentrations after sufficient length of time. The values determined from this effort have shown source flux values up to $10^3$ times greater than that measured by Spangler et al. 1975. Detailed technical reports on this effort will be published by Leggett et al. in the future.

Task Three – Laboratory Scale Experiments

The laboratory scale experiments have been subcontracted to New Mexico Institute of Mining and Technology (NM Tech). This effort is currently on schedule with experimental designs complete. The column testing equipment is being acquired and configured for use starting in February 1999. The basis for the testing will be soil columns with detailed soil moisture monitoring with capability for measurement of surface vapor flux and sorbed soil concentrations.

Task Four – Operational Strategy

No work was scheduled for this task in 1998.

Task Five – Ordnance Source Term

The ordnance source term effort began in September 1998. This effort includes acquisition of live/unfused ordnance (105 mm cartridges, 60 and 81 mm mortars), testing

for external contamination, performing immersion tests to evaluate long term source flux, firing the ordnance into the ground, and performing post-firing long-term source flux. One pallet of each ordnance group (12 individual ordnance items) has been located from a demil account at Redstone Army Depot and is currently in transit to Sandia National Laboratories. Fuses will be obtained that can be disassembled to remove the primary charge. In this way, the fuse impact into soils will be similar to live UXO.

The external swipe tests will be performed in early January 1999 and a six-week long pre-firing immersion test will follow. Careful consideration was taken in the design of the firing of the cartridges and mortars. Damaged explosive devices have severe constraints with transportation on public byways. Therefore, collection of actual UXO from current range cleanup operations and transportation to Sandia National Laboratories was not likely. However, Sandia National Laboratories has the capabilities to fire ordnance into soils, recover the items, and provide on-site transportation.

Two designs were evaluated for firing the ordnance into soils. An above ground soil berm of compacted soil with concrete containment walls was considered; however, consultation with penetrator testing groups at Sandia National Laboratories discouraged this method as containment is typically not guaranteed. Using an Army manual (Technical Manual TM 5-855-1, July 1965), penetration of the 105 mm cartridge is expected to be about 7 to 9 feet at an impact velocity of 800 to 900 fps. A low angle (15 to 20°) shot into native, undisturbed soil with a penetration depth of 20 feet yields a depth below grade of about 10 feet. By probing the soil trajectory path, the angle and total penetration length can be determined, and recovery of the target can be performed with traditional excavation equipment. Explosive Ordnance Disposal trained services area available to recover the fired ordnance. Therefore, a trench will be excavated that will serve as the face for the low angle shot into undisturbed soil.

## List of Symbols

$\rho_b$ – soil bulk density ($g/cm^3$)
$\rho_s$ – soil particle density ($g/cm^3$)
$\rho_w$ – density of water (1.0 $g/cm^3$)
$\theta$ – volumetric moisture content ($cm^3/cm^3$)
w – gravimetric soil moisture content (g/g)
$w_4$ – water content at 4 monomolecular layers of water (g/g)
$\varphi$ – soil porosity ($cm^3/cm^3$)
a – air filled porosity ($cm^3/cm^3$)
$\gamma$ – activity of water (~1)

$C_T$ – Total soil concentration ($g/cm^3$)
$C_S$ – Concentration on solid phase ($g/cm^3$)
$C_L$ – Concentration in soil aqueous phase ($g/cm^3$)
$C_G$ – Concentration in the soil gas ($g/cm^3$)
$C_{SG}$ – Concentration on soil solid phase from vapor sorption ($g/cm^3$)
$C_{SL}$ – Concentration on soil solid phase from liquid sorption ($g/cm^3$)
$R_S$ – Soil solid phase partitioning factor ($g/cm^3$)
$R_G$ – Soil gas phase partitioning factor ($cm^3/cm^3$)
$R_L$ – Soil liquid phase partitioning factor ($cm^3/cm^3$)
$R_{SG}$ – Soil solid-vapor phase partitioning factor ($g/cm^3$)
$R_{SL}$ – Soil solid-liquid phase partitioning factor ($g/cm^3$)

$K_d$ – soil water partition coefficient ($cm^3/g$)
$K_H$ – Henry's Law Constant ($cm^3$,air/$cm^3$,water)
$K_{SG}$ – soil vapor partition coefficient ($cm^3/g$)
K'd – soil vapor partition coefficient ($cm^3/g$)
$A_0$ – log of K'd at oven dry conditions ($cm^3/g$)
$A_4$ – log of K'd at moisture content of 4 monomolecular layers of water
$\beta(w)$ – fitting parameter
$\alpha$ – fitting parameter for $K'_d(w)$
$S_A$ – soil specific surface area ($m^2/g$)
$MW_w$ – molecular weight of water (18 g/mole)
$MA_w$ – molecular area of water (10.8E-20 $m^2$/molecule)
$A_n$ – Avogadro's Number (6.02E23 molec/mole)

## References


[1] Braud, I., A.C. Dantas-Antonino, M. Vauclin, J.L. Thony, P. Ruelle, 1995. A simple soil-plant-atmosphere transfer model (SiSPAT) development and field verification. Journal of Hydrology 166 (1995) 213-250.

[2] Braud, I., 1996, SiSPAT User's Manual – Simple Soil Plant Atmosphere Transfer Model, Version 2.0, LTHE, Grenoble, France.

[3] Boulet, G., I. Braud, and M. Vauclin, 1997. Study of the mechanisms of evaporation under arid conditions using a detailed model of the soil-atmosphere continuum. Application to the EFEDA I experiment. Journal of Hydrology 193 (1997) 114-141.

[4] Farmer, W.J., M.S. Yang, J. Letey, and W.F. Spencer. 1980. Hexachlorobenzene: its vapor pressure and vapor phase diffusion in soil. Soil Sci. Soc. Am. Proc. 44:676-680.

[5] Hogan, A., D. Leggett, T. Jenkins, P. Miyares. 1992. Results of Preliminary Analysis, Surface Contamination of Depot-Stored Land mines, Prepared as a briefing guide for planning DARPA mine detector trials. USACRREL. June 23, 1992. Includes: Test Plan Summary: Sampling of Mine Surfaces to Determine the Extent of Explosive Contamination.

[6] Mayer, R., J. Letey, and W.J. Farmer. 1974. Models for predicting volatilization of soil-incorporated pesticides. Soil Sci. Soc. Am. Proc. 38:563-568.

[7] Jury, W.A., R. Grover, W.F. Spencer, and W. J. Farmer. 1980. Modeling Vapor Lossess of Soil-Incorporated with Triallate. Soil Sci. Soc. of Am. J., 44, 445-50 (May-June 1980).

[8] Jury, W.A., W.F. Spencer, and W.J. Farmer. 1983. Behavior Assessment Model for Trace Organics in Soil: I. Model Description. J. Environ. Qual., Vol 12, no. 4, 558-564.

[9] Jury, W.A., W.J. Farmer, and W.F. Spencer. 1984a. Behavior Assessment Model for Trace Organics in Soil: II. Chemical Classification and Parameter Sensitivity. J. Environ. Qual., Vol. 13, no. 4, 567-572.

[10] Jury, W.A., W.F. Spencer, and W.J. Farmer. 1984b. Behavior Assessment Model for Trace Organics in Soil: III. Application of Screening Model. J. Environ. Qual., Vol 13, no. 4, 573-579.

[11] Jury, W.A., W.F. Spencer, and W.J. Farmer. 1984c. Behavior Assessment Model for Trace Organics in Soil: IV. Review of Experimental Evidence. J. Environ. Qual., Vol 13, no. 4, 580-586.

[12] Jury, W.A., D. Russo, G. Streile, and H. Abd. 1990. Evaluation of Volatilization by Organic Chemicals Residing Below the Surface. Water Resources Research vol 26, no 1, p 13-20, January 1990.

[13] May, W.E. and S.P. Wasik, 1978. Determination of the Aqueous Solubility of Polynuclear Aromatic Hydrocarbons by a Coupled Column Liquid Chromatographic Technique. Analytical Chemistry, Vol. 50, No. 1, January 1978.

[14] Ong, S.K., T.B. Culver, L.W. Lion, and C.A. Shoemaker, 1992. Effects of soil moisture and physical-chemical properties of organic pollutants on vapor-phase transport in the vadose zone. Journal of Contaminant Hydrology, 11(1992) 273-290.

[15] Petersen, L.W., P. Moldrup, Y.H. El-Farhan, O.H. Jacobsen, T. Yamaguchi, and D.E. Rolston, 1995. The Effect of Moisture and Soil Texture on the Adsorption of Organic Vapors. J. Environ. Qual. 24:752-759 (1995).

[16] Phelan, J.M. and S. W. Webb. 1997. Environmental Fate and Transport of Chemical Signatures from Buried Landmines - Screening Model Formulation and Initial Simulations. Sandia National Laboratories, SAND97-1426. June 1997.

[17] Phelan, J.M. and S.W. Webb, 1998. Chemical Detection of Buried Landmines. Proceeding of the 3rd International Symposium on Technology and the Mine Problem, April 6-9, 1998. Mine Warfare Association.

[18] Spangler, G.E.. 1975. Measurements on the Availability of TNT Vapor from Antitank Mines. Report No: MERADCOM-R-2159

[19] Spencer, W.F., M.M. Cliath, W.A. Jury, and L.-Z. Zhang. 1988. Volatilization of Organic Chemicals from Soil as Related to Their Henry's Law Constants. J. Environ. Qual. 17:504-509.

[20] U.S. Army, 1965. Fundamentals of Protective Design (non-nuclear). TM 5-855-1. Headquarters, Department of the Army, July 1965.

[21] U.S. Army, 1971. Engineering Design Handbook: Explosives Series. Properties of Explosives of Military Interest. AMPC 706-177, Headquarters, U.S. Army Material Command, January 1971.

## Appendices

A Phelan, J.M. and S.W. Webb, 1998. Chemical Detection of Buried Landmines. Proceedings of the 3rd International Symposium on Technology and the Mine Problem, April 6-9, 1998. Mine Warfare Association.

B Phelan, J.M. and S.W. Webb, 1998. Simulation of the Environmental Fate and Transport of Chemical Signatures from Buried Landmines. Part of the SPIE Conference on Detection and Remediation Technologies for Mines and Minelike Targets III. Orlando, FL. April 1998.

C Webb, S.W., S.A. Finsterle, K. Pruess, and J.M. Phelan, 1998. Prediction of the TNT Signature from Buried Landmines. Proceedings of the TOUGH '98 Workshop. Berkeley, CA.

D Jury, W.A. and L. Guo, 1998. One Dimensional Transport of Vapor From A Buried Landmine. Project report. University of California, Riverside. July 20, 1998.

E Jury, W.A. and L. Guo, 1998. Two Dimensional Transport of Vapor From A Buried Landmine. Draft project report. University of California, Riverside. September 1, 1998.

# APPENDIX A

Phelan, J.M. and S.W. Webb, 1998. Chemical Detection of Buried Landmines. Proceedings of the 3rd International Symposium on Technology and the Mine Problem, April 6-9, 1998. Mine Warfare Association.

# Chemical Detection of Buried Landmines

James M. Phelan[1] and Stephen W. Webb[2]

Of all the buried landmine identification technologies currently available, sensing the chemical signature from the explosive components found in landmines is the only technique that can classify non-explosive objects from the real threat. In the last two decades, advances in chemical detection methods have brought chemical sensing technology to the foreground as an emerging technological solution. In addition, advances have been made in the understanding of the fundamental transport processes that allow the chemical signature to migrate from the buried source to the ground surface. A systematic evaluation of the transport of the chemical signature from inside the mine into the soil environment, and through the soil to the ground surface is being explored to determine the constraints on the use of chemical sensing technology. This effort reports on the results of simulation modeling using a one-dimensional screening model to evaluate the impacts on the transport of the chemical signature by variation of some of the principal soil transport parameters.

**landmines, chemical sensors, soil transport**

## I. Introduction

The organic chemicals of the explosives in the buried landmine environment can exist in or on four phases: solid phase of the neat explosive material, vapor phase in the soil air, aqueous phase in the soil water solution, and sorbed onto soil solid phases. The chemical signature begins as a surface coating from production or depot storage and through continuous emission by permeation through the mine case or through leaks in seals and seams. Once the chemicals enter the soil environment, they experience phase transitions, partitioning into the soil air, soil water and sorbing onto soil particles. The impact of temperature and chemical gradients, and precipitation/evaporation will cause movement of the chemical signature. Part of this transport is upward to the soil surface where chemical detection technology is envisioned to be used. Simulation modeling is a technique that can evaluate the impacts of many of the environmental variables that can dampen or accentuate the surface expression of the chemical signature. Model results will be shown that describe the magnitude of the changes that accompany variations due to chemical properties of the explosive and properties of the soil environment.

[1] Environmental Restoration Technologies Department,
[2] Mission Analysis and Simulation Department,
at Sandia National Laboratories, Albuquerque, NM.

## II. Chemicals in the Soil Environment

Soils are porous media with a number of physico-chemical properties that affect the transport of explosive chemicals. Soil bulk density is a measure of the compaction of the soil and is defined as

$$\rho_b = \frac{M_s}{V_s} \quad [1]$$

where $\rho_b$ is the soil bulk density (g/cm$^3$), $M_s$ is the mass of soil particles (g), and $V_s$ is the volume of soil (cm$^3$). Soils under natural conditions have bulk densities ranging from 1.0 to 1.8 g/cm$^3$. However, soils that have been excavated and replaced, such as during the emplacement of a landmine, may have bulk densities much less than 1. The soil bulk density is inversely proportional to the soil porosity as follows

$$\phi = 1 - \rho_b / \rho_s \quad [2]$$

where $\rho_s$ is the soil particle density (ranges from 2.6 to 2.8 g/cm$^3$ for most soils). The soil porosity, or void volume, is defined as

$$\phi = \frac{V_w + V_a}{V_s} \quad [3]$$

where $\phi$ is the soil porosity (cm$^3$/cm$^3$), $V_w$ is the volume of soil water (cm$^3$) and $V_a$ is the volume of soil air (cm$^3$). Soil porosity values range from 0.3 for sands to 0.6 for clay rich soils. The volumetric moisture content describes how much water is present in the soil and changes greatly during precipitation/drainage events and evaporation conditions. Volumetric water content is defined as

$$\theta = \frac{V_w}{V_s} \quad [4]$$

where $\theta$ is the volumetric water content (cm$^3$/cm$^3$). Soil moisture contents have values from near zero up to the soil porosity value. When the soils are not fully saturated, the balance of the soil pore space not filled with water is termed the air filled porosity, and is defined as

$$a = \frac{V_a}{V_s} \quad [5]$$

where $V_a$ is the volumetric air content (cm$^3$/cm$^3$).

It is often more convenient to use soil saturation ($S_l$) because it is a measure of the relative saturation of a particular soil pore space with water.

$$S_l = \frac{\theta}{\phi} \qquad [6]$$

Since the explosive chemicals can exist as solutes in the soil water and the movement of soil water can be a significant transport mechanism, water solubility is an important parameter. Water solubility is defined as

$$C_L = \frac{M_{chem}}{V_w} \qquad [7]$$

where $C_L$ is the concentration in aqueous phase ($g/cm^3$ soil water) and $M_{chem}$ is the mass of chemical (e.g. TNT) (g). Water solubility, however, is not constant and is typically an increasing function with temperature.

Henry's Law constant is a relative measure of the amount of the chemical that exists in the gas phase to that in the aqueous phase at equilibrium, and is defined as

$$K_H = \frac{C_G}{C_L} \qquad [8]$$

where $K_H$ is the Henry's Law constant (unitless) and $C_G$ is the concentration in gas phase (g/cm3 soil gas). Henry's Law constant is also a function of temperature because both $C_G$ and $C_L$ are functions of temperature.

The soil partition coefficient is a relative measure of how much of the chemical is temporarily bound to the soil to that in the soil aqueous phase

$$K_d = \frac{C_S}{C_L} \qquad [9]$$

where $K_d$ is the linear soil-water partition coefficient ($cm^3/g$) for water saturated soils and $C_S$ is the concentration sorbed on the soil solid phase (g/g of soil).

The soil water partition coefficient is often correlated with the fraction of organic carbon found in the soils. In this way, the variability between soils can be reduced. The organic carbon distribution coefficient is defined as

$$K_{oc} = \frac{K_d}{f_{oc}} \qquad [10]$$

where $K_{oc}$ is the organic carbon distribution coefficient and $f_{oc}$ is the fraction of organic carbon.

## III. Physical Chemical Properties of Explosives

The principal explosive chemicals found in landmines are TNT and RDX (NGIC, 1995). DNT, as a production by-product of TNT, is also considered to be a significant signature chemical for buried landmines. As a group, these chemicals have very low vapor densities and moderately low water solubilities. Table 1 shows these properties and the Henry's Law constant at 20°C (Phelan and Webb, 1997).

Table 1. Vapor Density, Water Solubility and Henry's Law Constant of Explosive Compounds at 20°C

| | TNT | DNT | RDX |
|---|---|---|---|
| Vapor Density ($\mu g/m^3$) | 43.5 | 122 | 0.024 |
| Water Solubility (mg/l) | 130 | 270 | 50 |
| Henry's Law Constant | 3.35E-7 | 4.51E-7 | 4.73E-10 |

Pennington and Patrick (1990) measured the soil water partition coefficient ($K_d$) of TNT in fourteen soils from locations across North America. The mean value was 3.8 $cm^3/g$ with a standard deviation of 1.34. The highest value was 6.8 $cm^3/g$ and the lowest value was 2.3 $cm^3/g$. Xue et al. (1995) evaluated two soils and showed mean values for TNT of 2.66 $cm^3/g$ and 3.64 $cm^3/g$. DNT and RDX have very little data. Xue et al. (1995) showed values for RDX of 1.59 $cm^3/g$ and 1.57 $cm^3/g$. McGrath (1995) showed a $K_{oc}$ value of 251 for DNT. For the fourteen soils evaluated by Pennington and Patrick (1990), the mean value for the fraction of organic carbon was 0.0173 with a standard deviation of 0.011. Using these values, the $K_d$ for DNT has a mean value of $4.4 \pm 2.7$ $cm^3/g$ (one std. dev.). In summary, the soil water partitioning coefficients for TNT, DNT and RDX all fall into an approximate range between 1.5 and 7.0 $cm^3/g$. This is a rather narrow range as common chemicals can have values one to two orders of magnitude lesser and greater than these.

The biochemical half-life of explosives in near surface soils has not been studied well outside of the biotreatment technology area for contaminated soils. However, long-term surface soil degradation tests at Los Alamos National Laboratory (LANL) followed the degradation of soils doped with 1000 mg/kg of various explosives over 20 years (Dubois and Baytos, 1991). Table 2 shows the half-lives estimated from these long-term experiments.

Table 2. Estimates of Half-Lives of Explosives from LANL Long-Term Surface Soil Tests

| Explosive | Half-Life (years) |
|---|---|
| TNT | 1 |
| RDX | 36 |
| HMX | 39 |
| PETN | 92 |

## IV. Screening Model

The environmental fate and transport of organic chemicals including volatilization and leaching losses has been used to explore the distribution of agricultural pesticides in soils (Mayer et al. 1974, Farmer et al. 1980, and Jury et al. 1980). These models were primarily intended to simulate specific circumstances. However, Jury et al. (1983, 1984a, 1984b, 1984c) developed and validated a general screening model (Behavior Assessment Model, BAM) that included volatilization, leaching, and degradation to explore the major loss pathways of agricultural pesticides as a function

of specific environmental conditions. The model simulations can be used to assess the behavior of different chemicals under particular environmental conditions, but is not intended to predict a definitive concentration distribution in the field. As such, the predictions from the screening model are only an indication of expected conditions.

This model is valuable in that it can express the total concentration of a chemical in the gas, aqueous and sorbed phases. The total concentration is expressed as

$$C_T = \rho_b C_S + \theta C_L + a C_G \qquad [11]$$

where $C_S$ is the concentration sorbed to the soil, $C_L$ is the solute concentration in the aqueous phase, and $C_G$ is the gas phase concentration. In addition, Jury (1983) shows how equation [11] can be rewritten in terms of one of the variables alone

$$C_T = R_S C_S = R_L C_L = R_G C_G \qquad [12]$$

where

$$R_S = \rho_b + \frac{\theta}{K_d} + a\frac{K_H}{K_d} \qquad [13]$$

$$R_L = \rho_b K_d + \theta + a K_H, \text{ and} \qquad [14]$$

$$R_G = \rho_b \frac{K_d}{K_H} + \frac{\theta}{K_H} + a \qquad [15]$$

are the solid, liquid and gas phase partition coefficients, respectively.

An adaptation of the BAM was developed to be applicable to the conditions of contaminated soil buried under a known depth of clean soil - Buried Chemical Model, BCM (Jury et al., 1990). Simulations based on a modification of Jury's BCM are used in this report to simulate the behavior of the chemical signature from buried landmines. The Buried Chemical Model of Jury et al. (1990) is based on the following assumptions. A detailed discussion of these assumptions is given in Jury et al. (1990).

1. The chemical may adsorb on the solid phase, be dissolved in the aqueous phase, or exist in the vapor phase.
2. The chemical flux is the sum of the vapor flux and the dissolved solute flux using Fick's law.
3. The porous medium factors for gas and liquid phase diffusion are given by the Millington and Quirk (1961) model as extended for liquid diffusion by Jury et al. (1983).
4. The chemical will undergo first-order degradation due to biological and chemical effects.
5. Chemical movement is one dimensional.
6. The adsorbed and dissolved phases undergo reversible, linear adsorption.
7. The dissolved and gaseous phase concentrations are related through Henry's law.
8. The soil properties are constant in space and time.
9. Water flux is constant in space and time (relaxed in the present application).
10. Volatilization of the chemical to the atmosphere is by vapor diffusion through an air boundary layer of constant thickness.

In the present implementation of Jury's model, a constant source term has been added to reflect the chemical source from the landmine at a specific location.

Under these assumptions (including the source term) the model formulation becomes

$$\frac{\partial C_T}{\partial t} + \mu C_T = D_E \frac{\partial^2 C_T}{\partial z^2} - V_E \frac{\partial C_T}{\partial z} + \sigma \qquad [16]$$

where $C_T$ is the total chemical concentration, $\mu$ is the bio-chemical decay constant, and $\sigma$ is the source term. The effective velocity ($V_E$) is defined as

$$V_E = \frac{J_w}{\rho_b K_d + \theta + a K_H} \qquad [17]$$

where $J_w$ is the precipitation/evaporation flux. The effective diffusion coefficient ($D_E$) of the chemical is defined as

$$D_E = \frac{a^{10/3} K_H D_g^a + \theta^{10/3} D_l^w}{\phi^2 \left(\rho_b K_d + \theta + a K_H\right)} \qquad [18]$$

where $D_g^a$ is the diffusivity of the gas phase of the chemical in air and $D_l^w$ is the diffusivity of the chemical in aqueous phase . The boundary conditions for the problem are diffusion through a boundary layer at the upper surface, and a zero chemical concentration at infinity at the lower boundary. These boundary conditions can be expressed as

$$-D_E \frac{\partial C_T}{\partial z} + V_E C_T = -H_E C_T \qquad [19]$$

where

$$H_E = \frac{h K_H}{\rho_b K_d + \theta + a K_H} \qquad [20]$$

and

$$h = \frac{D_g^a}{d} \qquad [21]$$

and

$$C_T(\infty, t) = 0.$$

The initial conditions are an initial concentration, $C_0$, over an interval from L to W, or

$$C_T(z,0) = 0 \qquad L \rangle z \rangle W$$
$$C_T(z,0) = C_0 \qquad L \le z \le W$$

The above model results in a closed form solution as a function of space and time; the results are rather lengthy and will not be presented here but are given by Jury et al. (1983, 1990). In the present simulation, the assumption of constant water flux in time will be relaxed. Therefore, sequences of water fluxes representing desired conditions (rainfall followed by evaporation) can be simulated to determine the effect of water flux variations on the location of TNT in the soil and the surface TNT vapor flux. A numerical solution was developed and verified by comparison to the results given by Spencer et al. (1988) and Jury et al. (1990) (Phelan and Webb, 1997).

Using this solution, simulations were performed using a landmine that has contributed an initial soil concentration ($C_o$) based on the surface contamination of the landmine. It has been assumed that the entire surface contamination was completely and uniformly transferred to the soil just prior to the beginning of the simulation runs. Surface contamination data (Hogan et al., 1992) showed a median surface contamination of 15 ng/cm$^2$ from 42 domestic and foreign landmines. Using the dimensions of an anti-tank (AT) mine of 30 cm diameter by 10 cm high, the surface contamination would provide $3.5 \times 10^{-5}$ g of TNT for initial distribution in the soil. Using the volume of the AT mine that this mass of TNT is distributed into, the initial concentration ($C_o$) would be ~$5 \times 10^{-3}$ µg/cm$^3$.

The constant source term emanation rate was derived from vapor collection chamber experiments on two mines (Spangler, 1975). Values ranged from $10^{-16}$ to $10^{-18}$ g/cm$^2$-s. The higher rate of $10^{-16}$ g/cm$^2$-s ($8.6 \times 10^{-6}$ µg/cm$^2$-day) was used in these simulations. If the top of the AT mine was buried at a depth of 10 cm, the burial zone of the initial contamination is from 10 to 20 cm, and the constant source term is placed at a depth of 15 cm.

The diffusivity of gas in air ($D_g^a$) and diffusivity of liquid in water ($D_l^w$) were selected from Jury et al. (1983). The biochemical half-life value of 365 days was selected from a long term field experiment (Dubois and Bayton, 1991).

The precipitation/evaporation rates and periods followed in all the simulations here were the low desert scenario from Phelan and Webb (1997). This scenario was derived from data found in HELP (Hydrological Evaluation of Landfill Performance) model (Schroeder et al., 1994a and 1994b). . The HELP model showed that the low desert had 1 day of precipitation followed by 7 days of evaporation. For simplicity, total precipitation and total evaporation for each cycle are assumed to be equal and for these simulations the cycles were continued for approximately four to ten years.

Table 2 shows the input parameters used in the simulations.

Table 2. Simulation Parameters

| parameter | units | base case | variant cases |
|---|---|---|---|
| $\theta$ | cm$^3$/ cm$^3$ | 0.25 | 0.375 |
| $\phi$ | cm$^3$/ cm$^3$ | 0.5 | * |
| $\rho_b$ | g/cm$^3$ | 1.5 | * |
| $K_d$ | cm$^3$/g | 1.6 | 3.8<br>6.0 |
| $K_H$ | -- | 5.9E-7 | 4.73E-10 |
| air boundary layer | cm | 0.5 | * |
| $t_{1/2}$ | days | 365 | 180<br>60 |
| $C_o$ | µg/cm$^3$ | 4.6E-3 | 0 |
| $J_c$ | µg/cm$^2$-day | 8.6E-6 | 0 |
| $D_l^w$ | cm$^2$/day | 0.432 | * |
| $D_g^a$ | cm$^2$/day | 4320 | * |
| burial depth, top | cm | 10 | * |
| burial depth, bottom | cm | 20 | * |
| cycles/yr | -- | 45 | * |
| precipitation | days | 1 | * |
| evaporation | days | 7 | * |
| precipitation rate | cm/day | 0.44 | * |
| evaporation rate | cm/day | - 0.063 | * |
| total precipitation/ evaporation | cm/year | 20 | * |

* - same as the base case

## V. Discussion

For each of the figures shown, there is a distinct oscillation of the surface vapor flux. This feature is a result of the cycling of precipitation and evaporation. To evaluate the effect of the Henry's Law constant, two simulations were performed where all parameters were kept constant with one case using a $K_H$ equal to that of TNT and one for RDX (both at 20°C). Figure 1 shows the results and indicate that the TNT surface vapor flux would be expected to reach a greater steady state value than RDX, approximately proportional to the ratio of Henry's Law constants. For TNT, a temperature increase from 0°C to 40°C will increase the $K_H$ value by a factor of about 100. It appears that seasonal and diurnal soil temperature changes could

make a significant effect on the subsurface transport and surface flux of explosive signatures.

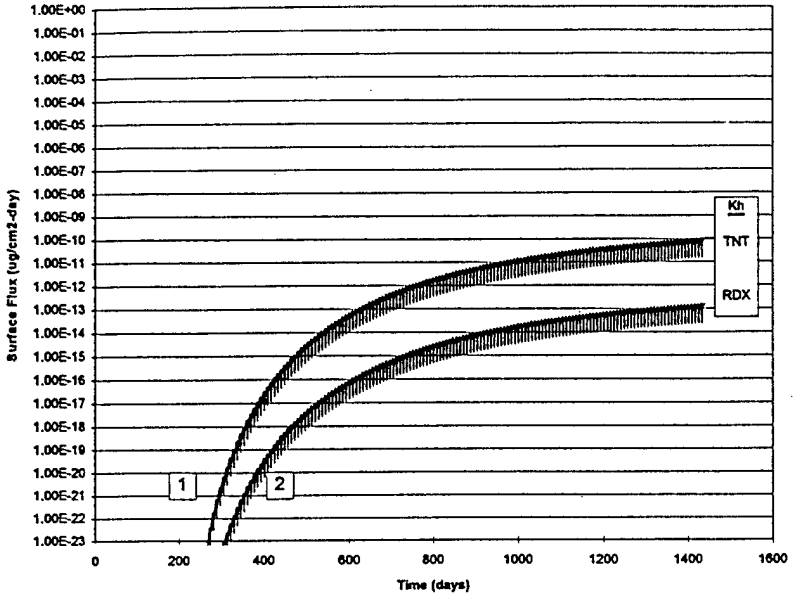


Figure 1. Effect of Henry's Law Constant on Surface Vapor Flux

Depth concentration profiles at the end of the simulation period show that for both cases the concentration of TNT and RDX are essentially equal. This implies that most of the transport upward to the ground surface is within the aqueous phase and that the release of the chemical into the vapor phase above the ground surface is directly proportional to the Henry's Law constant.

Next, simulations were performed to evaluate small changes in the soil water partitioning coefficient. The $K_d$ values for TNT, DNT and RDX have values from about 1.5 to 7. Figure 2 shows the surface flux over time for $K_d$ values of 1.6, 3.8 and 6.0 $cm^3/g$.

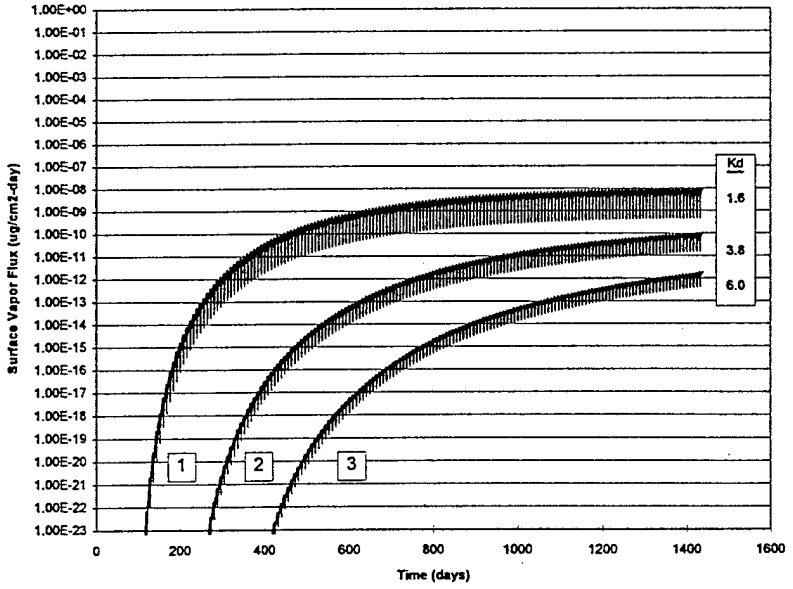


Figure 2. Effect of Soil Water Partitioning Coefficient on Surface Vapor Flux

These simulations show that even though the soil water partitioning coefficients appear to vary only slightly among many soils, there is a significant impact to the transport of the chemical to the ground surface. As the $K_d$ value increases, the lag period becomes much longer and the steady state concentrations stabilize at much lower levels. Also with the lower $K_d$ values, the effect of precipitation/ evaporation cycles becomes more pronounced. This is consistent with the lower $K_d$ value, since more of the mass of the chemical is found in the aqueous phase and is

affected by the upward and downward flux of water. Figure 3 shows the depth profiles from the simulations varying the soil water partitioning coefficients. These curves show that the simulations with lower $K_d$ values have more significant transport of the chemicals to soils both above and below the source zone than the higher $K_d$ values.

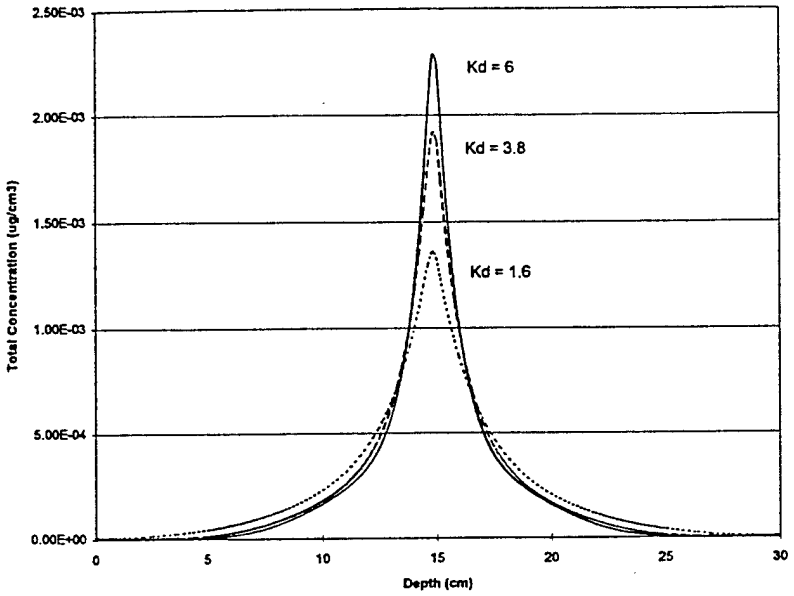


Figure 3. Depth Profile After 4 Years With Variant $K_d$ Values

The next simulations were an evaluation of the source term parameters. Very little data is available on the initial concentration of explosives coating the outer surface of a mine and even less so on the surface emission flux. Figure 4, curve one shows the effect of reducing the surface emission flux to essentially zero (a value of 1E-20 ug/cm2-day was used). This curve is essentially the same as curve one in Figure 1 where the surface emission flux ($J_c$) was equal to 8.6E-6 ug/cm2-day. This implies that the surface emission flux makes very little contribution to the overall mass transport in the soil. If one considers the total mass of explosive contributed by the initial concentration (35 ug) and the amount from the surface emission flux (0.02 ug/day), it would take about 4.8 years for the total mass of explosive from the surface emission flux to equal the amount from the initial surface contamination. Curve two in Figure 4 shows the effect where the initial concentration on the mine is essentially zero (a value of 1E-20 ug/cm3 was used). This shows a significantly longer lag time and about four orders of magnitude lower steady state surface vapor flux at the end of the simulation period. Figure 4 indicates that the initial concentration is a much more important parameter than the surface flux for the mass transport of chemicals to the ground surface.

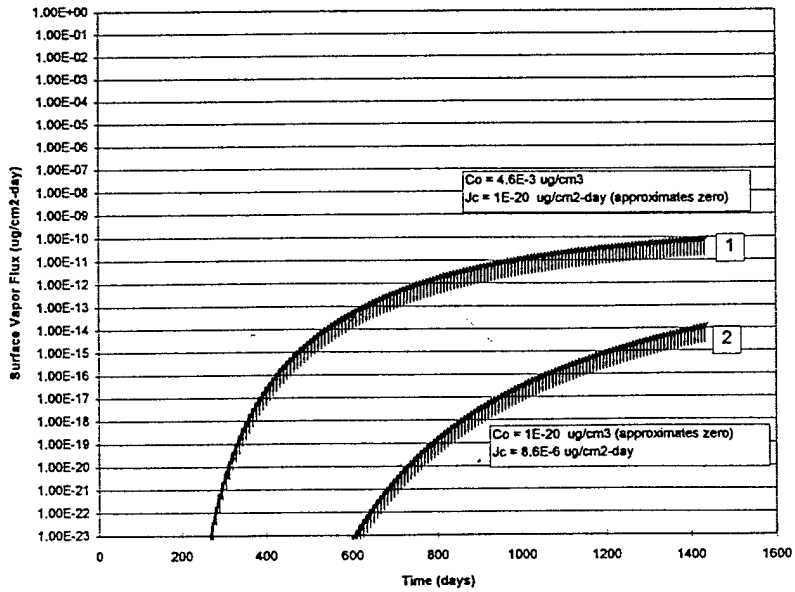


Figure 4. Effect of Source Term Variation on Surface Vapor Flux

Figure 5 shows the cases where the initial concentration is increased by a factor of 10 (curve 2) and a factor of 10E+5 (curve 1) over the base case (curve 3). These simulations show that the lag period remains about the same; however, the increase in steady state flux is proportional to the increase in initial concentration ($C_0$).

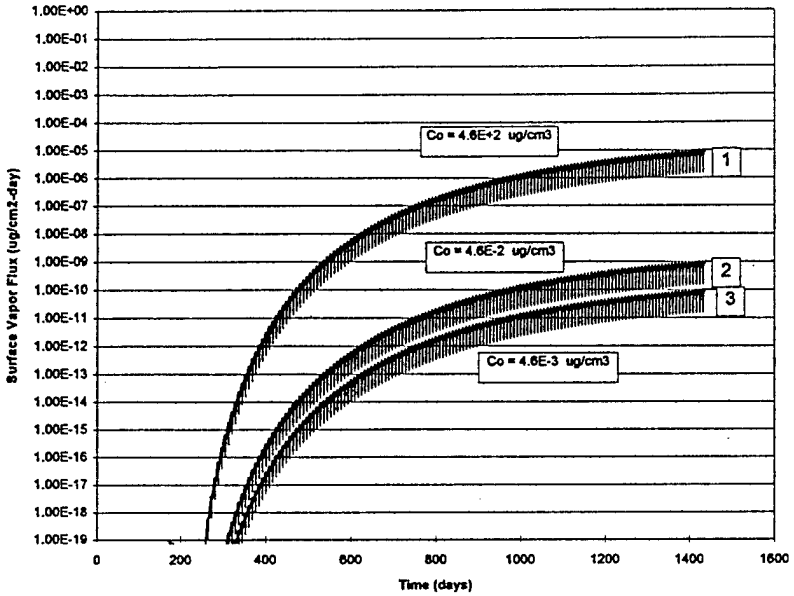


Figure 5. Effect of Source Term Variation on Surface Vapor Flux

Another parameter where there is very little data is the biochemical half life ($t_{1/2}$). There are many influences on the magnitude of this parameter and the variability is expected to be large. Simulations over ten (10) years were completed to assess the impact of decreases in the biochemical half-life from 365 days (curve 1) to 180 days (curve 2). Figure 6 shows that over the long-term, the shorter half-life will significantly decrease the steady state surface flux. Biochemical decay constants that are very large (e.g. RDX values over 30 years) appears to have minimal impact to the short term soil transport phenomena evaluated in these simulations.

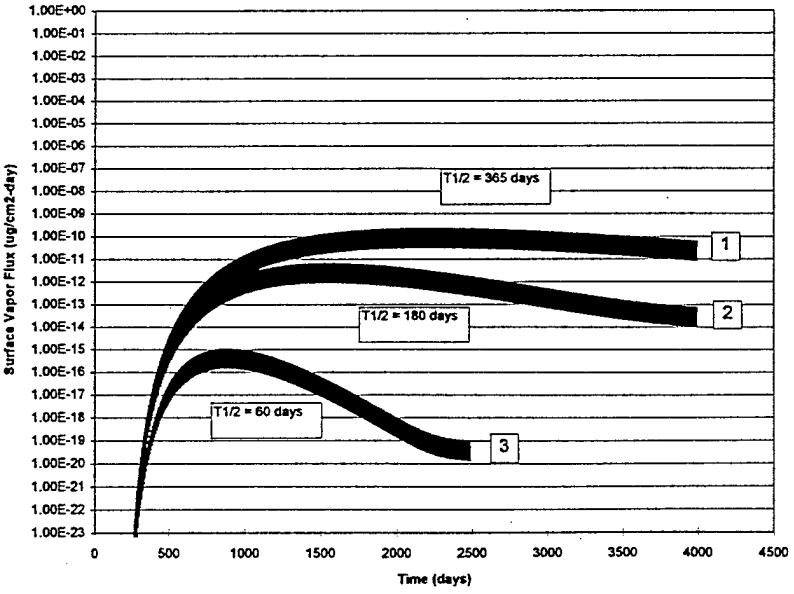


Figure 6. Effect of Half-Life on Surface Flux

Initial simulations using this approach showed that for a particular scenario, the constant moisture content value had a significant impact on the lag period (when the vapor flux reached the ground surface) and the steady state concentrations (Phelan and Webb, 1997). Higher moisture contents showed significantly shorter lag periods and greater steady state concentrations. Figure 7 shows how increasing the soil saturation from 0.5 to 0.75, decreases the

lag period substantially and increases the steady state surface flux by two orders of magnitude. The constant moisture content assumption in this screening model allows for a simplified mathematical solution to complex transport phenomena. One must recognize this assumption and not over generalize the information gleaned from these simulations. Future efforts will include the development of a numerical simulation capability that can explore the transport phenomena of chemical signatures from buried landmines in more detail and with fewer simplifying assumptions.

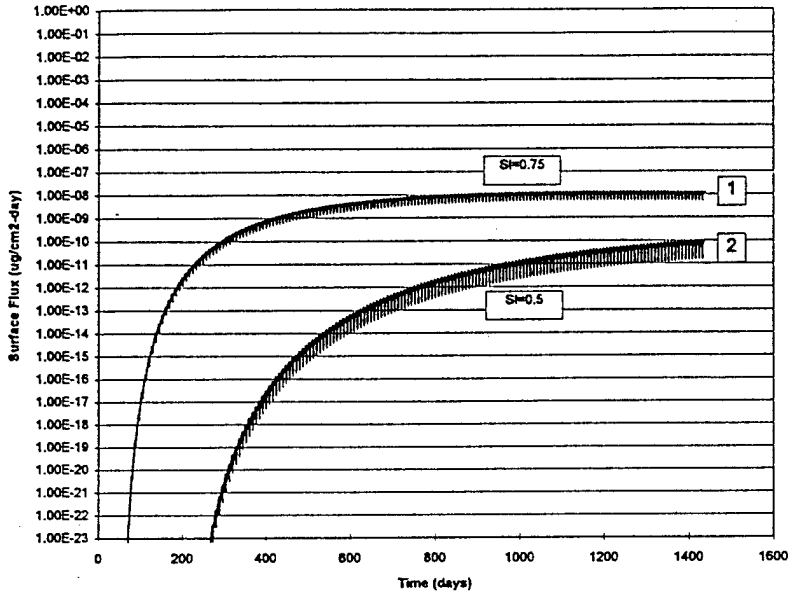


Figure 7. Effect of Soil Moisture Content on Surface Flux

In some parts of the world, minefields are located in areas that experience very distinct wet and dry climatic periods. Figure 8 shows the result of a simulation to assess the effect of a short-term continuos precipitation period followed by a short-term evaporation period. The baseline simulation (Figure 1, curve 1) was run for 1440 days followed by 1 cm/day of precipitation for 30 days which was then followed by -0.5 cm/day of evaporation for 60 days. This shows the immediate drop in the steady-state surface flux after precipitation begins. Once the evaporation period begins, there is a short lag period where the surface vapor flux stays nearly constant before rising to just above the flux before the precipitation began.

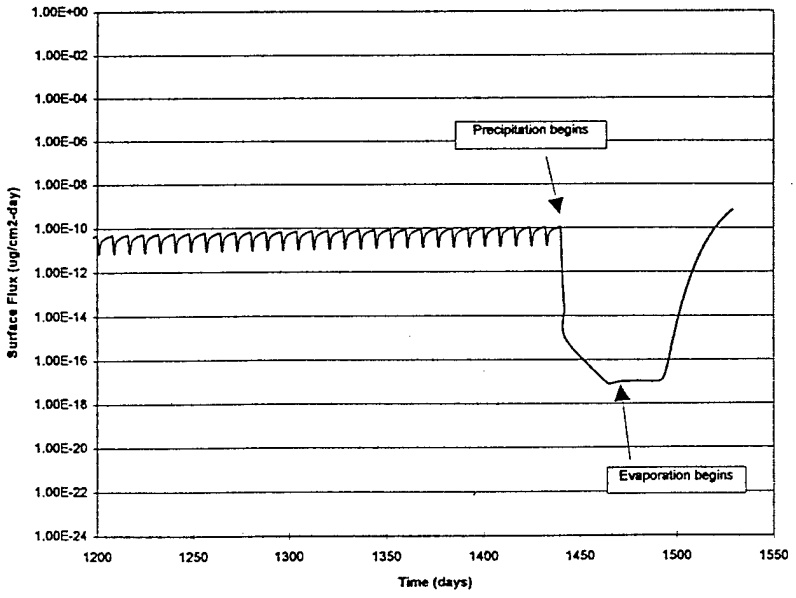


Figure 8. Effect of Continuous Precipitation Followed by Continuous Evaporation

## VI. SUMMARY

The detection of buried landmines has become a significant challenge to the technical community. The challenges of locating a buried object in near surface soils have driven the need for technology from traditional geophysical sensor systems to those looking for the chemical signatures of the explosives derived from within the landmine. The transport of the chemicals found in the explosive charge through soils is a complex process involving phase changes, interactions with the soils, and biochemical reactions.

An investigation with computational simulation was initiated to explore the impacts of several of the various input parameters with a pesticide screening model adapted to the landmine chemical sensing problem. It was found that the variations in the Henry's Law constant are directly proportional to the changes seen in the steady-state surface vapor flux. Small changes in the soil water partitioning coefficient made large changes in the lag period and steady-state surface vapor flux. The initial source term and continuous source flux of chemicals from the landmines is poorly understood and expected to be highly variable. These simulations found that with the baseline case, if the continuous source flux was absent, there was no significant difference in the surface vapor flux or subsurface distribution at the end of the simulation period. This implies that the continuous source flux may be much less important than the initial surface contamination. It appears that the magnitude of the surface vapor flux is directly proportional to the amount of the initial surface contamination. The biochemical half-life is another parameter that is likely to have very different values depending on the location and climatic conditions. Simulations over ten years showed that the steady state surface vapor flux declines steadily when the biochemical half-life becomes smaller than one year. Finally, the importance of heavy precipitation (such as a monsoon season) followed by a dry season was explored. The impact of the heavy precipitation was to lower the surface flux seven orders of magnitude; however, the evaporation period that followed returned the surface flux to approximately the pre-monsoon surface flux.

## VII. ACKNOWLEDGMENT

This work was performed with internal laboratory-directed research and development funds to explore applications for miniaturized chemical sensors. Follow-on work to develop a numerical model is just beginning with funds from the Strategic Environmental Research and Development Program (SERDP) for UXO and from the Defense Advanced Research Projects Agency (DARPA) for landmines. Sandia is a multiprogram laboratory operated by Sandia Corporation, a Lockheed Martin Company, for the United States Department of Energy under Contract DE-AC04-94AL85000.

[1] DuBois, F.W. and J. F. Baytos. 1991. Weathering of Explosives for Twenty Years. Los Alamos National Laboratory, Report LA-11931.

[2] Farmer, W.J., M.S. Yang, J. Letey, and W.F. Spencer. 1980. Hexachlorobenzene: its vapor pressure and vapor phase diffusion in soil. Soil Sci. Soc. Am. Proc. 44:676-680.

[3] Hogan, A., D. Leggett, T. Jenkins, P. Miyares. 1992. Results of Preliminary Analysis, Surface Contamination of Depot-Stored Land mines, Prepared as a briefing guide for planning DARPA mine detector trials. USACRREL. June 23, 1992. Includes: Test Plan Summary: Sampling of Mine Surfaces to Determine the Extent of Explosive Contamination.

[4] Mayer, R., J. Letey, and W.J. Farmer. 1974. Models for predicting volatilization of soil-incorporated pesticides. Soil Sci. Soc. Am. Proc. 38:563-568.

[5] Jury, W.A., R. Grover, W.F. Spencer, and W. J. Farmer. 1980. Modeling Vapor Lossess of Soil-Incorporated with Triallate. Soil Sci. Soc. of Am. J., 44, 445-50 (May-June 1980).

[6] Jury, W.A., W.F. Spencer, and W.J. Farmer. 1983. Behavior Assessment Model for Trace Organics in Soil: I. Model Description. J. Environ. Qual., Vol 12, no. 4, 558-564.

[7] Jury, W.A., W.J. Farmer, and W.F. Spencer. 1984a. Behavior Assessment Model for Trace Organics in Soil: II. Chemical Classification and Parameter Sensitivity. J. Environ. Qual., Vol. 13, no. 4, 567-572.

[8] Jury, W.A., W.F. Spencer, and W.J. Farmer. 1984b. Behavior Assessment Model for Trace Organics in Soil: III. Application of Screening Model. J. Environ. Qual., Vol 13, no. 4, 573-579.

[9] Jury, W.A., W.F. Spencer, and W.J. Farmer. 1984c. Behavior Assessment Model for Trace Organics in Soil: IV. Review of Experimental Evidence. J. Environ. Qual., Vol 13, no. 4, 580-586.

[10] Jury, W.A., D. Russo, G. Streile, and H. Abd. 1990. Evaluation of Volatilization by Organic Chemicals Residing Below the Surface. Water Resources Research vol 26, no 1, p 13-20, January 1990.

[11] McGrath, C. 1995. Review of Formulations for Processes Affecting the Subsurface Transport of Explosives. US Army Corps of Engineers, Waterways Experiment Station, Technical Report IRRP-95-2, August 1995.

[12] Millington, R.J., and J.M. Quirk. 1961. Permeability of porous solids. Trans. Faraday Soc., 57:1200-1207.

[13] NGIC. 1995. Landmines and Demining: A Global Problem CD-ROM. National Ground Intelligence Center, Charlottesville, VA.

[14] Pennington, J.C. and W.H. Patrick. 1990. Adsorption and desorption of 2,4,6-trinitrotoluene by soils. J. Environ. Qual. 19:559-567.

[15] Phelan, J.M. and S. W. Webb. 1997. Environmental Fate and Transport of Chemical Signatures from Buried Landmines - Screening Model Formulation and Initial Simulations. Sandia National Laboratories, SAND97-1426. June 1997.

[16] Schroeder, P.R., C.M. Lloyd, and P.A. Zappi. 1994a. The Hydrological Evaluation of Landfill Performance (HELP) Model User's Guide for Version 3. EPA/600/R-94/168a. U.S. Environmental Protection Agency, Risk Reduction Engineering Laboratory, Cincinnati, Ohio.

[17] Schroeder, P.R., T.S. Dozier, P.A. Zappi, B.M. McEnroe, J.W. Sjostrom, and R.L. Peyton. 1994b. The Hydrological Evaluation of Landfill Performance (HELP) Model: Engineering Documentation for Version 3. EPA/600-R-94/168b. U.S. Environmental Protection Agency, Risk Reduction Engineering Laboratory, Cincinnati, Ohio.

[18] Spangler, G.E.. 1975. Measurements on the Availability of TNT Vapor from Antitank Mines. Report No: MERADCOM-R-2159

[19] Spencer, W.F., M.M. Cliath, W.A. Jury, and L.-Z. Zhang. 1988. Volatilization of Organic Chemicals from Soil as Related to Their Henry's Law Constants. J. Environ. Qual. 17:504-509.

[20] Xue, S.K., I.K. Iskandar, and H.M. Selim. 1995. Adsorption-Desorption of 2,4,6-Trinitrotoluene and Hexahydro-1,3,5-Trinitro-1,3,5-Triazine in Soils. Soil Science, Vol. 160, No. 5. November 1995.

# APPENDIX B

Phelan, J.M. and S.W. Webb, 1998. Simulation of the Environmental Fate and Transport of Chemical Signatures from Buried Landmines. Part of the SPIE Conference on Detection and Remediation Technologies for Mines and Minelike Targets III. Orlando, FL. April 1998.

# Simulation of the Environmental Fate and Transport of Chemical Signatures from Buried Landmines

James M. Phelan[a] and Stephen W. Webb[b]

Sandia National Laboratories, [a]Environmental Restoration Technologies Department and [b]Mission Analysis and Simulation Department, Albuquerque, NM 87185

## ABSTRACT

The fate and transport of chemical signature molecules that emanate from buried landmines is strongly influenced by physical chemical properties and by environmental conditions of the specific chemical compounds. Published data have been evaluated as the input parameters that are used in the simulation of the fate and transport processes. A one-dimensional model developed for screening agricultural pesticides was modified and used to simulate the appearance of a surface flux above a buried landmine and estimate the subsurface total concentration. The physical chemical properties of TNT cause a majority of the mass released to the soil system to be bound to the solid phase soil particles. The majority of the transport occurs in the liquid phase with diffusion and evaporation driven advection of soil water as the primary mechanisms for the flux to the ground surface. The simulations provided herein should only be used for initial conceptual designs of chemical pre-concentration subsystems or complete detection systems. The physical processes modeled required necessary simplifying assumptions to allow for analytical solutions. Emerging numerical simulation tools will soon be available that should provide more realistic estimates that can be used to predict the success of landmine chemical detection surveys based on knowledge of the chemical and soil properties, and environmental conditions where the mines are buried. Additional measurements of the chemical properties in soils are also needed before a fully predictive approach can be confidently applied.

Keywords: Mine detection, chemical sensing, soil transport, computational simulation

## 1. INTRODUCTION

The goal of locating buried landmines is a significant challenge to science and technology (Dugan, 1996). The chemical signature of landmines is affected by multiple environmental phenomena that can enhance or reduce its presence and transport, and can affect the distribution of the chemical signature in the environment. For example, the chemical can be present in the vapor, aqueous, and solid phases. The distribution of the chemical among these phases, including the spatial distribution, is key in designing appropriate detectors, e.g. gas, aqueous or solid phase sampling instruments, and their optimum use. A fundamental understanding of the environmental conditions that affect the chemical signature is needed to describe the favorable and unfavorable conditions of a chemical detector based survey to minimize the consequences of a false negative. The fate and transport of the chemical signature emanating from the buried landmine is a fundamental property that is poorly understood. As an initial step in the evaluation of the landmine chemical signature, a screening model based on pesticide and Volatile Organic Compound (VOC) movement in soils has been adapted to evaluate landmine chemical behavior. This report addresses an initial evaluation of the fate and transport of this chemical signature including the dominant effects environmental conditions may have on the success of a chemical detector survey. Future efforts to develop more mechanistic and sophisticated chemical transport models and the low concentration physical chemical properties are needed to bridge the gap to more realistic fate and transport conditions.

Figure 1 shows a conceptual model of the environmental fate and transport processes that impact the movement of landmine chemical constituents to the surface for chemical detection. Chemical vapors emanate from a buried landmine by permeation through plastic case materials or through seals and seams, and from the initial surface contamination of the case. Vapor phase diffusion transports molecules away from the landmine. The vapors may partition into the aqueous phase of the soil water which may then be transported to the surface through advection, driven by evapotranspiration or to depth by precipitation infiltration, and through diffusion driven by concentration gradients. Under extremely dry soil conditions near the ground surface, vapor phases may be directly sorbed to soil particles. When in the liquid phase, chemicals may also sorb

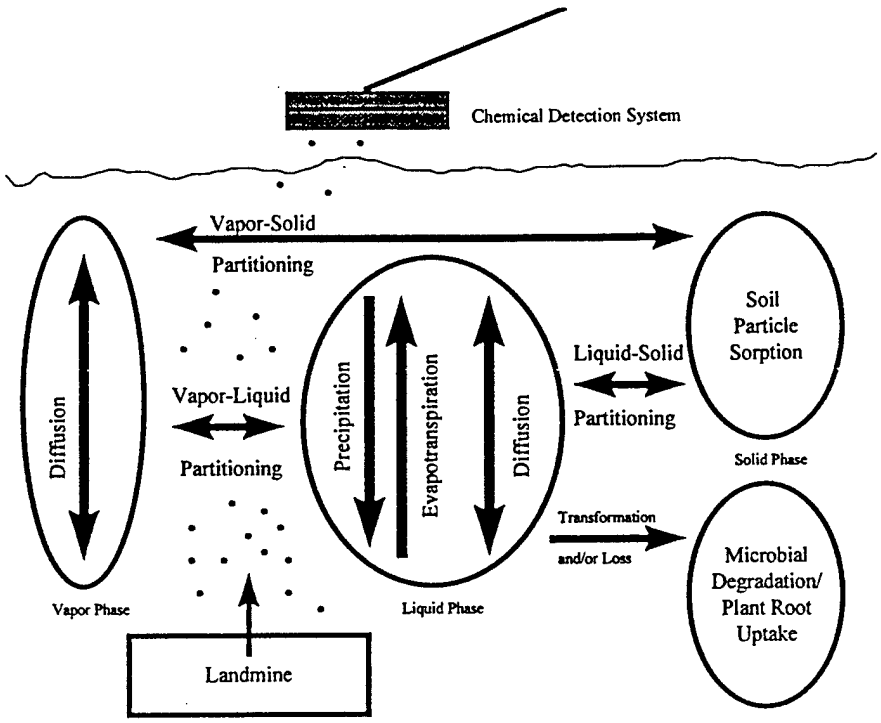


Figure 1. Environmental Fate and Transport Model for Chemical Detection of Buried Landmines

to the soil particles. Soil particle sorption can be considered a temporary storage reservoir for the explosive constituents, where they may be released under reversible partitioning reactions, but some proportion may also permanently bound through chemisorption reactions. Transformation and loss of explosive constituents also occurs during microbial degradation and uptake by the roots of certain plant species.

## 2. CHEMICAL TRANSPORT IN SOILS

Soils are porous media with a number of physico-chemical properties that affect the transport of explosive chemicals. Soil bulk density is a measure of the compaction of the soil and is defined as

$$\rho_b = \frac{M_s}{V_s} \qquad [1]$$

where $\rho_b$ is the soil bulk density (g/cm$^3$), $M_s$ is the mass of soil particles (g), and $V_s$ is the volume of soil (cm$^3$). Soils under natural conditions have bulk densities ranging from 1.0 to 1.8 g/cm$^3$. However, soils that have been excavated and replaced, such as during the emplacement of a landmine, may have bulk densities much less than 1. The soil bulk density is inversely proportional to the soil porosity as follows

$$\phi = 1 - \rho_b / \rho_s \qquad [2]$$

where $\rho_s$ is the soil particle density (ranges from 2.6 to 2.8 g/cm$^3$ for most soils). The soil porosity, or void volume, is defined as

$$\phi = \frac{V_w + V_a}{V_s} \qquad [3]$$

where $\phi$ is the soil porosity (cm$^3$/cm$^3$), $V_w$ is the volume of soil water (cm$^3$) and $V_a$ is the volume of soil air (cm$^3$). Soil porosity values range from 0.3 for sands to 0.6 for clay rich soils. The volumetric moisture content describes how much water is present in the soil and changes greatly during precipitation/drainage events and evaporation conditions. Volumetric water content is defined as

$$\theta = \frac{V_w}{V_s} \quad [4]$$

where $\theta$ is the volumetric water content ($cm^3/cm^3$). Soil moisture contents have values from near zero up to the soil porosity value. When the soils are not fully saturated, the balance of the soil pore space not filled with water is termed the air filled porosity, and is defined as

$$a = \frac{V_a}{V_s} \quad [5]$$

where $V_a$ is the volumetric air content ($cm^3/cm^3$). It is often more convenient to use soil saturation ($S_l$) because it is a measure of the relative saturation of a particular soil pore space with water.

$$S_l = \frac{\theta}{\phi} \quad [6]$$

Since the explosive chemicals can exist as solutes in the soil water and the movement of soil water can be a significant transport mechanism, water solubility is an important parameter. Water solubility is defined as

$$C_L = \frac{M_{chem}}{V_w} \quad [7]$$

where $C_L$ is the concentration in aqueous phase ($g/cm^3$ soil water) and $M_{chem}$ is the mass of chemical (e.g. TNT) (g). Water solubility, however, is not constant and is typically an increasing function with temperature.

Henry's Law constant is a relative measure of the amount of the chemical that exists in the gas phase to that in the aqueous phase at equilibrium, and is defined as

$$K_H = \frac{C_G}{C_L} \quad [8]$$

where $K_H$ is the Henry's Law constant (unitless) and $C_G$ is the concentration in gas phase (g/cm3 soil gas). Henry's Law constant is also a function of temperature because both $C_G$ and $C_L$ are functions of temperature. The soil partition coefficient is a relative measure of how much of the chemical is temporarily bound to the soil to that in the soil aqueous phase

$$K_d = \frac{C_S}{C_L} \quad [9]$$

where $K_d$ is the linear soil-water partition coefficient ($cm^3/g$) for water saturated soils and $C_S$ is the concentration sorbed on the soil solid phase (g/g of soil). The soil water partition coefficient is often correlated with the fraction of organic carbon found in the soils. In this way, the variability between soils can be reduced. The organic carbon distribution coefficient is defined as

$$K_{oc} = \frac{K_d}{f_{oc}} \quad [10]$$

where $K_{oc}$ is the organic carbon distribution coefficient and $f_{oc}$ is the fraction of organic carbon.

## 3. SCREENING MODELS

The environmental fate and transport of organic chemicals including volatilization and leaching losses has been used to explore the distribution of agricultural pesticides in soils (Mayer et al. 1974, Farmer et al. 1980, and Jury et al. 1980). These models were primarily intended to simulate specific circumstances. However, Jury et al. (1983, 1984a, 1984b, 1984c) developed and validated a general screening model (Behavior Assessment Model, BAM) that included volatilization, leaching, and degradation to explore the major loss pathways of agricultural pesticides as a function of specific environmental conditions. The model simulations can be used to assess the behavior of different chemicals under particular environmental conditions, but is not intended to predict a definitive concentration distribution in the field. As such, the predictions from the screening model are only an indication of expected conditions.

This model is valuable in that it can express the total concentration of a chemical in the gas, aqueous and sorbed phases. The total concentration is expressed as

$$C_T = \rho_b C_S + \theta C_L + a C_G \quad [11]$$

where $C_S$ is the concentration sorbed to the soil, $C_L$ is the solute concentration in the aqueous phase, and $C_G$ is the gas phase concentration. In addition, Jury (1983) shows how equation [11] can be rewritten in terms of one of the variables alone

$$C_T = R_S C_S = R_L C_L = R_G C_G \quad [12]$$

where

$$R_S = \rho_b + \frac{\theta}{K_d} + a\frac{K_H}{K_d} \quad [13]$$

$$R_L = \rho_b K_d + \theta + a K_H, \text{ and} \quad [14]$$

$$R_G = \rho_b \frac{K_d}{K_H} + \frac{\theta}{K_H} + a \quad [15]$$

are the solid, liquid and gas phase partition coefficients, respectively.

An adaptation of the BAM was developed to be applicable to the conditions of contaminated soil buried under a known depth of clean soil - Buried Chemical Model, BCM (Jury et al., 1990). Simulations based on a modification of Jury's BCM are used in this report to simulate the behavior of the chemical signature from buried landmines. The Buried Chemical Model of Jury et al. (1990) is based on the following assumptions. A detailed discussion of these assumptions is given in Jury et al. (1990).

1. The chemical may adsorb on the solid phase, be dissolved in the aqueous phase, or exist in the vapor phase.
2. The chemical flux is the sum of the vapor flux and the dissolved solute flux.
3. The porous medium factors for gas and liquid phase diffusion are given by the Millington and Quirk (1961) model as extended for liquid diffusion by Jury et al. (1983).
4. The chemical will undergo first-order degradation due to biological and chemical effects.
5. Chemical movement is one dimensional.
6. The adsorbed and dissolved phases undergo reversible, linear adsorption.
7. The dissolved and gaseous phase concentrations are related through Henry's law.
8. The soil properties are constant in space and time.
9. Water flux is constant in space and time (relaxed in the present application).
10. Volatilization of the chemical to the atmosphere is by vapor diffusion through an air boundary layer of constant thickness.

In the present implementation of Jury's model, a constant source term has been added to reflect the chemical source from the landmine at a specific location.

Under these assumptions (including the source term) the model formulation becomes

$$\frac{\partial C_T}{\partial t} + \mu C_T = D_E \frac{\partial^2 C_T}{\partial z^2} - V_E \frac{\partial C_T}{\partial z} + \sigma \quad [16]$$

where $C_T$ is the total chemical concentration, $\mu$ is the biochemical decay constant, and $\sigma$ is the source term. The effective velocity ($V_E$) is defined as

$$V_E = \frac{J_w}{\rho_b K_d + \theta + aK_H} \quad [17]$$

where $J_w$ is the precipitation/evaporation flux. The effective diffusion coefficient ($D_E$) of the chemical is defined as

$$D_E = \frac{a^{10/3} K_H D_g^a + \theta^{10/3} D_l^w}{\phi^2 \left(\rho_b K_d + \theta + aK_H\right)} \quad [18]$$

where $D_g^a$ is the diffusivity of the gas phase of the chemical in air and $D_l^w$ is the diffusivity of the chemical in aqueous phase . The boundary conditions for the problem are diffusion through a boundary layer at the upper surface, and a zero chemical concentration at infinity at the lower boundary. These boundary conditions can be expressed as

$$-D_E \frac{\partial C_T}{\partial z} + V_E C_T = -H_E C_T \quad [19]$$

where

$$H_E = \frac{hK_H}{\rho_b K_d + \theta + aK_H} \quad [20]$$

and

$$h = \frac{D_g^a}{d} \quad [21]$$

and

$$C_T(\infty, t) = 0$$

The initial conditions are an initial concentration, $C_0$, over an interval from L to W, or

$$C_T(z,0) = 0 \qquad L \rangle z \rangle W$$

$$C_T(z,0) = C_0 \qquad L \le z \le W$$

The above model without the source term results in a closed form solution as a function of space and time; the results are rather lengthy and will not be presented here but are given by Jury et al. (1983, 1990). In the present simulations, the assumption of constant water flux in time is relaxed. Therefore, sequences of water fluxes representing desired conditions (rainfall followed by evaporation) can be simulated to determine the effect of water flux variations on the location of TNT in the soil and the surface TNT vapor flux. A numerical solution was developed and verified by comparison to the results given by Spencer et al. (1988) and Jury et al. (1990) (Phelan and Webb, 1997).

## 4. LANDMINE SOURCE TERM

The total mass of the initial deposit of chemicals after first emplacement of the landmine in soils is critical in the estimation of soil concentrations and surface vapor fluxes (Phelan and Webb, 1988). For the model used in this analysis, it has been assumed that the entire surface contamination was completely and uniformly transferred to the soil just prior to the beginning of the simulation runs. Surface contamination data (Hogan et al., 1992) showed a median surface contamination of 15 ng/cm$^2$ from 42 domestic and foreign landmines. However, the surface contamination values ranged from below instrument detection limits to 300-500 ng/cm2 and some outliers as high as 1000-5000 ng/cm2. Using the median surface contamination and the dimensions of an anti-tank (AT) mine of 30 cm diameter by 10 cm high, the surface contamination would provide $3.5 \times 10^{-5}$ g of TNT for initial distribution in the soil. Using the volume of the AT mine that this mass of TNT is distributed into, the initial concentration ($C_o$) would be $5 \times 10^{-3}$ µg/cm$^3$.

The continuous release of chemicals by permeation or leaks through seals and seams is also important if the rate is significantly large enough. However, few data exist. One effort established constant source term emanation rates derived from vapor collection chamber experiments on two mines (Spangler, 1975). Values ranged from $10^{-16}$ to $10^{-18}$ g/cm$^2$-s. The higher rate of $10^{-16}$ g/cm$^2$-s ($8.6 \times 10^{-6}$ µg/cm$^2$-day) was used in these simulations.

## 5. PHYSICAL CHEMICAL PROPERTIES OF EXPLOSIVES

The principal explosive chemicals found in landmines are TNT and RDX (NGIC, 1995). DNT, as a production by-product of TNT, is also considered to be a significant signature chemical for buried landmines. As a group, these chemicals have very low vapor densities and moderately low water solubility's. Table 1 shows these properties and the Henry's Law constant at 20°C (Phelan and Webb, 1997).

Table 1. Vapor Density, Water Solubility and Henry's Law Constant of Explosive Compounds at 20°C

| | TNT | DNT | RDX |
|---|---|---|---|
| Vapor Density ($\mu g/m^3$) | 43.5 | 122 | 0.024 |
| Water Solubility (mg/l) | 130 | 270 | 50 |
| Henry's Law Constant | 3.35E-7 | 4.51E-7 | 4.73E-10 |

Pennington and Patrick (1990) measured the soil water partition coefficient ($K_d$) of TNT in fourteen soils from locations across North America. The mean value was 3.8 $cm^3/g$ with a standard deviation of 1.34. The highest value was 6.8 $cm^3/g$ and the lowest value was 2.3 $cm^3/g$. Xue et al. (1995) evaluated two soils and showed mean values for TNT of 2.66 $cm^3/g$ and 3.64 $cm^3/g$. DNT and RDX have very little data. Xue et al. (1995) showed values for RDX of 1.59 $cm^3/g$ and 1.57 $cm^3/g$. McGrath (1995) showed a $K_{oc}$ value of 251 for DNT. For the fourteen soils evaluated by Pennington and Patrick (1990), the mean value for the fraction of organic carbon was 0.0173 with a standard deviation of 0.011. Using these values, the $K_d$ for DNT has a mean value of 4.4±2.7 $cm^3/g$ (one std. dev.). In summary, the soil water partitioning coefficients for TNT, DNT and RDX all fall into an approximate range between 1.5 and 7.0 $cm^3/g$. This is a rather narrow range as common chemicals can have values one to two orders of magnitude lesser and greater than these.

The biochemical half-life of explosives in near surface soils has not been studied well outside of the biotreatment technology area for contaminated soils. However, long-term surface soil degradation tests at Los Alamos National Laboratory (LANL) followed the degradation of soils doped with 1000 mg/kg of various explosives over 20 years (Dubois and Baytos, 1991). Table 2 shows the half-lives estimated from these long-term experiments.

Table 2. Estimates of Half-Lives of Explosives from LANL Long-Term Surface Soil Tests

| Explosive | Half-Life (years) |
|---|---|
| TNT | 1 |
| RDX | 36 |
| HMX | 39 |
| PETN | 92 |

## 6. SIMULATION PARAMETERS

Using the modified Buried Chemical Model (BCM), simulations were performed using a landmine that has contributed an initial soil concentration ($C_o$) based on the median surface contamination of the landmine (Hogan et al., 1992) and the constant flux ($J_c$) from Spangler, 1975. The diffusivity of gas in air ($D_g^a$) and diffusivity of liquid in water ($D_l^w$) were selected from Jury et al. (1983). The biochemical half-life value of 365 days was selected from a long term field experiment (Dubois and Bayton, 1991). The physico-chemical properties of TNT were used at 25°C.

The precipitation/evaporation rates and periods followed in several of the simulations here were the low desert scenario from Phelan and Webb (1997). This scenario was derived from data found in HELP (Hydrological Evaluation of Landfill Performance) model (Schroeder et al., 1994a and 1994b). The HELP model showed that the low desert had 1 day of precipitation followed by 7 days of evaporation. For simplicity, total precipitation and total evaporation for each cycle are assumed to be equal and for these simulations the cycles were continued for approximately four years. Table 3 shows the input parameters used in the simulations.

Table 3. Simulation Parameters

| parameter | units | base case | variant cases |
|---|---|---|---|
| $\theta$ | $cm^3/cm^3$ | 0.20 | Figure 2: 0.243, 0.287 |
| $\phi$ | $cm^3/cm^3$ | 0.434 | * |
| $\rho_b$ | $g/cm^3$ | 1.5 | Figure 2: 1.25, 1.0 |
| $K_d$ | $cm^3/g$ | 3.8 | * |
| $K_H$ | -- | 5.9E-7 | * |
| air boundary layer | cm | 0.5 | * |
| $t_{1/2}$ | days | 365 | * |
| $C_o$ | $\mu g/cm^3$ | 5E-3 | * |
| $J_c$ | $\mu g/cm^2$-day | 8.6E-6 | * |
| $D_l^w$ | $cm^2$/day | 0.432 | * |
| $D_g^a$ | $cm^2$/day | 4320 | * |
| burial depth, top | cm | 10 | Figure 3: 5, 1, 0<br>Figure 6, 7, 8 & 9: 5 |
| burial depth, bottom | cm | 20 | Figure 3: 15, 11, 10<br>Figure 6, 7, 8 & 9: 15 |
| precipitation | days | 1 | varies |
| evaporation | days | 7 | varies |
| precipitation rate | cm/day | 0.44 | Figure 4, 5: 0 |
| evaporation rate | cm/day | - 0.063 | Figure 4, 5: 0 |

* - same as the base case

## 7. DISCUSSION

Initial application of the screening model (Phelan and Webb, 1997) showed that explosive compounds such as TNT, DNT and RDX will have over 90% of the mass fraction sorbed to the soil solid phase, up to 10% present in the soil aqueous phase and less than 1E-6% in the soil vapor phase. The implications for this are that transport of these chemicals in soils will be dominated by movement as a solute in the aqueous phase. In addition, at soil water contents above about 0.1 $cm^3/cm^3$, the effective diffusivity ($D_E$) is dominated by liquid diffusion by one to five orders of magnitude. Next, the screening model was applied to three different environmental scenarios and results showed that maximum surface vapor fluxes were very low, requiring a sampling and concentration factor of $10^3$ using currently available laboratory instrument detection limits. Surface soil concentrations showed that sampling modest amounts of soil would require a preconcentration factor of about 2.

Next, the impact of variations in several of the various input parameters was explored (Phelan and Webb, 1998). It was found that the variations in the Henry's Law constant are directly proportional to the changes seen in the steady-state surface vapor flux. Small changes in the soil water partitioning coefficient made large changes in the lag period and steady-state surface vapor flux. The initial source term and continuous source flux of chemicals from the landmines is poorly understood and expected to be highly variable. These simulations found that with the baseline case, if the continuous source flux was absent, there was no significant difference in the surface vapor flux or subsurface distribution at the end of the simulation period. This implies that the continuous source flux may be much less important than the initial surface contamination. It appears that the magnitude of the surface vapor flux is directly proportional to the amount of the initial surface contamination. The biochemical half-life is another parameter that is likely to have very different values depending on the location and climatic conditions. Simulations over ten years showed that the steady state surface vapor flux declines steadily when the biochemical half-life becomes smaller than one year. Finally, the importance of heavy precipitation (such as a monsoon season) followed by a dry season was explored. The impact of the heavy precipitation was to lower the surface

flux seven orders of magnitude; however, the evaporation period that followed returned the surface flux to approximately the pre-monsoon surface flux.

This current effort has evaluated the impact of changes to the soil bulk density, burial depth, concentration in the soil layer, water flux, and the conditions that promote an enhanced surface layer. When a landmine is placed, the soil surrounding the mine is not compacted to the original bulk density. Over time the soil bulk density will increase. Figure 2 shows that soils with smaller soil bulk densities will have a shorter lag period and a steady state surface flux about two orders of magnitude greater than the base case.

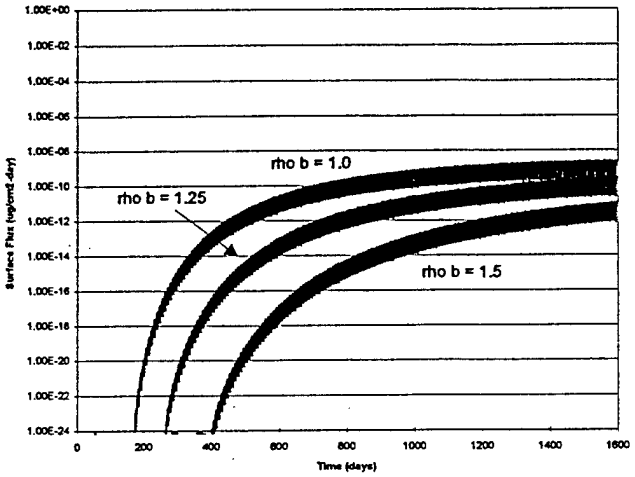


Figure 2. Effect of Soil Bulk Density Changes on Surface Flux

The effect of burial depth appears to be a very critical parameter, even over small distances of a few centimeters. Figure 3 shows how the lag time for the surface vapor flux becomes dramatically shorter by moving the top of the initial source zone up from 10 cm to 5 cm to 1 cm and 0 cm.

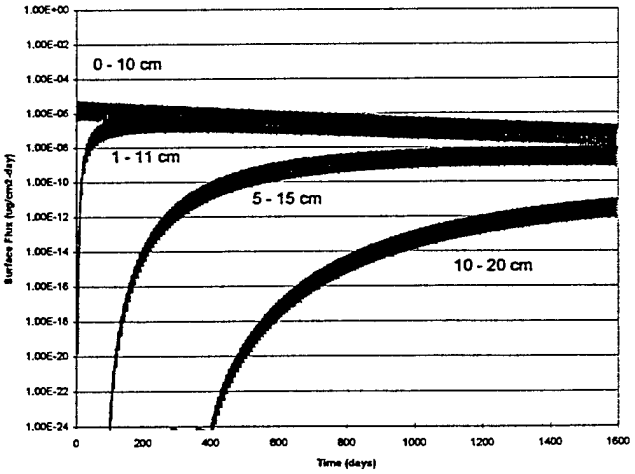


Figure 3. Effect of Burial Depth on Surface Flux

An important assumption made in the current numerical application to the landmine problem is the assumption of a uniform explosive concentration between the top and bottom of the mine. In reality, the explosive is concentrated on the top and the bottom surfaces, the mine is an impediment to transport, and the mine is not porous media. In order to assess the implication of smearing the concentration over the entire depth, Jury's original BCM without a source term and with zero water flux has been applied to the case of two buried chemical sources. The top source started at the top of the landmine location, while the bottom source ended at the bottom of the landmine, with a zero concentration region in the center of the landmine location.

A constant mass was used, and the concentration changed with the source width, which varied from 5.0 cm, the base case, down to 0.0005 cm. The 5.0 cm base case results in a uniform initial concentration between the top and bottom of the mine, while the 0.0005 cm case approximates two sources at the top and bottom surfaces. Fig 4 shows the vapor flux at the ground surface as a function of time for the various source widths. The parameters in this case are the same as for the base case in Table 3 without a source term and with no precipitation/evaporation. The results are similar, though not identical, to results given in Figure 2 (rho b = 1.5).

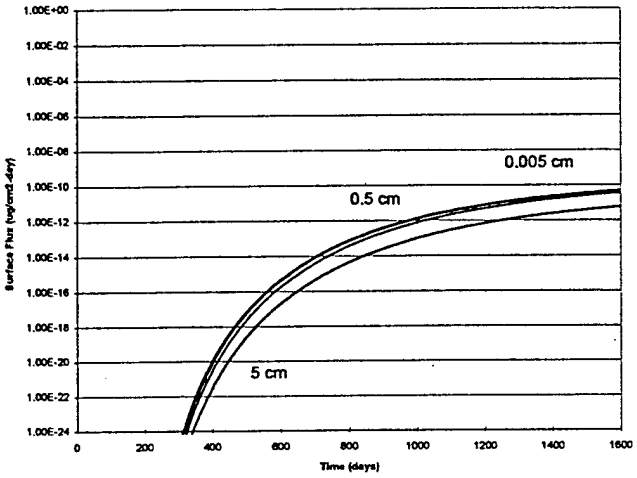


Figure 4. Effect of Layer Concentration on Surface Vapor Flux

Even if the parameters were the same, some differences would exist, particularly at earlier times and at lower concentrations, due to numerical issues such as roundoff and numerical diffusion. From Figure 4, the vapor flux increases as the width decreases, which is expected because a reduction in the width essentially moves the top source closer to the ground surface. Figure 5 shows the ratio of the vapor flux from the 0.0005 cm width case to the 5 cm case. The ratio decreases with time from about 50 to a value of 10 at late times.

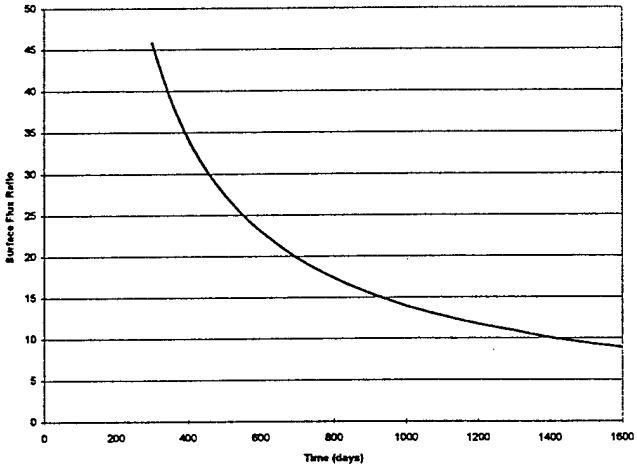


Figure 5. Ratio of Surface Flux from a 0.0005 cm Layer to 5 cm Layer

In addition to the effect of soil moisture content, the effect of precipitation (positive water flux, $J_w$) and evaporation (negative water flux, $J_w$) is probably one of the most important environmental factors in the transport of explosive chemicals in soils. Figure 6 shows that with only precipitation occurring, the surface flux is about 3 orders of magnitude less than the case of zero precipitation or evaporation. The case of constant evaporation is about 2 orders of magnitude greater than the zero water flux case. If one examines the model formulation, the mass transport upwards is controlled by the effective diffusion ($D_E$) and the effective chemical velocity ($V_E$). In the constant precipitation case, upward mass transport is a function of $D_E$

minus $V_E$. In the zero precipitation/evaporation, upward mass transport is a function of only $D_E$. In the constant evaporation case, upward mass transport is a function of $D_E$ plus $V_E$.

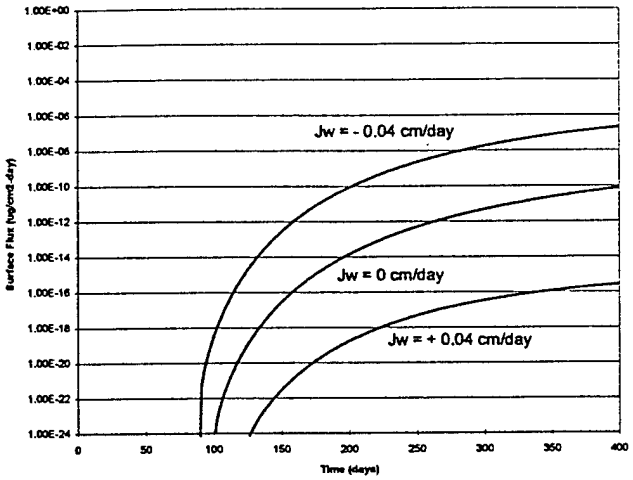


Figure 6. Effect of Water Flux (Precipitation/Evaporation) on Surface Flux

The occurrence of a surface soil layer that is greater in concentration than the subsurface soil layers, or a surface "crust", has been observed and modeled with agricultural pesticides (Spencer et al., 1988). This type of behavior is also thought to occur with explosive compounds due to similarities in the physical/chemical properties and some evidence from field surveys and lab experiments. Simulation runs were completed to evaluate what influences the creation of the enhanced concentrations in the surface soil layers. Initial simulation runs (Phelan and Webb, 1997) used cyclic precipitation/evaporation that was equal in magnitude. This condition did not create an enhanced surface layer. In order to create an enhanced surface layer, enough of the mass must be transported from deeper regions to the ground surface. This condition only occurs during evaporation conditions and in Figure 7 the buried chemical layer is shown to move upward until it intersects with the ground surface. Figure 8 shows more detail on the depth and magnitude of the enhanced layer. It is believed that the air boundary layer and the low Henry's Law Constant ($K_H$) contribute to the formation of the enhanced surface layer (Spencer et al., 1988). It appears that the upward transport through the soil exceeds the loss through the air boundary layer. Transport though the air boundary layer is controlled by vapor diffusion and limited by the transfer of chemical from the aqueous phase to the gas phase by the very low $K_H$.

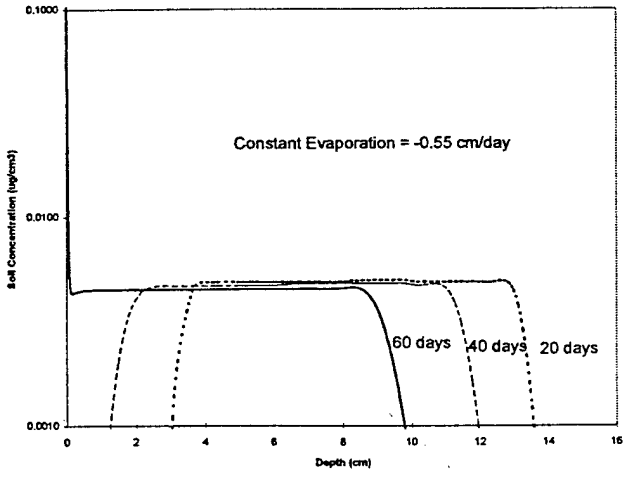


Figure 7. Upward Transport and Development of a Surface Layer

Figure 9 shows the effect of developing the enhanced surface layer with 60 days of evaporation (-0.5 cm/day), followed by precipitation for 5 days (0.5 cm/day). The enhanced surface layer found in the top 0.1 cm of soil is transported down leaving just a small enhancement at a depth of about 0.5 cm. Another simulation was run that included the same evaporation and

precipitation, but was followed by another 5 day evaporation period (-0.5 cm/day) and the surface enhancement returned at about the same concentration.

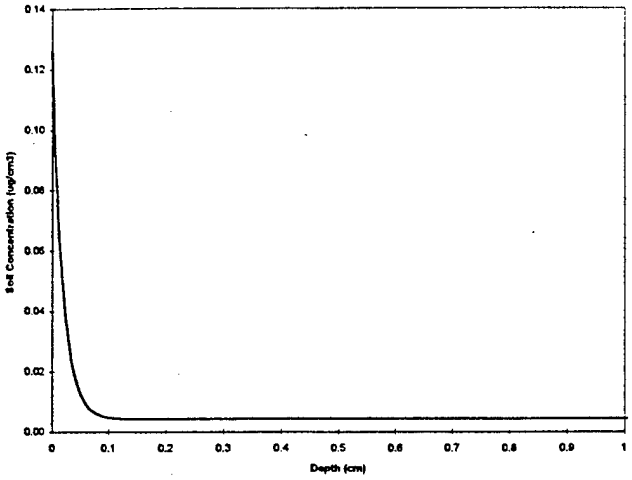


Figure 8. Detail of the Surface Layer Formed by Evaporation

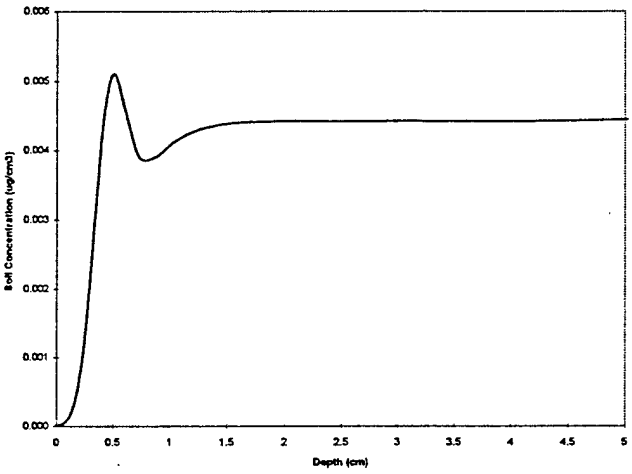


Figure 9. Effect of Precipitation on the Enhanced Surface Layer

## 8. SUMMARY AND CONCLUSIONS

Two previous efforts have evaluated the environmental fate and transport of chemical signature molecules from buried landmines (Phelan and Webb, 1997 and 1998). This effort evaluated the effect of changes in soil bulk density, burial depth, source term thickness, precipitation or evaporation, and the elements that produce an enhanced surface layer. Smaller soil bulk densities change the soil porosity and moisture content at constant soil saturations. Lower soil bulk densities increase the rate of transport as indicated by a shorter lag time and reach a higher steady state surface vapor flux. Burial depth has a dramatic effect on the lag time. With just a one centimeter soil cover, there appears to be almost no lag time and the surface vapor flux is five orders of magnitude greater than a soil cover of ten centimeters. The assumption of a uniform concentration over the depth of the landmine leads to under prediction of the vapor flux at the land surface by about an order of magnitude or more. The appearance of an enhanced surface layer is the result of evaporation driven mass transport that is constrained by vapor diffusion through the air boundary at the ground surface and the low aqueous to vapor transfer as a function of the low Henry's Law Constant. However, there are probably many other uncertainties in the present model which affect the quantitative results as well. The one-dimensional assumption demands that the mine itself is permeable, and the assumption of constant liquid content, both spatially and temporally, is obviously a great simplification. In order to address these and other issues, a multidimensional mechanistic code is being developed for application to the landmine

problem. This code, which is based on the TOUGH code from Lawrence Berkeley Laboratory (Pruess, 1987,1991), will consider air, water vapor, and explosive vapor mass and heat flow in a porous media and will be able to address many of these questions.

## 9. ACKNOWLEDGEMENTS

This work was performed with internal laboratory-directed research and development funds at Sandia National Laboratories to explore applications for miniaturized chemical sensors. Follow-on work to develop a numerical model is just beginning with funds from the Strategic Environmental Research and Development Program (SERDP) for application to unexploded ordnance chemical sensing and from the Defense Advanced Research Projects Agency (DARPA) for application to buried landmines. Sandia is a multiprogram laboratory operated by Sandia Corporation, a Lockheed Martin Company, for the United States Department of Energy under Contract DE-AC04-94AL85000.

## 10. REFERENCES

[1] Dugan, R.E., 1996. Detection of Land Mines and Unexploded Ordanance by Exploitation of the Chemical Signature. Defense Advanced Research Projects Agency, Conference presentation. April 1996.

[2] DuBois, F.W. and J. F. Baytos. 1991. Weathering of Explosives for Twenty Years. Los Alamos National Laboratory, Report LA-11931.

[3] Farmer, W.J., M.S. Yang, J. Letey, and W.F. Spencer. 1980. Hexachlorobenzene: its vapor pressure and vapor phase diffusion in soil. Soil Sci. Soc. Am. Proc. 44:676-680.

[4] Hogan, A., D. Leggett, T. Jenkins, P. Miyares. 1992. Results of Preliminary Analysis, Surface Contamination of Depot-Stored Land mines, Prepared as a briefing guide for planning DARPA mine detector trials. USACRREL. June 23, 1992. Includes: Test Plan Summary: Sampling of Mine Surfaces to Determine the Extent of Explosive Contamination.

[5] Jury, W.A., R. Grover, W.F. Spencer, and W. J. Farmer. 1980. Modeling Vapor Losses of Soil-Incorporated with Triallate. Soil Sci. Soc. of Am. J., 44, 445-50 (May-June 1980).

[6] Jury, W.A., W.F. Spencer, and W.J. Farmer. 1983. Behavior Assessment Model for Trace Organics in Soil: I. Model Description. J. Environ. Qual., Vol 12, no. 4, 558-564.

[7] Jury, W.A., W.J. Farmer, and W.F. Spencer. 1984a. Behavior Assessment Model for Trace Organics in Soil: II. Chemical Classification and Parameter Sensitivity. J. Environ. Qual., Vol. 13, no. 4, 567-572.

[8] Jury, W.A., W.F. Spencer, and W.J. Farmer. 1984b. Behavior Assessment Model for Trace Organics in Soil: III. Application of Screening Model. J. Environ. Qual., Vol 13, no. 4, 573-579.

[9] Jury, W.A., W.F. Spencer, and W.J. Farmer. 1984c. Behavior Assessment Model for Trace Organics in Soil: IV. Review of Experimental Evidence. J. Environ. Qual., Vol 13, no. 4, 580-586.

[10] Jury, W.A., D. Russo, G. Streile, and H. Abd. 1990. Evaluation of Volatilization by Organic Chemicals Residing Below the Surface. Water Resources Research vol 26, no 1, p 13-20, January 1990.

[11] Mayer, R., J. Letey, and W.J. Farmer. 1974. Models for predicting volatilization of soil-incorporated pesticides. Soil Sci. Soc. Am. Proc. 38:563-568.

[12] McGrath, C. 1995. Review of Formulations for Processes Affecting the Subsurface Transport of Explosives. US Army Corps of Engineers, Waterways Experiment Station, Technical Report IRRP-95-2, August 1995.

[13] Millington, R.J., and J.M. Quirk. 1961. Permeability of porous solids. Trans. Faraday Soc., 57:1200-1207.

[14] NGIC. 1995. Landmines and Demining: A Global Problem CD-ROM. National Ground Intelligence Center, Charlottesville, VA.

[15] Pennington, J.C. and W.H. Patrick. 1990. Adsorption and desorption of 2,4,6-trinitrotoluene by soils. J. Environ. Qual. 19:559-567.

[16] Phelan, J.M. and S. W. Webb. 1997. Environmental Fate and Transport of Chemical Signatures from Buried Landmines - Screening Model Formulation and Initial Simulations. Sandia National Laboratories, SAND97-1426. June 1997.

[17] Phelan, J.M. and S.W. Webb, 1998. Chemical Detection of Buried Landmines. Proceedings of the 3rd International Symposium on Technology and the Mine Problem, April 6-9, 1998. Mine Warfare Association.

[18] Pruess, K. 1987. TOUGH User's Guide, NUREG/CR-4645, SAND86-7104, LBL-20700, US Nuclear Regulatory Commission.

[19] Pruess, K. 1991. TOUGH2 - A General-Purpose Numerical Simulator for Multiphase Fluid and Heat Flow. LBL-29400, Lawrence Berkeley Laboratory.

[20] Schroeder, P.R., C.M. Lloyd, and P.A. Zappi. 1994a. The Hydrological Evaluation of Landfill Performance (HELP) Model User's Guide for Version 3. EPA/600/R-94/168a. U.S. Environmental Protection Agency, Risk Reduction Engineering Laboratory, Cincinnati, Ohio.

[21] Schroeder, P.R., T.S. Dozier, P.A. Zappi, B.M. McEnroe, J.W. Sjostrom, and R.L. Peyton. 1994b. The Hydrological Evaluation of Landfill Performance (HELP) Model: Engineering Documentation for Version 3. EPA/600-R-94/168b. U.S. Environmental Protection Agency, Risk Reduction Engineering Laboratory, Cincinnati, Ohio.

[22] Spangler, G.E.. 1975. Measurements on the Availability of TNT Vapor from Antitank Mines. Report No: MERADCOM-R-2159

[23] Spencer, W.F., M.M. Cliath, W.A. Jury, and L.-Z. Zhang. 1988. Volatilization of Organic Chemicals from Soil as Related to Their Henry's Law Constants. J. Environ. Qual. 17:504-509.

[24] Xue, S.K., I.K. Iskandar, and H.M. Selim. 1995. Adsorption-Desorption of 2,4,6-Trinitrotoluene and Hexahydro-1,3,5-Trinitro-1,3,5-Triazine in Soils. Soil Science, Vol. 160, No. 5. November 1995.

# APPENDIX C

Webb, S.W., S.A. Finsterle, K. Pruess, and J.M. Phelan, 1998. Prediction of the TNT Signature from Buried Landmines. Proceedings of the TOUGH '98 Workshop. Berkeley, CA.

# Prediction of the TNT Signature from Buried Landmines

Stephen W. Webb[1], Stefan A. Finsterle[2], Karsten Pruess[2], and James M. Phelan[1]
[1]Sandia National Laboratories, Albuquerque, NM 87185
[2]Lawrence Berkeley National Laboratory, Berkeley, CA 94720

## ABSTRACT

The detection, and removal, of buried landmines is one of the most important international problems facing the world today. Numerous detection strategies are being developed, including infrared, electrical conductivity, ground-penetrating radar, and chemical sensors. Chemical sensors rely on the detection of TNT molecules from buried landmines, which are transported by advection and diffusion in the soil. As part of this effort, numerical models are being developed to predict TNT transport in soils including the effect of precipitation and evaporation. Modifications will be made to TOUGH2 for application to the TNT chemical sensing problem. The understanding of the environmental fate and transport of TNT in the soil will affect the design, performance and operation of chemical sensors by indicating preferred sensing strategies.

## INTRODUCTION

The goal of locating buried landmines is a significant challenge to science and technology. The chemical signature of landmines is affected by multiple environmental phenomena that can enhance or reduce its presence and transport behavior, and can affect the distribution of the chemical signature in the environment. For example, the chemical can be present in the vapor, aqueous, and solid phases. The distribution of the chemical among these phases, including the spatial distribution, is key in designing appropriate detectors, e.g., gas, aqueous or solid phase sampling instruments. A fundamental understanding of the environmental conditions that affect the chemical signature is needed to describe the favorable and unfavorable conditions of a chemical detector based survey to minimize the consequences of a false negative.

The fate and transport of the chemical signature emanating from the buried landmine is poorly understood. As an initial step in the evaluation of the landmine chemical signature, a screening model based on pesticide and Volatile Organic Compound (VOC) movement in soils has been adapted to evaluate landmine chemical behavior. Future efforts to develop more mechanistic and sophisticated chemical transport models are needed to bridge the gap to more realistic fate and transport conditions.

Figure 1 shows a conceptual model of the environmental fate and transport processes that impact the movement of landmine chemical constituents, such as TNT and DNT, to the land surface for chemical detection. Chemical vapors emanate from a buried landmine by permeation through plastic case materials or "leakage" through seals and seams, and from surface contamination of the case.

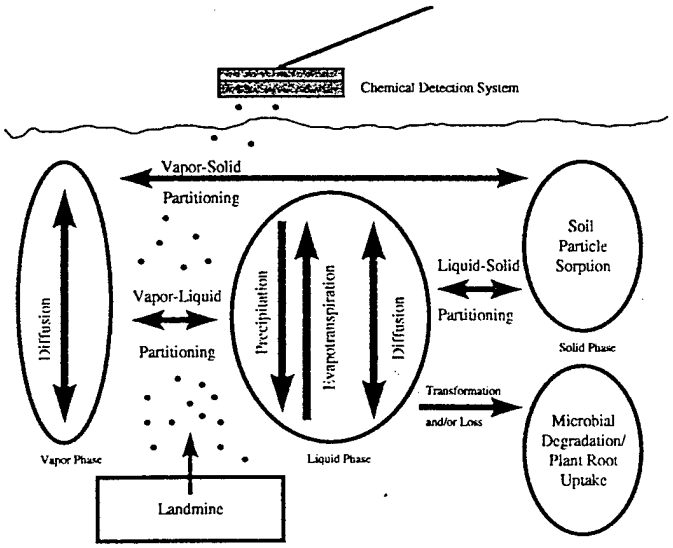


**Figure 1. Environmental Fate and Transport Model for Chemical Detection of Buried Landmines.**

Table 1. TNT and DNT Properties at 20°C

| | TNT | DNT |
|---|---|---|
| Vapor Density ($\mu g/m^3$) | 43.5 | 122 |
| Water Solubility (mg/l) | 130 | 270 |
| Henry's Law Constant | 3.35E-7 | 4.51E-7 |
| Sorption Coefficient ($cm^3/g$) | 3.8 | 4.4 |

## CHEMICAL PROPERTIES

The chemical properties of TNT and DNT are important in determining the transport rate of these vapors through the soil. These chemical vapors exist in the gas, liquid, and solid phases of the soil. Typical properties for TNT and DNT are shown in Table 1. Because of the low value of Henry's constant and the value of the soil water partition coefficient, about 90% of the explosive mass fraction is sorbed to the soil solid phase, about 10% is in the water; and less than $10^{-6}$% is in the gas phase as shown in Figure 2.

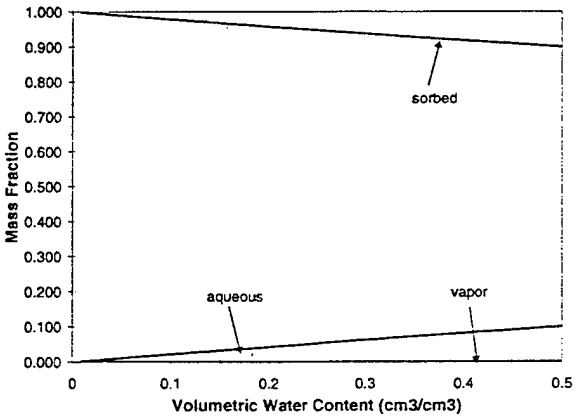


**Figure 2. Phase Mass Fraction of TNT**

The transport rate of TNT in soil can be estimated by evaluating pure diffusion conditions. An effective diffusivity can be defined for the total chemical concentration by considering the distribution among the phases (Jury et al., 1983). By applying the Millington and Quirk (1961) tortuosity relationship to the liquid phase, the effective diffusivity for the total chemical concentration can be expressed as

$$D_E = \frac{a^{10/3} K_H D_g^a + \theta^{10/3} D_l^w}{\phi^2 (\rho_b K_d + \theta + a K_H)} \qquad (1)$$

Figure 3 shows the variation in this effective diffusivity with water content. Note that the diffusivity value is low due to the value of Henry's constant and sorption onto the solid phase that acts as a sink for the explosive chemical. The effective diffusivity is generally much higher at higher moisture contents.

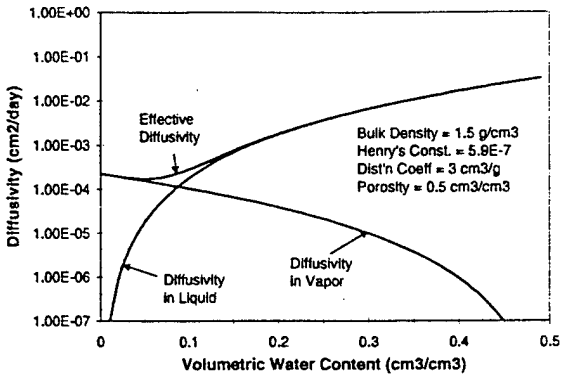


**Figure 3. TNT Effective Diffusivity**

## INITIAL TRANSPORT STUDIES

Jury and his colleagues (Jury et al., 1983, 19841,b,c) developed a one-dimensional screening model to study the behavior of various pesticides under different environmental conditions. This model was subsequently extended to buried chemicals, such as VOCs, by Jury et al. (1990). TNT properties (Henry's constant and sorption coefficient) are very similar to some pesticides, especially Prometron. Therefore, Jury's screening model has been used for some initial studies of the TNT transport in soils from buried landmines.

In addition, Prometron exhibits some interesting behavior that may be particularly important for the sensing of TNT for landmine detection. Under evaporation conditions, a surface "crust", or a soil layer that is greater in concentration than the subsurface soil, has been observed in laboratory tests; this surface "crust" is also predicted by Jury's screening model (Spencer et al., 1988). Some evidence of this type of behavior for TNT has also been noted in some field surveys and lab experiments, although the data are not definitive. The occurrence of a surface "crust" would greatly enhance the concentration available to chemical sensors and the efficiency of the technique.

Initial studies of the transport rate of TNT in soils from landmines have been conducted by Phelan and Webb (1997, 1998a,b) using Jury's model. The results of Phelan and Webb for landmine detection indicated a significant influence of the soil type and environmental conditions, including precipitation and evaporation, on the TNT flux at the soil surface which is available to chemical detectors.

| Table 2. Phase Specific Concentration of TNT at the Ground Surface After One Year | | | | |
|---|---|---|---|---|
| | | Volumetric Water Content/Saturation | | |
| Concentration | Units | 0.20/0.46 | 0.25/0.58 | 0.30/0.69 |
| Solid Phase | µg TNT/g soil | 1.8E-8 | 3.1E-6 | 2.8E-5 |
| Liquid Phase | µg TNT/ml soil water | 4.8E-9 | 8.4E-7 | 7.6E-6 |
| Gas Phase | µg TNT/cm$^3$ soil air | 2.8E-15 | 5.0E-13 | 4.5E-12 |

Results from this screening model are shown below for a landmine buried from 5 cm to 15 cm beneath the surface; details are given by Phelan and Webb (1997, 1998a,b). Note that the screening model was developed to assess the behavior of different chemicals under specific environmental conditions; it is not intended as a purely predictive model due to a number of simplifying assumptions, such as constant soil moisture content. Therefore, these results are only an indication of expected conditions, and more detailed numerical methods, such as TOUGH2, are necessary for a fully predictive simulation.

Figure 4 shows the TNT surface flux at the land surface for a Gulf coastal lowlands soil type as a function of soil saturation. The oscillations in the surface flux are a result of precipitation/evaporation cycles, which were constant over the simulation. As the soil saturation increases, the surface flux increases dramatically.

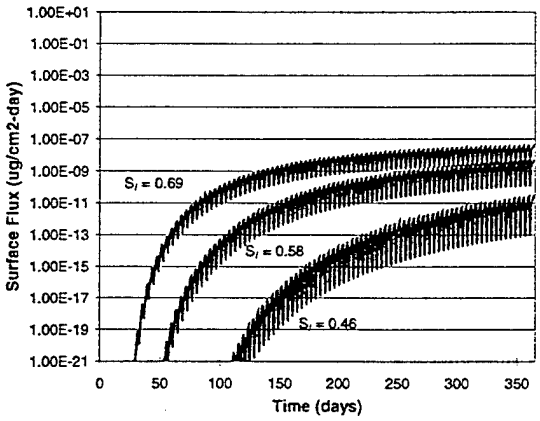


**Figure 4. Surface Flux of TNT**

Figure 5 shows the surface distribution of TNT after 1 year for the three soil saturations. The landmine was buried from 5 to 15 cm below the ground with an initial concentration based on contamination on the landmine casing. In addition, landmines "leak" TNT through the casing, which was represented by a source at 10 cm. The movement of the TNT away from the landmine is slow and is a function of the liquid saturation.

Note the low total concentrations in Figure 5. These total concentrations can be further broken down into solid, liquid, and gas phase values as summarized in Table 2, which indicate the extremely small concentrations available in the gas phase. This information will be valuable in the design and operation of chemical sensors for landmine detection.

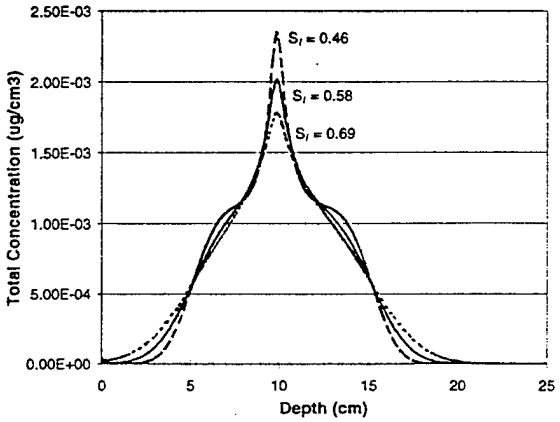


**Figure 5. Subsurface Distribution of TNT After One Year**

The effect of burial depth is a critical parameter. Figure 6 shows how the lag time for the surface vapor flux becomes dramatically shorter by moving the top of the initial source zone up from 10 cm to 5 cm to 1 cm and 0 cm.

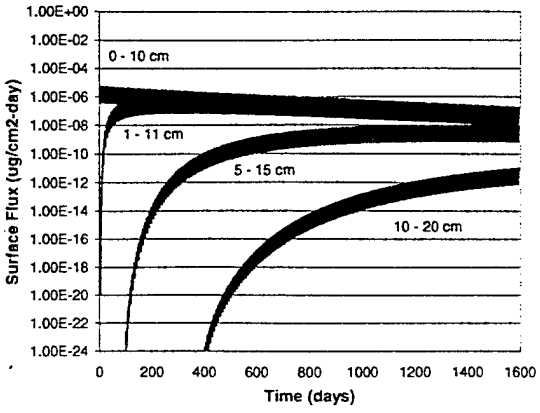


**Figure 6. Effect of Burial Depth on Surface Flux**

The effect of precipitation (positive water flux, $J_w$) and evaporation (negative water flux, $J_w$) is one of the most important environmental factors in the transport of explosive chemicals in soils. Figure 7 shows that with only precipitation occurring, the surface flux is about 3 orders of magnitude less than the case of zero precipitation or evaporation. The case of constant evaporation is about 2 orders of magnitude greater than the zero water flux case. If one examines the model formulation, the mass transport upwards is controlled by the effective diffusion ($D_E$) and the effective chemical velocity ($V_E$). In the constant precipitation case, upward mass transport is a function of $D_E$ minus $V_E$. For the case of zero precipitation/evaporation, upward mass transport is a function of only $D_E$. In the constant evaporation case, upward mass transport is a function of $D_E$ plus $V_E$.

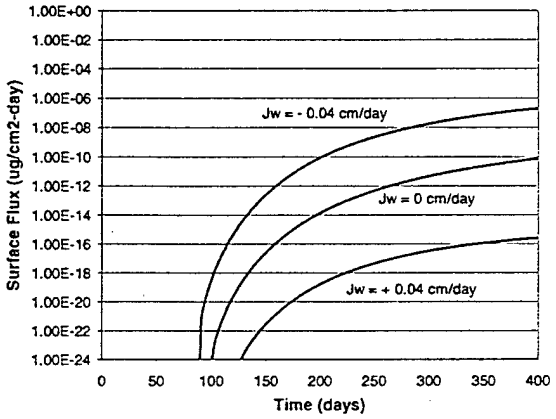


**Figure 7. Effect of Water Flux (Precipitation/Evaporation) on Surface Flux**

The occurrence of a surface soil layer that is greater in concentration than the subsurface soil layers, or a surface "crust", was discussed earlier. Simulations were performed to evaluate what influences the creation of the enhanced concentrations in the surface soil layers. Initial simulation runs (Phelan and Webb, 1997, 1998a) used cyclic precipitation/evaporation that was equal in magnitude; this condition did not create an enhanced surface layer. In order to create an enhanced surface layer, enough of the mass must be transported from deeper regions to the ground surface. This condition only occurs during evaporation conditions. In Figure 8 the buried chemical layer is shown to move upward until it intersects with the ground surface. Figure 9 shows the depth and magnitude of the enhanced layer. It is believed that the air boundary layer and the low Henry's Law Constant ($K_H$) contribute to the formation of the enhanced surface layer (Spencer et al., 1988). It appears that the upward transport through the soil exceeds the loss through the air boundary layer. Transport though the air boundary layer is controlled by diffusion and limited by the transfer of chemical from the aqueous phase to the gas phase by the very low $K_H$.

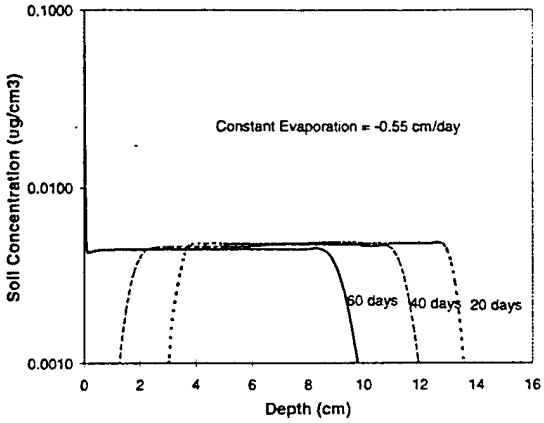


**Figure 8. Upward Transport and Development of a Surface Layer**

Figure 10 shows the effect of developing the enhanced surface layer with 60 days of evaporation (-0.5 cm/day), followed by precipitation for 5 days (0.5 cm/day). The enhanced surface layer found in the top 0.1 cm of soil is transported down leaving just a small enhancement at a depth of about 0.5 cm. Another simulation was run that included the same evaporation and precipitation, but was followed by another 5 day evaporation period (-0.5 cm/day) and the surface enhancement returned at about the same concentration.

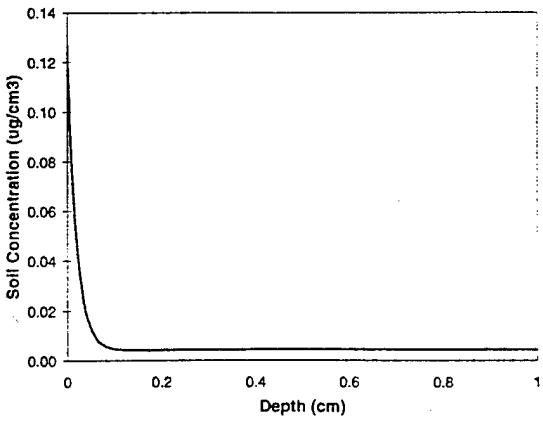


**Figure 9. Detail of the Surface Layer Formed by Evaporation**

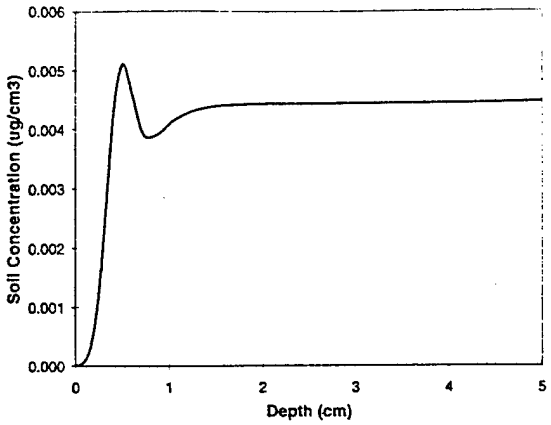


**Figure 10. Effect of Precipitation on the Enhanced Surface Layer**

## DISCUSSION

As a result of these initial results, a more detailed mechanistic numerical model is being developed. This model is being based on TOUGH2 (Pruess, 1991) with modifications pertinent to the landmine application and will be called T2TNT. Modifications being made or planned to be made include:

1. Addition of TNT and DNT vapor components. - Landmines typically emit TNT and DNT vapors. The vapor pressure of DNT is higher than TNT and, if present, will probably reach any chemical sensor before TNT.
2. Dusty Gas Model for gas diffusion. – Gas diffusion is a dominant transport mode for TNT and DNT vapors in the subsurface. Therefore, the Dusty Gas Model (Webb, 1998) will be implemented.
3. Liquid diffusion of dissolved TNT and DNT. – Liquid diffusion is not present in the standard version, although some special EOS modules include it. Liquid diffusion analogous to gas diffusion will be included because of the significant chemical concentration in the liquid phase.
4. Partition coefficient as a function of saturation. – The solid partition coefficient may be a strong function of saturation, especially at low moisture content where the partition coefficient may increase dramatically (Petersen, et al. 1995).
5. Boundary layer specifications for transport at soil surface. – For transport from the soil to the atmosphere, a boundary layer for heat and mass transfer will be implemented. The exact modifications are still being developed.
6. Precipitation and evaporation boundary conditions. – Precipitation boundary conditions will be added. The evaporation boundary condition may simply involve specification of a boundary layer and a boundary relative humidity, which will be time dependent.
7. Diurnal and seasonal variations in atmospheric conditions – In order to simulate daily and seasonal fluctuations, time-dependent boundary conditions for the pressure, temperature, and relative humidity will be implemented.

The resulting code will be used to develop an effective operational strategy for the design and deployment of landmine chemical sensors. The code will also be used within the ITOUGH framework to assist in the design of column experiments to be conducted at New Mexico Tech during the next few years. T2TNT will play an important part in the effective use of chemical sensors for landmine detection and removal.

## CONCLUSIONS

The environmental fate and transport of chemical signatures from landmines is important for the design and operation of chemical sensors. The explosive vapors are predominantly found sorbed to soil particles or in the liquid phase; only a small fraction is present in the gas phase. As a result, diffusion and advection of the liquid water dominates the transport of the chemicals from the buried landmine to the land surface. Precipitation and evaporation also strongly influence the movement of the chemical signature.

The results of initial screening studies have confirmed the influence of environmental conditions and soil parameters. The burial depth of the landmine is a significant factor. For shallow landmines, the chemical appears much sooner and at a much higher concentration than for deeper landmines. Precipitation and evaporation have a significant effect on the transport of TNT in the subsurface. The chemical concentration at the surface varies by many orders of magnitudes depending upon whether precipitation or evaporation is occurring. Under evaporation conditions, a surface "crust" can form where the surface concentration is higher than in the subsurface. These conditions would greatly enhance the detection capability of chemical sensors. As a result, a mechanistic numerical model based on TOUGH2 (Pruess, 1991), called T2TNT, is currently being developed. T2TNT will include a number of modifications and enhancements that should be of general interest to many TOUGH2 users. The use of T2TNT in understanding the environmental fate and transport of TNT in the soil will contribute to the improved design, performance and operation of chemical sensors in the detection of buried landmines.

## NOMENCLATURE

a air volume fraction = $\phi - \theta$
D diffusion coefficient
$K_d$ distribution coefficient for sorption
$K_H$ Henry's Law constant
$\theta$ volumetric moisture content
$\phi$ porosity
$\rho$ density

Subscripts
E effective
g gas
l liquid

Superscripts
a air
w water


## ACKNOWLEDGMENTS

This work was performed with internal laboratory-directed research and development funds at Sandia National Laboratories to explore applications for miniaturized chemical sensors. Follow-on work to develop a numerical model is just beginning with funds from the Strategic Environmental Research and Development Program (SERDP) for application to unexploded ordnance chemical sensing and from the Defense Advanced Research Projects Agency (DARPA) for application to buried landmines. Sandia is a multiprogram laboratory operated by Sandia Corporation, a Lockheed Martin Company, for the United States Department of Energy under Contract DE-AC04-94AL85000.


## REFERENCES


Jury, W.A., Spencer, W.F., and Farmer, W.J., 1983, "Behavior Assessment Model for Trace Organics in Soil: I. Model Description," *J. Environ. Qual.*, 12:558-564.

Jury, W.A., Farmer, W.J., and Spencer, W.F., 1984a, "Behavior Assessment Model for Trace Organics in Soil: II. Chemical Classification and Parameter Sensitivity," *J. Environ. Qual.*, 13:567-572.

Jury, W.A., Spencer, W.F., and Farmer. W.J., 1984b, "Behavior Assessment Model for Trace Organics in Soil: III. Application of Screening Model," *J. Environ. Qual.*, 13:573-579.

Jury, W.A., Spencer, W.F., and Farmer, W.J., 1984c, "Behavior Assessment Model for Trace Organics in Soil: IV. Review of Experimental Evidence," *J. Environ. Qual.*, 13:580-586.

Jury, W.A., Russo, D., Streile, G., and Abd, H., 1990, "Evaluation of Volatilization by Organic Chemicals Residing Below the Surface," *Water Resour. Res.*, 26:13-20.

Millington, R.J., and Quirk, J.M., 1961, "Permeability of porous solids," *Trans. Faraday Soc.*, 57:1200-1207.

Petersen, L.W., Rolston, D.E., Moldrop, P., and Yamaguchi, T., 1994, "Volatile Organic Vapor Diffusion and Adsorption in Soils," *J. Environ. Qual.* 23:799-805.

Phelan, J.M. and Webb, S.W., 1997, *Environmental Fate and Transport of Chemical Signatures from Buried Landmines - Screening Model Formulation and Initial Simulations*, Sandia National Laboratories, SAND97-1426.

Phelan, J.M. and Webb, S.W., 1998a, "Chemical Detection of Buried Landmines," Proceedings of the 3rd International Symposium on Technology and the Mine Problem, April 6-9, 1998. Mine Warfare Association.

Phelan, J.M. and Webb, S.W., 1998b, "Simulation of the Environmental Fate and Transport of Chemical Signatures from Buried Landmines," International Symposium on Aerospace/Defense Sensing, Simulation, and Controls, Orlando, FL, April 13-17, 1998, SPIE.

Pruess, K., 1991, *TOUGH2 - A General-Purpose Numerical Simulator for Multiphase Fluid and Heat Flow*, LBL-29400, Lawrence Berkeley Laboratory.

Spencer, W.F., Cliath, M.M., Jury, W.A., and Zhang, L.-Z., 1988, "Volatilization of Organic Chemicals from Soil as Related to Their Henry's Law Constants," *J. Environ. Qual.* 17:504-509.

Webb, S.W., 1998, "*Gas Diffusion in Porous Media: Comparison of Models*," TOUGH '98 Workshop, Lawrence Berkeley National Laboratory, May 4-6, 1998.

# APPENDIX D

Jury, W.A. and L. Guo, 1998. One Dimensional Transport of Vapor From A Buried Landmine. Project report. University of California, Riverside. July 20, 1998.

July 20, 1998

# One Dimensional Transport of Vapor From a Buried Land Mine

William Jury and Lei Guo, University of California, Riverside

## Introduction

Constructing a general strategy for detecting emissions at the soil surface from buried land mines requires an understanding of the effect of soil and environmental conditions on signal strength and location. While too simple to simulate in detail the actual transport and reaction processes occurring in a natural setting, screening models are useful tools for elucidating the relationships between soil parameters and output characteristics of interest. This first model is one dimensional, representing steady emissions from a buried source of TNT vapor. It is an extension of the screening model papers of Jury et al. (1983; 1984abc; 1990)

## Model Description

**Transport Equations:** The analysis of the original screening model paper (Jury et al. 1983) produces the familiar transport equation

$$\frac{\partial C_t}{\partial t} = D_E \frac{\partial^2 C_t}{\partial z^2} - V_E \frac{\partial C_t}{\partial z} - \mu_E C_t \tag{1}$$

where

$$C_t = \rho_b C_a + \theta C_\ell + a C_g \tag{2}$$

is the total concentration of TNT in the soil, $C_a, C_\ell, C_g$ are the concentrations in the sorbed, dissolved, and vapor phases, respectively, $\rho_b$ is soil bulk density, and $\theta$ is volumetric water content.

The effective diffusion coefficient $D_E$ is the combined diffusion in the dissolved and gaseous phases, given by

$$D_E = \frac{K_H \xi_g D_g^{air} + \xi_w D_\ell^w}{R} \tag{3}$$

where $K_H$ is the dimensionless Henry's constant, $D_g^{air}, D_\ell^w$ are the binary diffusion coefficients of the chemical in air and water respectively, and $\xi_g, \xi_w$ are the tortuosity factors, given by the modified Millington-Quirk tortuosity law

$$\xi(x) = \frac{x^2}{\phi^{4/3}}; \quad x = \theta, a \tag{4}$$

(Jin and Jury, 1993). The effective solute velocity is given by

$$V_E = \frac{J_w}{R} \tag{5}$$

where $J_w$ is the water flux rate.

The retardation factor $R$ is given by

$$R = 1 + \frac{\rho_b K_d}{\theta} \tag{6}$$

where $K_d$ is the slope of the linearized adsorption isotherm (the distribution coefficient).

The upper boundary condition is assumed to be controlled by diffusion through a stagnant air boundary layer above the soil surface, and is expressed as:

$$-D_E\frac{\partial C_t}{\partial z} + V_E C_t = H_E C_t \qquad z = 0 \tag{7}$$

where $H_E$ is the effective mass transfer coefficient through the boundary layer, given by

$$H_E = \frac{K_H D_g^{air}}{R d_{bl}} \tag{8}$$

where $d_{bl}$ is the boundary layer thickness, typically about 0.5 cm (Jury et al. 1984c).

**Constant Flux Emission From the Land Mine:** The lower boundary condition describing emission of a constant flux from the land mine is expressed mathematically as

$$-D_E\frac{\partial C_t}{\partial z} + V_E C_t = F \qquad z = -P \tag{9}$$

where $F$ is the flux of gas across the plane at $z = -P$.

The system described by these equations will come to a steady state eventually. We can easily solve for the steady profile and flux emission from the surface. At steady state, the concentration at $z = -P$ will also be constant, so that the solution will also apply to the case where the bottom of the profile is held at a constant value.

The steady form of the transport equation is

$$D_E\frac{d^2 C_t}{dz^2} - V_E\frac{dC_t}{dz} - \mu_E C_t = 0 \tag{10}$$

which has the solution

$$C_t(z) = A\exp[\frac{V_E z}{2D_E}(1-\xi)] + B\exp[\frac{V_E z}{2D_E}(1+\xi)] \quad ; \quad \xi = \left(1 + \frac{4\mu_E D_E}{V_E^2}\right)^{1/2} \tag{11}$$

The corresponding general solution for the flux is given by

$$J_S(z) = \frac{V_E}{2}\Big[A(1+\xi)\exp[\frac{V_E z}{2D_E}(1-\xi)] + B(1-\xi)\exp[\frac{V_E z}{2D_E}(1+\xi)]\Big] \tag{12}$$

The boundary conditions (2-3) can be applied to (11)-(12), producing

$$C_t(z) = \frac{2F}{\beta V_E}\Big[(2H_E + V_E(\xi-1))\exp[\Omega z(1-\xi)] - (2H_E - V_E(\xi+1))\exp[\Omega z(1+\xi)]\Big] \quad \Omega = \frac{V_E}{2D_E} \tag{13}$$

$$J_S(z) = \frac{F}{\beta}\Big[(2H_E(1+\xi) + \frac{4\mu_E D_E}{V_E})\exp[\Omega z(1-\xi)] + (2H_E(\xi-1) - \frac{4\mu_E D_E}{V_E})\exp[\Omega z(1+\xi)]\Big] \tag{14}$$

where

$$\beta = (2H_E(1+\xi) + \frac{4\mu_E D_E}{V_E})\exp[-\Omega P(1-\xi)] + (2H_E(\xi-1) - \frac{4\mu_E D_E}{V_E})\exp[-\Omega P(1+\xi)] \tag{15}$$

Of particular interest are the flux from the surface

$$J_S(0) = \frac{4H_E\xi F}{\beta} \tag{16}$$

and the concentration at $z = -P$

$$C_t(-P) = C_0 = \frac{2F\eta}{\beta V_E} \tag{17}$$

where

$$\eta = (2H_E + V_E(\xi - 1))\exp[-\Omega P(1-\xi)] - (2H_E - V_E(\xi+1))\exp[-\Omega P(1+\xi)] \tag{18}$$

Note that the surface concentration is given by $J_S(0)/H_E$.

We can rewrite (16) in terms of three dimensionless variables

$$\mathcal{J} = \frac{\mathrm{J_S(0)}}{\mathrm{F}} = \frac{2}{[1 + 1/\xi + 2\delta/(\omega\gamma)]\mathrm{e}^{-\gamma/2*(1-\xi)} + [1 - 1/\xi - 2\delta/(\omega\gamma)]\mathrm{e}^{-\gamma/2*(1+\xi)}} \tag{19}$$

where

$$\gamma = \frac{PV_E}{D_E} \quad \delta = \frac{P\mu_E}{V_E} \quad \omega = \frac{H_E}{V_E} \quad \xi = \sqrt{1 + \frac{4\delta}{\gamma}} \tag{20}$$

In the case where there is no evaporation ($V_E = 0$), this reduces to

$$\mathcal{J} = \frac{\mathrm{J_S(0)}}{\mathrm{F}} = \frac{2}{(1+\kappa\epsilon)\mathrm{e}^{\kappa} + (1-\kappa\epsilon)\mathrm{e}^{-\kappa}} \quad \kappa = \mathrm{P}\sqrt{\frac{\mu_e}{\mathrm{D_E}}} \quad \epsilon = \frac{\mathrm{D_E}}{\mathrm{PH_E}} \tag{21}$$

Focusing first on (21), we interpret $\kappa$ as the ratio of the diffusion time (i.e. the travel time to the surface) to the decay time. A large value of $\kappa$ will mean that most of the flux will be consumed en route to the surface. The second dimensionless variable $\epsilon$ can be interpreted as the ratio of the transfer coefficient to the boundary layer and the transfer coefficient through the boundary layer. Using all of the definitions for these coefficients, we can express $\epsilon$ as

$$\epsilon = \frac{d_B}{P}[\xi_v(a) + \zeta\xi_w(\theta)] \quad \zeta = \frac{D_\ell^{water}}{K_H D_g^{air}} \approx \frac{10^{-4}}{K_H} \tag{22}$$

where $\xi_v(a)$ is the tortuosity factor for the gas phase in soil, $\xi_w(\theta)$ is the tortuosity factor for the dissolved phase in soil, $d_B \approx 0.5$ cm is the thickness of the air boundary layer$K_H$ is Henrys constant, and $D_\ell^{water}, D_g^{air}$ are the diffusion coefficient of the chemical in water and air, respectively. The parameter $\zeta$ expresses the chemical's preference for the dissolved or vapor phase.

**Constant Concentration at the Depth of the Land Mine:** The boundary condition for the case of a constant concentration at the lower boundary is given by

$$C_t(-P) = C_0 \tag{23}$$

We may write down the solutions for the steady profile and flux for the case of constant concentration (23) using (17)

$$C_t(z) = \frac{C_0}{\eta}\Big[(2H_E + V_E(\xi-1))\exp[\Omega z(1-\xi)] - (2H_E - V_E(\xi+1))\exp[\Omega z(1+\xi)]\Big] \tag{24}$$

$$J_S(z) = \frac{V_E C_0}{2\eta}\Big[(2H_E(1+\xi) + \frac{4\mu_E D_E}{V_E})\exp[\Omega z(1-\xi)] + (2H_E(\xi-1) - \frac{4\mu_E D_E}{V_E})\exp[\Omega z(1+\xi)]\Big] \tag{25}$$

$$J_S(0) = \frac{2H_E\xi V_E C_0}{\eta} \tag{26}$$

This solution will later be superimposed on the constant flux solution to allow an analysis of the relative importance of the two signals for typical values of the boundary parameters.

# Results

**Constant Flux Emissions:** Calculations are performed for TNT using values of $K_H = 6 \times 10^{-7}$ and $K_{oc} = 300$ cm$^3$/g for a range of half lives. Figure 1 shows the predicted relative flux from the surface as a function of the steady upward evaporation rate, showing a significant enhancement due to upward advection. Note that the rate of loss is higher when the water

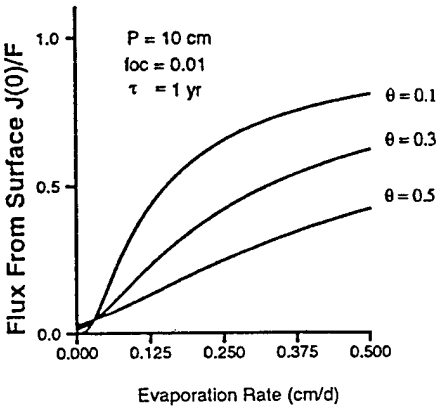


Figure 1: Flux from the surface as a function of evaporation rate for the case of a buried mine at 10 cm depth. Soil conditions: $\rho_b$ =1.5 g/cm$^3$, f$_{oc}$ = .01 Chemical properties: $K_{oc}$=300 cm$^3$/g, $K_H = 6 \times 10^{-7}$, $\tau_{1/2} = 1$ yr$^{-1}$

content is lower. This is because the transport is primarily in the dissolved phase, and the travel time to the surface by advection is inversely proportional to $\theta$.

Figure 2 shows the predicted relative flux from the surface as a function of water content for various values of evaporation. At high evaporation rate, the loss is dominated by advec-

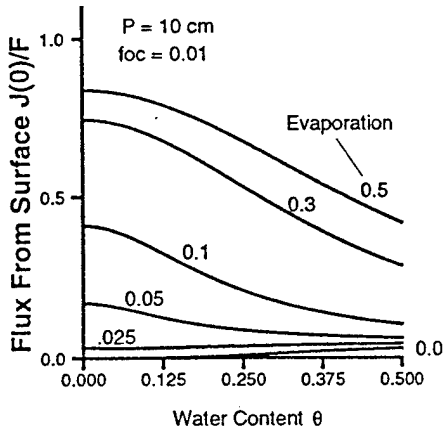


Figure 2: Flux from the surface as a function of water content for the case of a buried mine at 10 cm depth. Soil conditions: $\rho_b$ =1.5 g/cm$^3$, f$_{oc}$ = .01 Chemical properties: $K_{oc}$=300 cm$^3$/g, $K_H = 6 \times 10^{-7}$, $\tau_{1/2} = 1$ yr$^{-1}$

tion, and therefore increases with decreasing $\theta$. At low evaporation, the system shifts over to diffusion-dominated, showing a modest increase with increasing $\theta$. Vapor diffusion is insignificant compared to liquid diffusion over much of the range of water content because of the low Henry's constant. The ratio $r$ of liquid to vapor diffusive transport for a given concentration

gradient is given by

$$r = \frac{D_\ell^{soil}}{K_H D_g^{soil}} = \frac{D_\ell^{water}\xi_w(\theta)}{K_H D_g^{air}\xi_g(a)} \approx \frac{10^{-4}}{K_H}[\frac{S}{(1-S)}]^2 \quad S = \frac{\theta}{\phi} = 1 - \frac{a}{\phi} \tag{27}$$

Table 1 shows various values of r calculated with (27) as a function of S.

| S | r | S | r |
|---|---|---|---|
| 1.0 | $\infty$ | 0.2 | 10 |
| 0.6 | 375 | 0.071 | 1 |
| 0.4 | 74 | 0.0 | 0.0 |

Table 1: Ratio of liquid to vapor diffusion for TNT as a function of water saturation

Figure 3 shows the predicted relative flux from the surface as a function of organic carbon fraction.

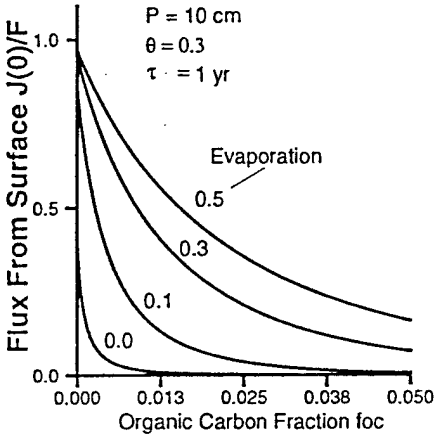


Figure 3: Flux from the surface as a function of organic carbon fraction for the case of a buried mine at 10 cm depth. Soil conditions: $\rho_b$ =1.5 g/cm$^3$, $\theta = 0.3$; Chemical properties: $K_{oc}$=300 cm$^3$/g, $K_H = 6 \times 10^{-7}$, $\tau_{1/2} = 1$ yr$^{-1}$

Since the value used for $K_{oc}$ is 300, the range of $K_d$ simulated in this figure is 0 to 15. This figure holds no surprises, merely illustrating the effect of increasing residence time on decreasing volatilization loss because of degradation.

Figure 4 shows the predicted relative flux from the surface as a function of the chemical half life. Half life is obviously a sensitive parameter, and unfortunately is also one for which no data is available. Significant in Figure 4 is the much smaller loss when no upward flow is occurring. The enhanced loss under upward water flow is caused by accumulation of TNT at the surface by deposition from the evaporation process, which causes a buildup of vapor concentration and an increased driving force for vapor diffusion across the boundary layer.

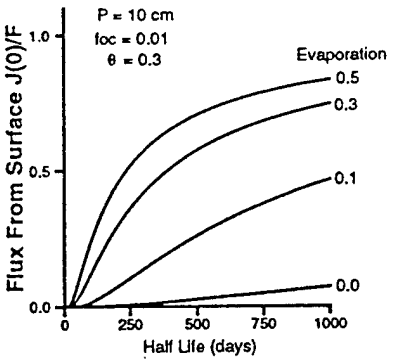


Figure 4: Flux from the surface as a function of chemical half life.

Figure 5 shows the predicted relative flux from the surface as a function of water content for the case of no evaporation (note expanded scale).

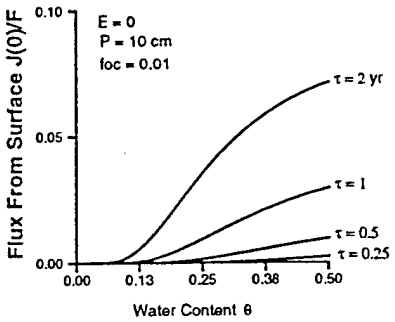


Figure 5: Flux from the surface as a function of water content and no evaporation.

Figure 6 shows the falloff in flux with depth of land mine, which is not too significant in the 5-15 cm range.

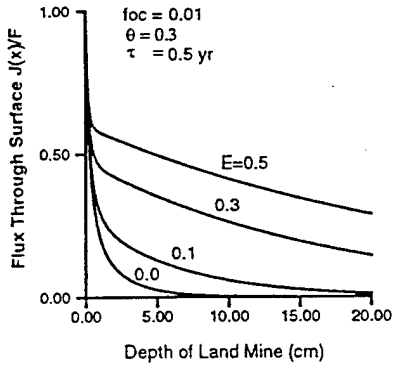


Figure 6: Flux from surface as a function of land mine depth.

**The Surface Concentration:** According to the model, the total surface concentration is given by $J_S(0)/H_E$. Thus, all of the graph results for the surface flux are proportional to the surface concentration. Since the Y-axis gives relative flux, we can convert to actual surface concentration by multiplying the axis value by $F/H_E$ As a rough estimate, we can use the following data (Table 2) from the report.

| Parameter | Value | Units |
|---|---|---|
| $K_H$ | $6 \times 10^{-7}$ | - |
| $K_d$ | 5 | $cm^3/g$ |
| $R_\ell$ | 15 | - |
| $h$ | 8600 | cm/d |
| $H_E$ | $3.5 \times 10^{-4}$ | cm/d |
| $F$ | $10^{-16} - 10^{-18}$ | $g/cm^2/s$ |
| $F/H_E$ | 0.25-25 | $\mu g/L$ |

Table 2: Representative parameters for TNT adopted from the report: *SAND97-1426*

The concentration profile in the soil can build up substantially near the surface because the boundary layer is the limiting step to loss from the soil. Figure 7 shows a plot of concentration (log scale) versus depth as a function of water content for the highest rate (E=0.5 cm/d) of evaporation.

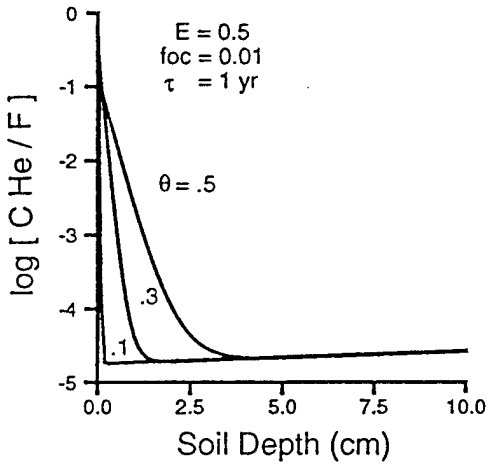


Figure 7: Soil concentration profile as a function of water content for the case of a buried mine at 10 cm depth. Soil conditions: $E = 0.5$ cm/d, $\rho_b$ =1.5 g/cm$^3$, $f_{oc} = 0.01$; Chemical properties: $K_{oc}$=300 cm$^3$/g, $K_H = 6 \times 10^{-7}$

As the evaporation rate declines, the profile becomes less extreme, as shown in Figure 8.

## Discussion

The one dimensional simulations are of limited value for estimating the magnitude of the surface flux, but they do show the main features the govern the true process. Compounds such as TNT, with extremely low Henrys constant, will be substantially influenced by upward flow, both because advection will provide the most rapid transport pathway to the surface, and because the air boundary layer will impede removal from the surface.

The loss of chemical under zero evaporation forms a lower limit to accumulation at the surface, where over time the concentration in the soil will form a decreasing gradient to the surface. Table 3 shows various values of $H_E C(0)/F$ for the case of zero evaporation, a water content of 0.3, a depth of 10 cm for the upper surface of the land mine, and an organic carbon

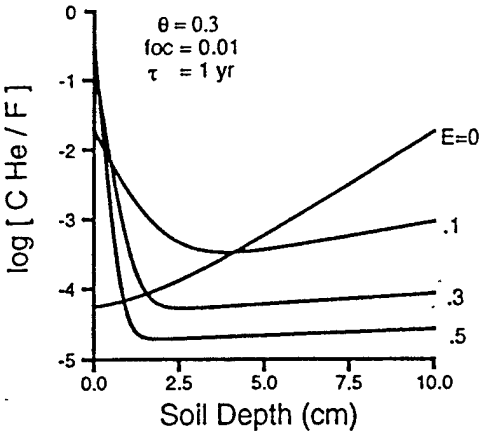


Figure 8: Soil concentration profile as a function of evaporation rate for the case of a buried mine at 10 cm depth. Soil conditions: $\theta$ =0.3, $\rho_b$ =1.5 g/cm$^3$, $f_{oc}$ = 0.01; Chemical properties: $K_{oc}$=300 cm$^3$/g, $K_H = 6 \times 10^{-7}$

fraction of 0.01. These can be multiplied by the values of $F/H_E$ in Table 2 to estimate surface concentrations.

| $\tau$ | $H_E C(0)/F$ |
|---|---|
| 3 | .072 |
| 2 | .045 |
| 1 | .014 |
| .5 | .003 |
| .25 | .0003 |

Table 3: Estimated values of the dimensionless surface concentration for various values of the half life for the case of zero upward flow of water to the surface.

**Constant Concentration at Lower Boundary:** The relation between the flux value and the corresponding concentration, as expressed in (17), is given in Figure 9 for representative conditions.

This relationship is nearly linear under a range of soil and environmental conditions. For the case where evaporation is nonzero, it becomes

$$F \approx \frac{[H_E V_E(1+\xi) + 2\mu_E D_E]}{[2H_E + V_E(\xi - 1)]} C_0 \tag{28}$$

and if evaporation is zero it becomes simply

$$F \approx \sqrt{\mu_E D_E} C_0 \tag{29}$$

For the conditions represented in Figure 9, the range of F values ($10^{-16} - 10^{-18}$ g/cm$^2$/s) typical of land mine emissions correspond to soil concentrations $C_0$ at the lower boundary of $7.1 \times 10^{-4} - 7.5 \times 10^{-6}$ $\mu$ g/cm$^3$. In other words, a soil concentration of this magnitude would give rise to the same surface emissions as the flux in this range. Figure 10 illustrates the case where both land mine flux emission of TNT and constant soil concentrations are present, where

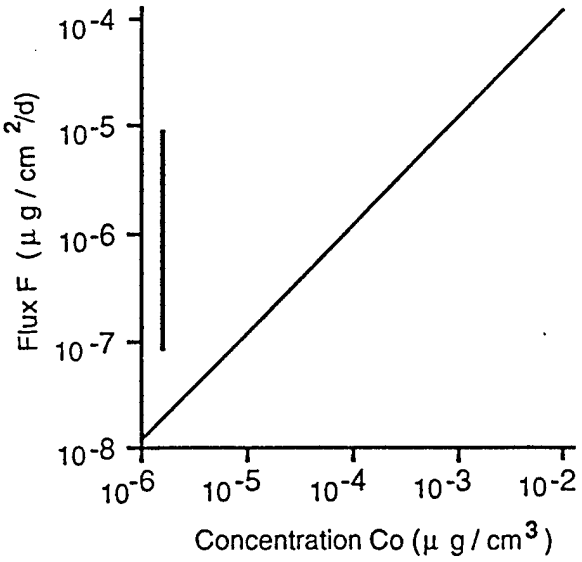


Figure 9: Relation between the flux F from depth $z = -P$ and the concentration $C_0$ at that depth. Solid vertical line brackets the range of fluxes $F \approx 10^{-16} - 10^{-18}$ g/cm$^2$/s given in report *SAND97-1426* . Soil conditions: $\rho_b$ =1.5 g/cm$^3$, $\theta = 0.3$, $f_{oc} = 0.01$; Chemical properties: $K_{oc}$=300 cm$^3$/g, $K_H = 6 \times 10^{-7}$, $\tau_{1/2} = 1$ yr$^{-1}$

F= $10^{-16}$ g/cm$^2$/s and $C_0 = 4.6 \times 10^{-3}$ $\mu$ g/cm$^3$, the latter taken from the screening calculations of the Sandia report *SAND97-1426* . As seen in this figure, under these conditions the signal from the soil concentrations at 10 cm would dominate the surface emissions.

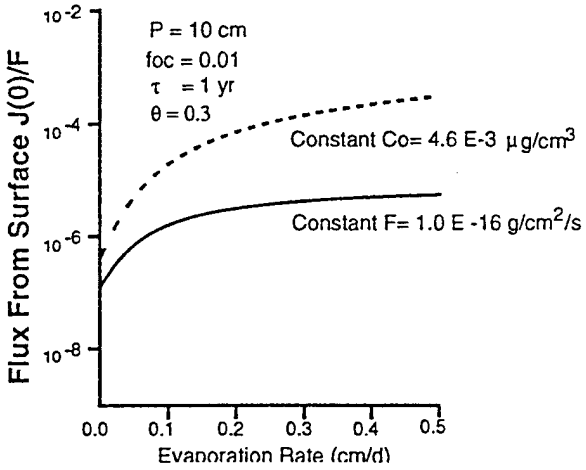


Figure 10: Flux at the surface arising from both land mine flux emissions F= $10^{-16}$ g/cm$^2$/s and soil concentrations $C_0 = 4.6 \times 10^{-3}$ $\mu$ g/cm$^3$ at $z = -P$.

**Transient Conditions:** The transient problem is more complex to analyse, but an approximate estimate of the time required to reach equilibrium can be calculated for the case of zero evaporation (the longest time to reach equilibrium) from the diffusion time

$$t_d = \frac{P^2}{16 D_E} \tag{30}$$

Table 4 gives the equilibration times calculated for TNT using Eq. 18.

| $\theta$ | $t_d$ (d) |
|---|---|
| .1 | 919 |
| .2 | 244 |
| .3 | 115 |
| .4 | 68 |
| .5 | 46 |

Table 4: Approximate time to reach steady state for the case of zero evaporation for the conditions $f_{oc} = 0.005, P = 10., K_H = 6 \times 10^{-7}, K_{oc} = 300.$

Prior to these times after insertion of the signal at the depth of the land mine, the fluxes and concentrations at the surface would be less than the amounts calculated from the steady model.

## References Cited


Jin, Yan, and William A. Jury, 1996. Measurement and prediction of gaseous diffusion coefficients in soil. Soil Sci. Soc. Amer. J. 60:66-71.

Jury, W. A., W. F. Spencer, and W. J. Farmer, 1983. Model for assessing behavior of pesticides and other trace organics using benchmark properties. I. Description of model. J. Environ. Qual. 12:558-564.

Jury, W. A., W. J. Farmer, and W. F. Spencer, 1984. Model for assessing behavior of pesticides and other trace organics using benchmark properties. II. Chemical classification and parameter sensitivity. J. Environ. Qual. 13:567-572.

Jury, W. A., W. F. Spencer, and W. J. Farmer, 1984. Model for assessing behavior of pesticides and other trace organics using benchmark properties. III. Application of screening model. J. Environ. Qual. 13:573-579.

Jury, W. A., W. F. Spencer, and W. J. Farmer, 1984. Model for assessing behavior of pesticides and other trace organics using benchmark properties. IV. Review of experimental evidence. J. Environ. Qual. 13:580-585.

Jury W. A.,D. Russo, G. Streile, and H. Elabd, 1990. Evaluation of volatilization by organic chemicals residing below the soil surface. Water Resour. Res. 26:13-20.

# APPENDIX E

Jury, W.A. and L. Guo, 1998. Two Dimensional Transport of Vapor From A Buried Landmine. Draft project report. University of California, Riverside. September 1, 1998.

# Two Dimensional Transport of Vapor from a Buried Land Mine

William Jury and Lei Guo, University of California, Riverside

## Introduction

Constructing a general strategy for detecting emissions at the soil surface from buried land mines requires an understanding of the effect of soil and environmental conditions on signal strength and location. While too simple to simulate in detail the actual transport and reaction processes occurring in a natural setting, screening models are useful tools for elucidating the relationships between soil parameters and output characteristics of interest. In a previous report we examined the release of TNT vapor from a subsurface land mine using a one-dimensional model. In this report we use a two dimensional model, representing steady emissions from a buried plane source of TNT vapor.

Figure 1 shows a schematic of the system represented with the model. The land mine is characterized by a constant flux plane at $z = -P$, which emits a constant upward flux within $-W < x < W$, and zero upward flux outside of this range. At a substantial lateral distance $x = \pm L$, the horizontal flux is set equal to zero. At the surface, chemical vapor can volatilize by diffusing through a stagnant air boundary layer of thickness $\delta z = d_{bl}$, above which the air is assumed to be at zero chemical concentration.

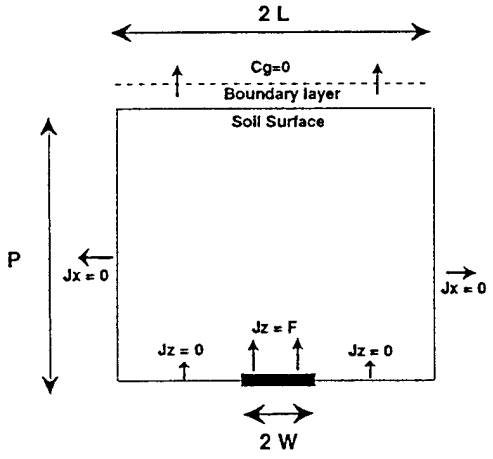


Figure 1: Schematic of the soil regime represented by the model

# Transport Equations

Two dimensional transport of TNT by vapor and liquid diffusion and liquid advection may be described by

$$\frac{\partial C_t}{\partial t} = D_E \frac{\partial^2 C_t}{\partial z^2} + D_E \frac{\partial^2 C_t}{\partial x^2} - V_E \frac{\partial C_t}{\partial z} - \mu_E C_t \tag{1}$$

where

$$C_t = \rho_b C_a + \theta C_\ell + a C_g \tag{2}$$

is the total concentration of TNT in the soil, $C_a, C_\ell, C_g$ are the concentrations in the sorbed, dissolved, and vapor phases, respectively, $\rho_b$ is soil bulk density, and $\theta$ is volumetric water content.

The effective diffusion coefficient $D_E$ is the combined diffusion in the dissolved and gaseous phases, given by

$$D_E = \frac{K_H \xi_g D_g^{air} + \xi_w D_\ell^w}{R} \tag{3}$$

where $K_H$ is the dimensionless Henry's constant, $D_g^{air}, D_\ell^w$ are the binary diffusion coefficients of the chemical in air and water respectively, and $\xi_g, \xi_w$ are the tortuosity factors, given by the modified Millington-Quirk tortuosity law

$$\xi(x) = \frac{x^2}{\phi^{4/3}}; \quad x = \theta, a \tag{4}$$

(Jin and Jury, 1993).

Figure 2 shows a plot of $D_E$ versus $\theta$ for TNT for several values of organic carbon fraction $f_{oc}$. Because of its low Henrys constant, TNT is dominated by liquid diffusion over most of the range of water content, and has an effective value that is nearly 200 times larger at saturation than at extremely low water content.

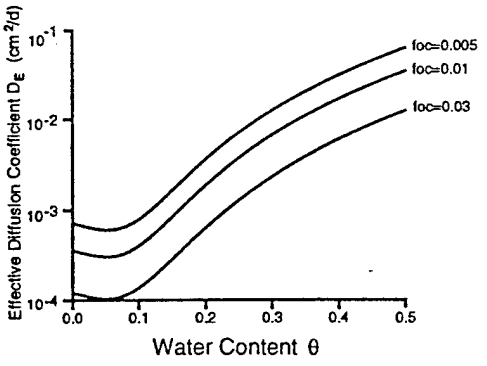


Figure 2: Effective diffusion coefficient of TNT calculated using Eq. (3).

The effective solute velocity is given by

$$V_E = \frac{J_{wz}}{R} \tag{5}$$

where $J_{wz}$ is the water flux rate, assumed to be one dimensional in the vertical direction.

The retardation factor $R$ is given by

$$R = 1 + \frac{\rho_b K_d}{\theta} \tag{6}$$

where $K_d$ is the slope of the linearized adsorption isotherm (the distribution coefficient).

The upper boundary condition is assumed to be controlled by diffusion through a stagnant air boundary layer above the soil surface, and is expressed as:

$$-D_E\frac{\partial C_t}{\partial z} + V_E C_t = H_E C_t \qquad z = 0; \quad 0 < x < L \tag{7}$$

where $H_E$ is the effective mass transfer coefficient through the boundary layer, given by

$$H_E = \frac{K_H D_g^{air}}{R d_{bl}} \tag{8}$$

where $d_{bl}$ is the boundary layer thickness, typically about 0.5 cm (Jury et al. 1984c).

**Constant Flux Emission From the Land Mine:** The lower boundary condition describing emission of a constant flux from the land mine is expressed mathematically as

$$-D_E\frac{\partial C_t}{\partial z} + V_E C_t = f(x) \qquad z = -P; 0 < x < L \tag{9}$$

where $f(x)$ is an arbitrary function representing the upward flux of TNT across the plane at $z = -P$.

The planes formed by the lines $x = 0$ and $x = L$ are planes of symmetry, which obey the conditions

$$\frac{\partial C_t}{\partial x} = 0 \qquad x = 0; \quad -P < z < 0 \tag{10}$$

$$\frac{\partial C_t}{\partial x} = 0 \qquad x = L; \quad -P < z < 0 \tag{11}$$

The system described by these equations will come to a steady state eventually. We can solve for the steady profile and flux emission by using separation of variables and Fourier series. We first let

$$C_t(x, z) = Z(z)X(x) \tag{12}$$

and plug this into the steady state form of the transport equation, with the result

$$D_E X\frac{d^2Z}{dz^2} - V_E X\frac{dZ}{dz} - \mu_E XZ + D_E Z\frac{d^2X}{dx^2} = 0 \tag{13}$$

Rearranging, we obtain

$$\frac{D_E}{X}\frac{d^2X}{dx^2} = \mu_E + \frac{V_E}{Z}\frac{dZ}{dz} - \frac{D_E}{Z}\frac{d^2Z}{dz^2} = -\omega^2 \tag{14}$$

where $\omega$ must be a constant. This produces two equations to solve.

$$D_E\frac{d^2X}{dx^2} + \omega^2 X = 0 \tag{15}$$

$$D_E\frac{d^2Z}{dz^2} - V_E\frac{dZ}{dz} - (\omega^2 + \mu_E)Z = 0 \tag{16}$$

The general solution to (15) is

$$X(x) = A_x\cos(\beta x) + B_x\cos(\beta x) \quad ; \quad \beta = \frac{\omega}{\sqrt{D_E}} \tag{17}$$

and the general solution to (16) is

$$Z(z) = A_z \exp[\frac{V_E z}{2D_E}(1-\xi)] + B_z \exp[\frac{V_E z}{2D_E}(1+\xi)] \quad ; \quad \xi = \left(1 + \frac{4(\omega^2+\mu_E)D_E}{V_E^2}\right)^{1/2} \tag{18}$$

The boundary conditions (5-6) can be applied to (17), producing

$$A_x = 0 \quad \text{and} \quad \beta = \frac{N\pi}{L} \quad N = 0, 1, 2, ... \tag{19}$$

This result means that there are an infinite number of values of $\beta, \xi$ which are functions now of $N$. Subsequently, any parameter depending on $N$ will have a subscript. In particular, all $X_N(x)$ satisfying

$$X_N(x) = B_{xN} \cos(\frac{N\pi x}{L}) \quad N = 0, 1, 2, ... \tag{20}$$

obey both the equation and the boundary conditions governing $X(x)$.

Applying the condition (7) to (18), we obtain

$$[\frac{V_E}{2}(1+\xi_N) - H_E]A_z + [\frac{V_E}{2}(1-\xi_N) - H_E]B_z = 0 \rightarrow B_z = \gamma_N A_z \tag{21}$$

where

$$\gamma_N = \frac{2H_E - V_E(1+\xi_N)}{V_E(1-\xi_N) - 2H_E} \tag{22}$$

and the most general form of $Z(z)$ satisfying the equation and the surface boundary condition is

$$Z_N(z) = A_{zN}\{\exp[\frac{V_E z}{2D_E}(1-\xi_N)] + \gamma_N \exp[\frac{V_E z}{2D_E}(1+\xi_N)]\} \tag{23}$$

By linear superposition, the sum of solutions to the linear transport equation is also a solution. Therefore, the most general solution to the original equation and all of the boundary conditions used thus far is

$$C_t(x,z) = \Sigma_{n=0}^{\infty} E_N Z_N(z) X_N(x) \quad E_N = A_{zN} B_{xN} \tag{24}$$

$$J_{wz}(x,z) = \Sigma_{n=0}^{\infty} E_N Q_N(z) X_N(x) \tag{25}$$

where

$$Q_N(z) = \frac{V_E}{2}[(1+\xi_N)\exp[\frac{V_E z}{2D_E}(1-\xi_N) + \gamma_N(1-\xi_N)\exp[\frac{V_E z}{2D_E}(1+\xi_N)] \tag{26}$$

Plugging in for the functions, we have

$$C_t(x,z) = \Sigma_{n=0}^{\infty} E_N \exp[\frac{V_E z}{2D_E}(1-\xi_N)] + \gamma_N \exp[\frac{V_E z}{2D_E}(1+\xi_N)] \cos[\frac{N\pi x}{L}] \tag{27}$$

Equation (27) has an infinite number of unknowns $E_N$, which are evaluated by applying the lower boundary condition (9) to the equation and making use of the orthogonal property of the cosine functions. Thus,

$$f(x) = \Sigma_{n=0}^{\infty} E_N Q_N(-P) \cos[\frac{N\pi x}{L}] \tag{28}$$

where $Q_N(-P)$ is calculated with (26). Equation (28) is a Fourier cosine series, and the coefficients $E_N$ can be evaluated by multiplying both sides by $\cos(M\pi x/L)$ and integrating from 0 to $L$. This yields

$$E_0 = \frac{1}{LQ_0(-P)} \int_0^L f(x')dx' \tag{29}$$

$$E_N = \frac{2}{LQ_N(-P)} \int_0^L f(x') \cos[\frac{N\pi x'}{L}]dx' \quad N = 1, 2, ... \tag{30}$$

It is also useful to calculate the flux at the surface as a function of position. To do this we plug (27) into the expression for the flux and evaluate it at z=0. This produces

$$J(x,0)) = -D_E \frac{\partial C_t}{\partial z}|_{z=0} + V_E C_t(0) = \Sigma_{n=0}^{\infty} E_N X_N(x) \Omega_N \quad \Omega_N = \frac{V_E}{2}[(1+\xi_N) + \gamma_N(1-\xi_N)] \tag{31}$$

**Constant Concentration at the Depth of the Land Mine:** Unlike the one dimensional case, the constant flux and constant concentration solutions are not mere multiples of each other. In the constant flux case above, for example, the concentration along $0 < x < W$ at $z = -P$ is not constant. Thus, the constant concentration problem must be solved separately. The lower boundary condition describing a constant concentration along the plane of the land mine is expressed mathematically as

$$C_t = g(x) \qquad z = -P; 0 < x < L \tag{32}$$

where $g(x)$ is an arbitrary function representing the chemical concentration across the plane at $z = -P$.

The rest of the boundary conditions are as before, and the method of solution is again separation of variables, producing the same general solution (27). The unknowns $E_N$ are evaluated in this case by applying the lower boundary condition (32) to the equation and making use of the orthogonal property of the cosine functions. Thus,

$$g(x) = \Sigma_{n=0}^{\infty} E_N Z_N(-P) \cos[\frac{N\pi x}{L}] \tag{33}$$

where

$$Z_N(-P) = \exp[\frac{V_E P}{2D_E}(\xi_N - 1)] + \gamma_N \exp[\frac{-V_E P}{2D_E}(1+\xi_N)]\} \tag{34}$$

Equation (33) is a Fourier cosine series, and the coefficients $E_N$ can be evaluated by multiplying both sides by $\cos(M\pi x/L)$ and integrating from 0 to $L$ as before. This yields

$$E_0 = \frac{1}{LZ_0(-P)} \int_0^L g(x')dx' \tag{35}$$

$$E_N = \frac{2}{LZ_N(-P)} \int_0^L g(x') \cos[\frac{N\pi x'}{L}]dx' \quad N = 1, 2, ... \tag{36}$$

The flux at the surface is simply equal to $H_E C_t(x, 0)$, or

$$J(x,0)) = H_E \Sigma_{n=0}^{\infty} E_N (1+\gamma_N) \cos[\frac{N\pi x}{L}] \tag{37}$$

We may now solve the problem for particular choices for the flux $f(x)$ or concentration $g(x)$ across the boundary at $z = -P$.

# Results

**Plane Source Flux Emission:** In this case

$$\begin{aligned} f(x) &= F \quad 0 < x < W \\ f(x) &= 0 \quad W < x < L \end{aligned} \tag{38}$$

Applying this to (29)-(30), we obtain

$$E_0 = \frac{FW}{LQ_0} \tag{39}$$

$$E_N = \frac{2F}{N\pi Q_N} \sin(\frac{N\pi W}{L}) \quad N = 1, 2, ... \tag{40}$$

and thus that

$$C_t(x,z) = \frac{FWZ_0(z)}{LQ_0} + \frac{2F}{\pi}\Sigma_{N=1}^{\infty} \cos[\frac{N\pi x}{L}] \sin[\frac{N\pi W}{L}] \frac{Z_N(z)}{NQ_N} \tag{41}$$

$$J(x,0)) = \frac{FW\Omega_0}{LQ_0} + \frac{2F}{\pi}\Sigma_{N=1}^{\infty} \cos[\frac{N\pi x}{L}] \sin[\frac{N\pi W}{L}] \frac{\Omega_N}{NQ_N} \tag{42}$$

Figure 3 shows a plot of the relative flux $J_{wz}(x,0)/F$ as a function of position on the surface for the extreme case of infinite half life for TNT, high water content (creating the maximum diffusion coefficient), and high evaporation rate.

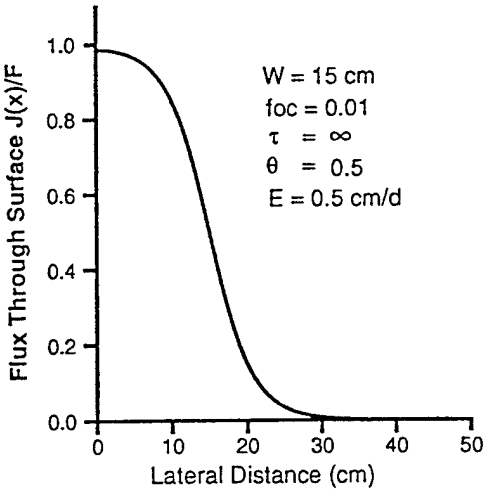


Figure 3: Flux from the surface as a function of lateral position for the case of a buried mine of width $2W = 30$ cm at 10 cm depth.

Figure 4 shows the effect of decreasing evaporation rate on the lateral spreading. As E declines, more lateral movement takes place because the travel time to the surface increases. This figure is possibly misleading however, because of the assumption of zero degradation. Whenever degradation is present, chemicals following paths with long travel times (as are the paths lateral to the vertical plane formed by the boundaries of the land mine) are attenuated prior to arrival

Figure 5 is a repeat of Figure 4, except that the half life of TNT is assumed to be 1 year.

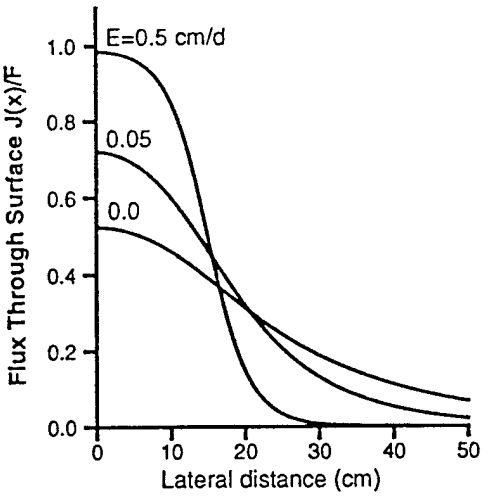


Figure 4: Effect of evaporation rate on the flux from the surface as a function of lateral position. Same conditions as in Fig. 3

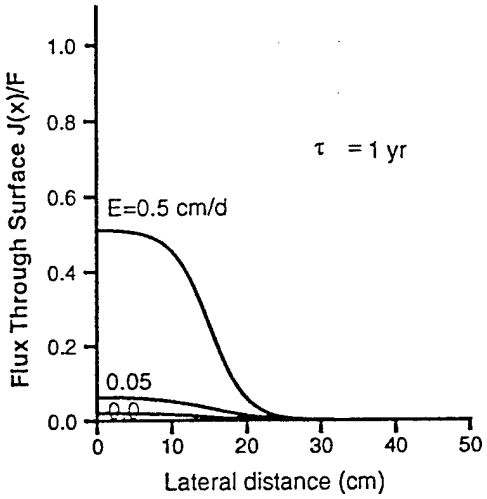


Figure 5: Effect of evaporation rate on the flux from the surface as a function of lateral position. Same conditions as in Fig. 4 except that $\tau = 1$ yr.

In contrast to the case where no degradation is occurring, the lateral extent of the surface flux is much less.

Water content also has a significant effect on signal strength and lateral spreading. Figure 6 is a recalculation of Figure 5 with the water content reduced from 0.5 to 0.25.

In this case, the advective travel time to the surface (which is inversely proportional to $\theta$) is decreased, causing higher surface flux above the land mine when $E \neq 0$. At the same time, however, diffusive travel time is lengthened significantly (see Figure 2), which decreases the lateral spreading when advection is present and extinguishes the signal when $E = 0$.

The effect of water content on lateral spreading is illustrated again in Figure 7, which is plotted logarithmically.

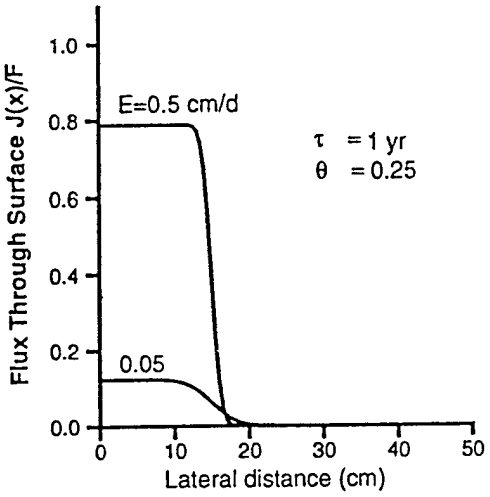


Figure 6: Effect of evaporation rate on the flux from the surface as a function of lateral position. Same conditions as in Fig. 4 except that $\theta = 0.25$. The flux reaching the surface when $E = 0$ is negligible.

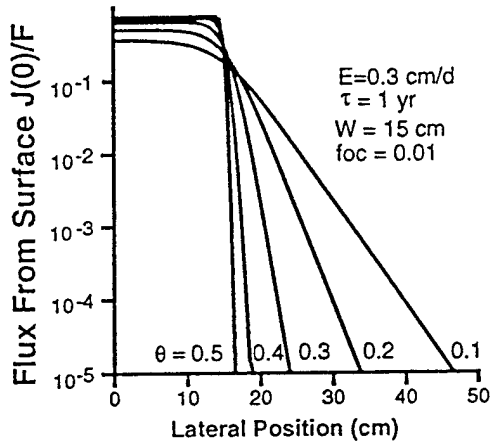


Figure 7: Effect of water content on lateral spreading of the surface flux.

**Plane Source Emission From Constant Concentration at the Depth of the Land Mine:** In this case

$$\begin{aligned} g(x) &= C_0 \qquad 0 < x < W \\ g(x) &= 0 \qquad W < x < L \end{aligned} \tag{43}$$

Applying this to (35)-(36), we obtain

$$E_0 = \frac{C_0 W}{L Z_0(-P)} \tag{44}$$

$$E_N = \frac{2C_0}{N\pi Z_N(-P)} \sin(\frac{N\pi W}{L}) \quad N = 1, 2, ... \tag{45}$$

and thus that

$$C_l(x,z) = \frac{C_0 W Z_0(z)}{L Z_0(-P)} + \frac{2C_0}{\pi}\Sigma_{N=1}^{\infty}\cos[\frac{N\pi x}{L}]\sin[\frac{N\pi W}{L}]\frac{Z_N(z)}{N Z_N(-P)} \tag{46}$$

$$J(x,0)) = \frac{C_0 W Q_0(0)}{L Z_0(-P)} + \frac{2C_0}{\pi}\Sigma_{N=1}^{\infty}\cos[\frac{N\pi x}{L}]\sin[\frac{N\pi W}{L}]\frac{Q_N(0)}{N Z_N(-P)} \tag{47}$$

Figures 8-10 show comparisons of the surface flux emission from a buried land mine emitting a constant flux of $F = 10^{-16}$ g/cm$^2$/sec, and a zone of constant concentration $C_0 = 4.6\times10^{-3}$ $\mu$g/cm$^3$ at the same location.

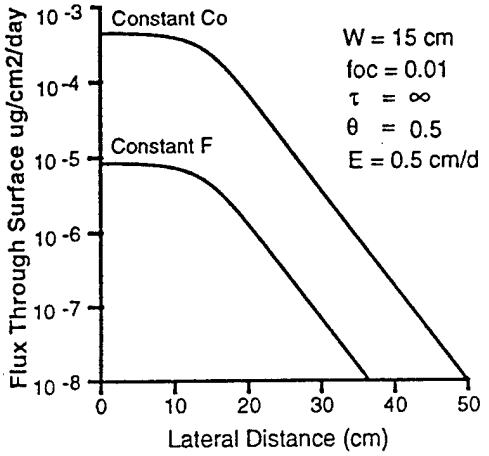


Figure 8: Comparison of constant flux $F = 10^{-16}$ g/cm$^2$/sec and constant concentration $C_0 = 4.6 \times 10^{-3}$ $\mu$g/cm$^3$ sources at $z = -10$ cm for the case of infinite half life and E= 0.5 cm/d.

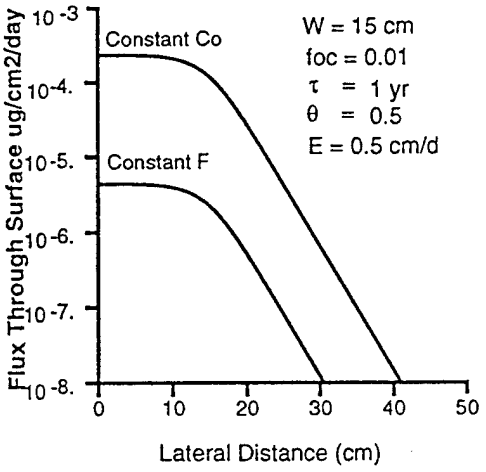


Figure 9: Comparison of constant flux $F = 10^{-16}$ g/cm$^2$/sec and constant concentration $C_0 = 4.6 \times 10^{-3}$ $\mu$g/cm$^3$ sources at $z = -10$ cm for the case of $\tau = 1$ yr half life and E= 0.5 cm/d.

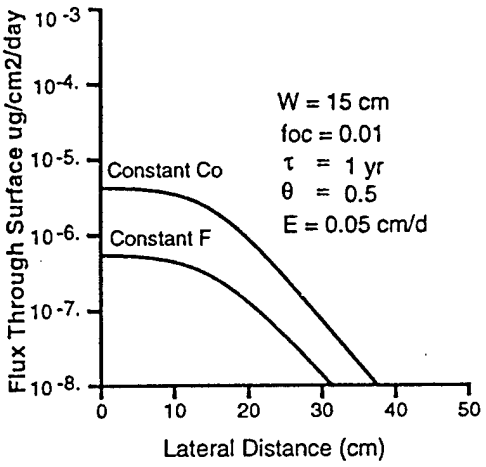


Figure 10: Comparison of constant flux $F = 10^{-16}$ g/cm$^2$/sec and constant concentration $C_0 = 4.6 \times 10^{-3}$ $\mu$g/cm$^3$ sources at $z = -10$ cm for the case of $\tau = 1$ yr half life and E= 0.05 cm/d.

**Continuous Point Source of Flux Emission:**

As the width $W$ of the land mine is decreased toward zero, while the product $\Xi = FW$ is held constant, we approach the delta function solution

$$f(x) = \Xi\delta(x) \tag{48}$$

which results in

$$C_l(x,z) = \frac{\Xi Z_0(z)}{LQ_0} + 2\Xi\Sigma_{N=1}^{\infty}\cos[\frac{N\pi x}{L}]\frac{Z_N(z)}{Q_N} \tag{49}$$

$$J(x,0)) = \frac{\Xi\Omega_0}{LQ_0} + 2\Xi\Sigma_{N=1}^{\infty}\cos[\frac{N\pi x}{L}]\frac{\Omega_N}{Q_N} \tag{50}$$

Figure 11 shows a comparison between the point source emission solution and one for which $W = 15$ cm and $F = 10^{-16}$ g/cm$^2$/sec.

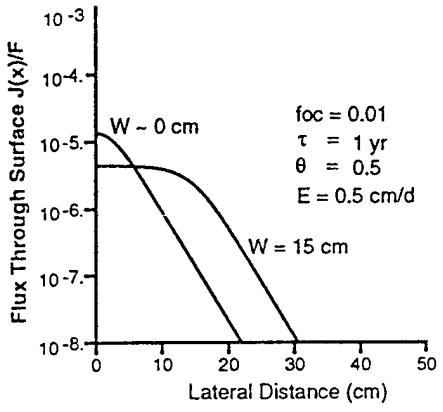


Figure 11: Comparison of delta function (W $\approx$ 0 cm) and distributed (W=15 cm) constant flux sources at $z = -10$ cm for the case of $\tau = 1$ yr half life , E= 0.5 cm/d, and $\Xi = FW = 1.3 \times 10^{-4}$ $\mu$g/cm/d.